TECHNICAL NOTES

NATIONAL ADVISORY COMMITTEE FOR AERONAUTICS

No. 264

TESTS OF THE N.P.L. AIRSHIP MODELS IN THE VARIABLE DENSITY WIND TUNNEL

By George J. Higgins
Langley Memorial Aeronautical Laboratory

Washington
September, 1927

NATIONAL ADVISORY COMMITTEE FOR AERONAUTICS.

TECHNICAL NOTE NO. 264.

TESTS OF THE N.P.L. AIRSHIP MODELS IN THE VARIABLE DENSITY WIND TUNNEL.

By George J. Higgins.

Summary

Tests have been conducted in the variable density wind tunnel of the National Advisory Committee for Aeronautics, on two airship models, known as the "N.P.L. Standardization Models, Long and Short." The resistance or shape coefficients were determined for each model through a range of Reynolds Numbers from 110,000 to 5,000,000. Comparison is made with previous tests on these models and other airship models.

Introduction

During the years of 1922 and 1923, comparative tests were made on two N.P.L. airship models in six American atmospheric wind tunnels to determine their resistance with particular reference to scale effect. These tests were made for the purpose of determining some idea of the "standardization of wind tunnels." The models used were developed and furnished by the British Aeronautical Research Committee.

It was desired that further tests on these models be made and, as the models had been returned to England, replicas were made at the Washington Navy Yard by the wind tunnel division of the Bureau of Construction and Repair. It was of particular importance that a greater "scale" or Reynolds Number be reached; simplicity in the method of support for the models was also recommended for the further tests.

The Navy replicas of the N.P.L. airship models were therefore forwarded to the Langley Memorial Aeronautical Laboratory for testing in the variable density wind tunnel where a Reynolds Number fifteen times that of the original tests could be obtained. The actual tests in the variable density tunnel were not performed until June, 1927.

These consisted of determining the resistance at the angle of zero pitch for both models through a range of Reynolds Numbers from 110,000 to 5,000,000.

Apparatus and Method of Test

The airship models used in these tests were cast of aluminum and turned in a lathe to specified ordinates measured on the original N.P.L. models. The model, designated as "long," is a 1/225 size replica of the "H.M.A.-R 33." The second model, designated as "short," is similar to the first in the shape of the nose and tail, but 1.5 diameters or 6.3 inches shorter in the cylindrical mid-portion. The actual dimensions of the two models are given in Table I. Here, also, is given the volume as determined by Simpson's rule and used in the computations. Photographs of the models are given in Figure 1.

The models were mounted in the test section of the variable density wind tunnel (Reference 1) in the manner shown in Figure 2. The suspension consisted of streamlined wires .025 inch by .094 inch in cross section. Two wires were screwed into the model 4 inches aft of the nose 90° apart and making 45° to the vertical. The outer ends of these wires were attached through small knife edges to the tunnel walls. Streamlined fairings covered the outer 16 inches and protected that portion of the suspension from the air stream. A single wire at the tail fastened by a pivot to a short 2-inch sting supported the rear of the models in a similar manner as the nose. A round wire, 0.043 inch in diameter, attached to a plug screwed in at the nose, transmitted the drag forces through a bell crank to the auxiliary drag balance (for use where resistance only is to be measured (Figure 3)). A similar round wire attached to the tail sting led through a bell crank to a counterweight. This served the purpose of keeping the system taut and maintaining a slight initial load on the balance. The lengths of these horizontal wires were adjusted by small turnbuckles at the ends away from the model so the model might assume its own position, thus eliminating any error due to a component of its weight exerting a force on the balance.

Each model was tested at a velocity of about 50 miles an hour and at densities ranging from that equivalent to 1/2 atmosphere to 20 atmospheres pressure, absolute. Using the $(\text{volume})^{1/3}$ as a characteristic length, the range in Reynolds Number covered was from 110,000 to 5,000,000. Readings of the resistance were obtained at six densities.

Results and Discussion

The results of the tests on these two airship models are given in Table II, and are plotted in Figures 4 and 5. Resistance or shape coefficients have been computed and plotted against Reynolds Number, where

$$D = C_S \, q \, (\text{Vol.})^{2/3}$$

$$R.N. = \frac{\rho V}{\mu} (\text{Vol.})^{1/3}$$

D = drag

q = dynamic pressure, $\frac{1}{2} \rho V^2$

R.N. = Reynolds Number

Vol. = volume of airship model

ρ = density of air

V = velocity of air

μ = viscosity of air

Figure 4 shows the values of C_S for the two models with reference to the change in R.N. In each case, the curve of C_S is regular, decreasing in value as the "scale" is increased and apparently approaching a minimum at the upper limit of the range tested. The 20-atmosphere run on the long model was irregular and the value of the C_S is too high. This is due to insufficient counterweight on the suspension system, which allowed the model to become unsteady and to oscillate. The value of the Reynolds Number of the "H.M.A.-R 33" cruising at 50 miles an hour is 60,500,000. Even though the scale reached is 1/10 that of full scale, these curves indicate that extrapolation to determine a full-scale value of C_S is perhaps unreliable.

In this same chart there are shown the C_S curves obtained for the N.P.L. originals of these same models in tests made at six American atmospheric wind tunnels. The range of R.N. covered by these tests is only about 1/15 that of the variable density tunnel. The curves are very widely scattered, particularly at the lower R.N. There is a decided tendency to converge as the scale is increased, approaching values of the same magnitude as obtained in the variable density tunnel.

The results from the Washington Navy Yard agree the best with those from the present tests; both are high compared to the average and it is possible that this is due to the relatively high degree of turbulence present in both wind tunnels.

The method of support used in the present tests was such that the tare drag amounted to about 45 per cent of the net drag and that interference to the model was small (see Fig. 2).

In Figure 5 there is shown a chart of C_S versus $\frac{\text{length}}{\text{diameter}}$

ratio, where a curve has been plotted representing the results of tests on other airships in the variable density tunnel at a Reynolds Number corresponding to 20 atmospheres. The values of C_S for the N.P.L. models are shown as points. The agreement is very good.

Conclusion

The shape or resistance coefficient of the N.P.L. airship models, as tested in the variable density wind tunnel, decreases in value as the scale or Reynolds Number is increased, tending to approach a minimum as the upper limit of the test range is reached. The results of these tests in comparison with tests at low scale in other wind tunnels show that further work is necessary in the standardization of wind tunnels. The values of resistance for these models are in accordance with other airship models tested in this wind tunnel.

Reference

1. Munk, Max M. and Miller, E. W. : The Variable Density Wind Tunnel of the National Advisory Committee for Aeronautics. N.A.C.A. Technical Report No. 227. (1926)

TABLE I.

Dimensions of N.P.L. Airship Models
in Inches.

Long Model				Short Model			
Sta.	Diam.	Sta.	Diam.	Sta.	Diam.	Sta.	Diam.
0.0	.000	15.0	4.200	0.0	.000	13.0	4.158
.5	1.320	16.0	4.199	.5	1.294	14.0	4.101
1.0	1.866	17.0	4.198	1.0	1.849	15.0	4.010
1.5	2.266	18.0	4.194	1.5	2.266	16.0	3.889
2.0	2.577	19.0	4.173	2.0	2.580	17.0	3.724
2.5	2.846	20.0	4.128	2.5	2.847	18.0	3.532
3.0	3.074	21.0	4.047	3.0	3.073	19.0	3.326
3.5	3.223	22.0	3.931	3.5	3.268	20.0	3.098
4.0	3.438	23.0	3.777	4.0	3.439	21.0	2.845
4.5	3.586	24.0	3.602	4.5	3.585	22.0	2.554
5.0	3.714	25.0	3.396	5.0	3.711	23.0	2.236
6.0	3.919	26.0	3.169	6.0	3.916	24.0	1.883
7.0	4.066	27.0	2.927	7.0	4.059	25.0	1.502
8.0	4.149	28.0	2.667	8.0	4.150	26.0	1.068
9.0	4.188	29.0	2.363	9.0	4.188	27.0	.592
10.0	4.200	30.0	2.013	10.0	4.196	27.953	.000
11.0	4.200	31.0	1.638	11.0	4.195		
12.0	4.2005	32.0	1.222	12.0	4.184		
13.0	4.2005	33.0	.752				
14.0	4.201	34.0	.217				
		34.280	.000				

Total length = 34.280 in.

Vol. = .00535 m^3

$(\text{Vol.})^{2/3}$ = .0360 m^2

$(\text{Vol.})^{1/3}$ = .1748 m

Total length = 27.953 in.

Vol. = .00391 m^3

$(\text{Vol.})^{2/3}$ = .02485 m^2

$(\text{Vol.})^{1/3}$ = .1577 m

TABLE II.

Resistance or Shape Coefficients.

$$C_S = \frac{\text{Drag}}{q\ (\text{Vol.})^{2/3}}$$

Long Model		Short Model	
R.N.	C_S	R.N.	C_S
118,000	.0372	108,500	.0341
118,000	.0368	108,500	.0341
254,000	.0346	228,000	.0327
254,000	.0348	228,000	.0328
254,000	.0350	545,000	.0290
254,000	.0349	545,000	.0292
610,000	.0294	1,175,000	.0257
610,000	.0294	1,175,000	.0257
1,285,000	.0260	2,320,000	.0231
1,285,000	.0261	2,320,000	.0230
2,570,000	.0233	4,550,000	.0209
2,570,000	.0233	4,550,000	.0213
5,050,000	.0236	4,550,000	.0213
5,050,000	.0238		

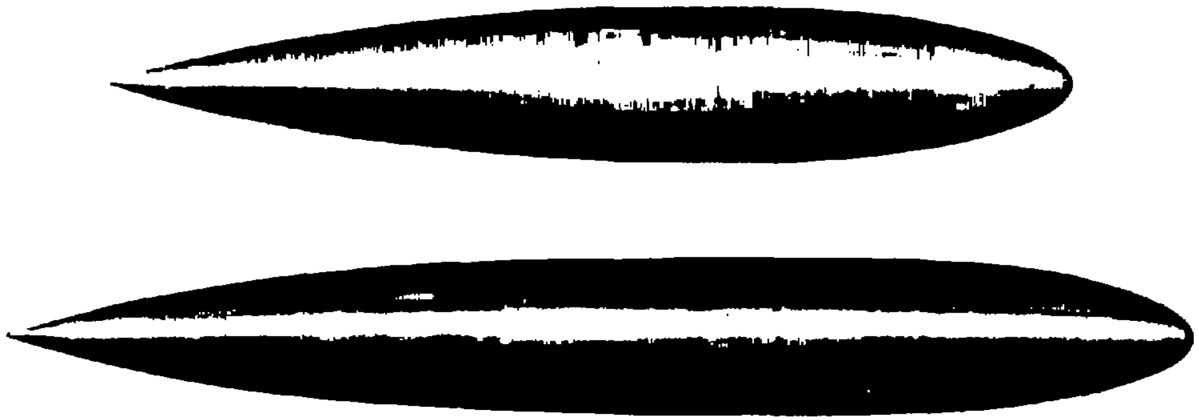

Fig.1 N.P.L. Standard airship models. U.S.N. replicas

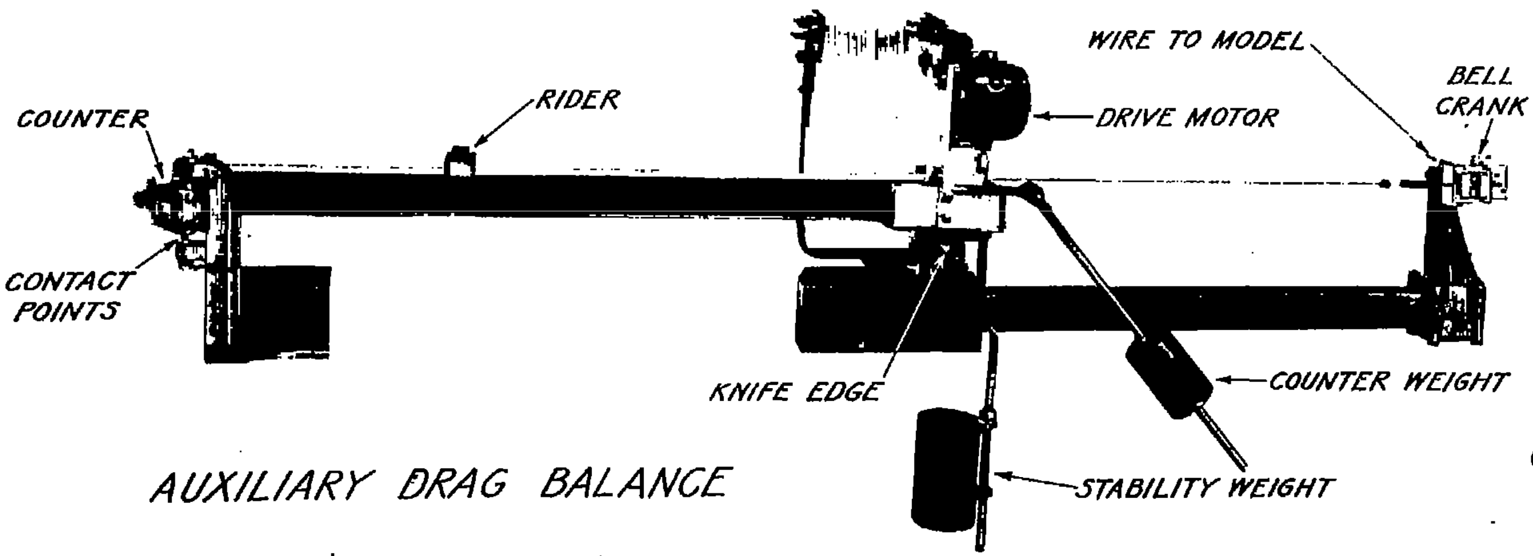

Fig.3 Auxiliary drag balance. Variable density tunnel.

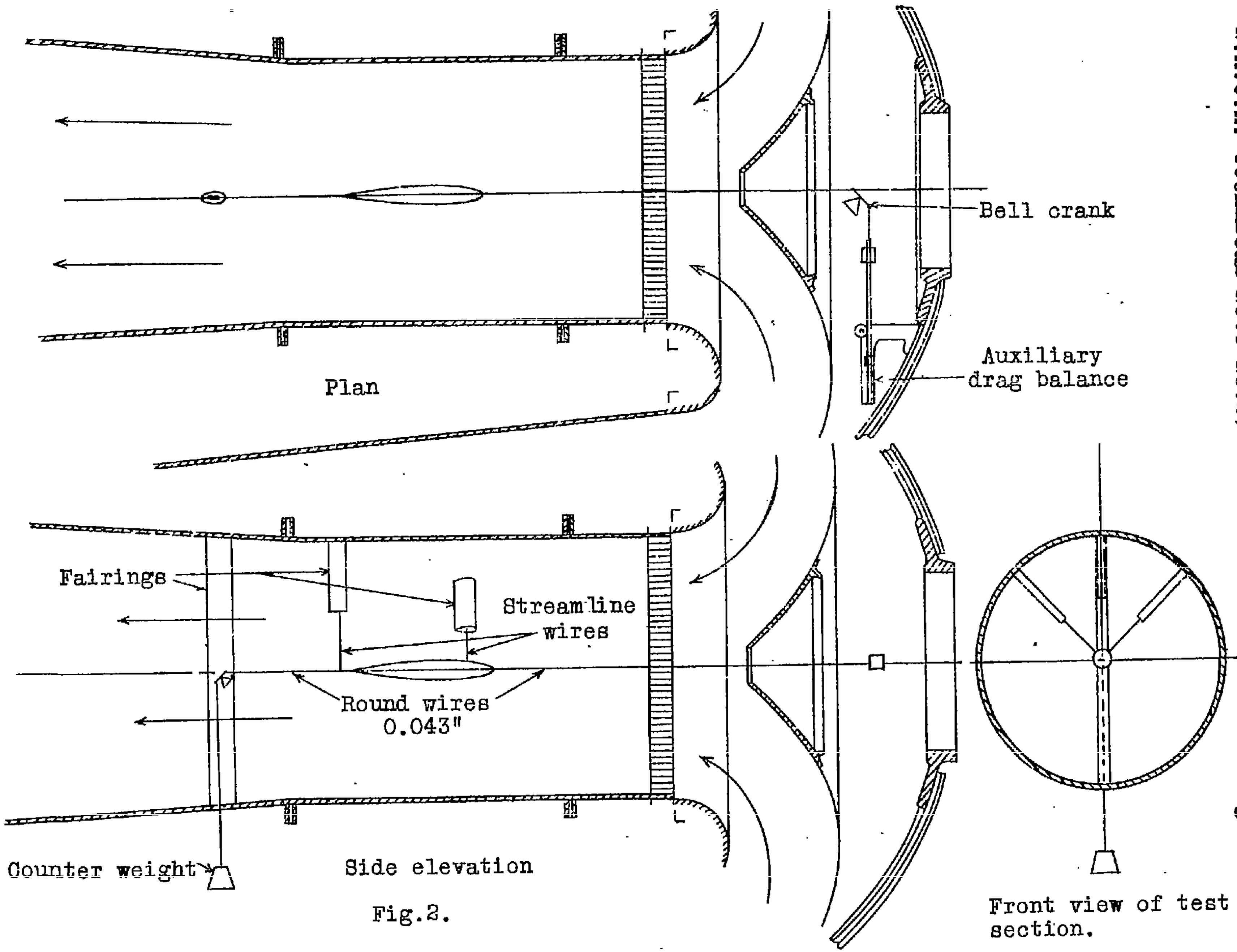

Bell crank
Auxiliary drag balance
Plan
Fairings
Streamline wires
Round wires 0.043"
Counter weight
Side elevation
Front view of test section.

Fig.2.

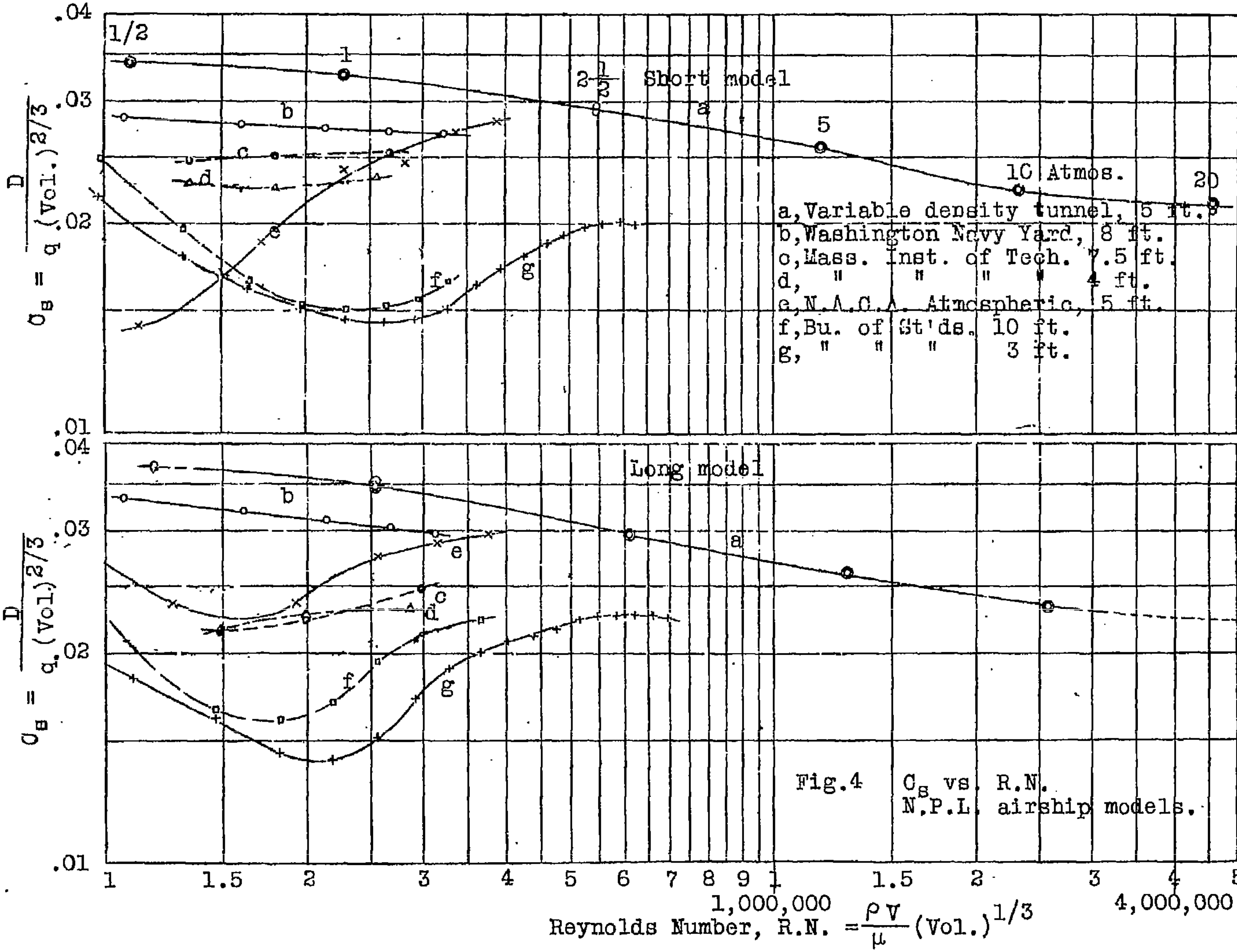

Fig.4 C_s vs. R.N. N.P.L. airship models.

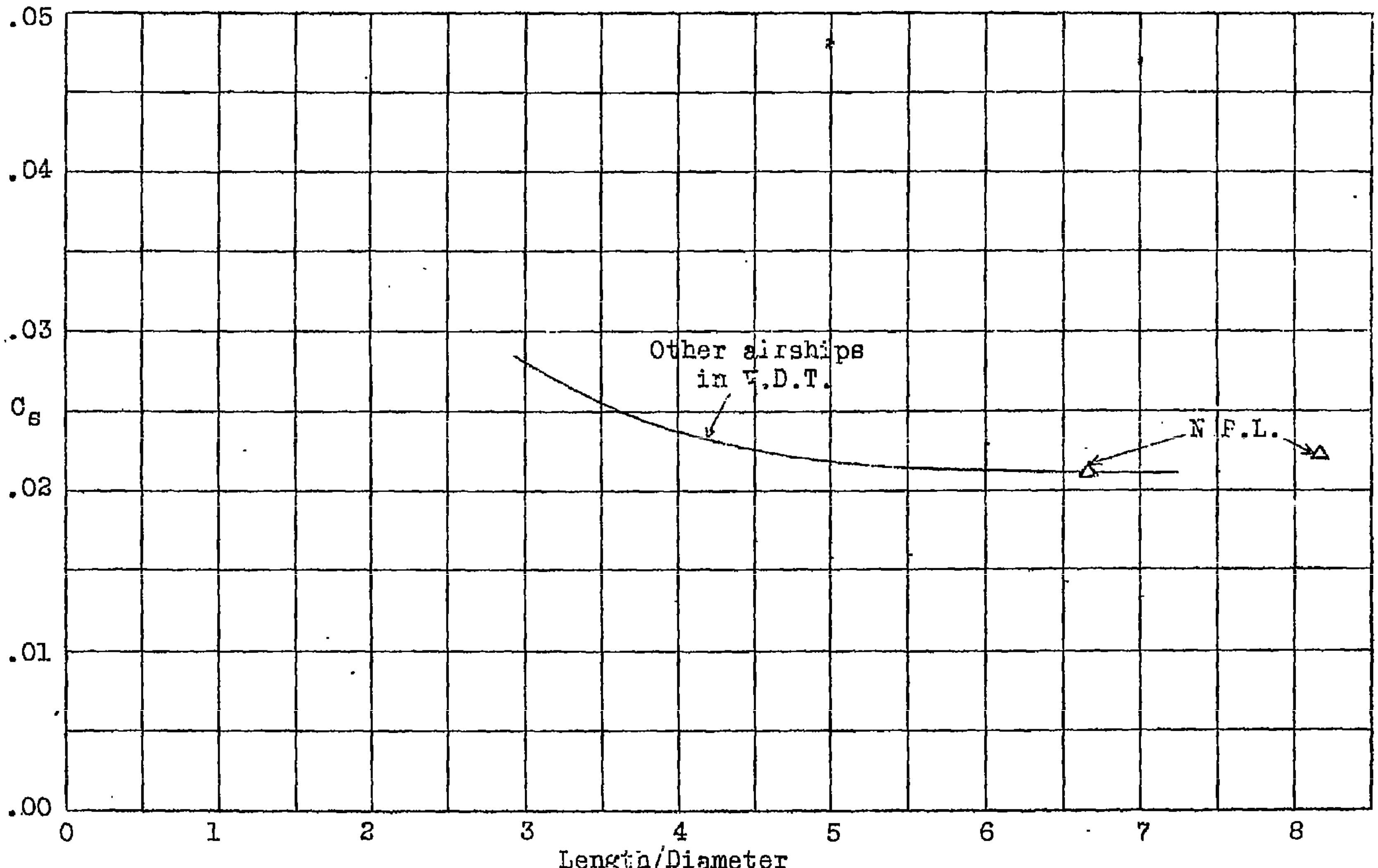

Fig.5 C_s vs. Length/Diameter. N.P.L. airship models.

where x and y are the abscissas and ordinates of the airfoil and φ is the central angle of the unit circle. The functions $\Delta x(\varphi)$ and $\Delta y(\varphi)$ are related either by the conjugate Fourier series, directly derivable from equation (A2) upon substitution of $p = e^{i\varphi}$, or by the integral relations:

$$\Delta x(\varphi) = -\frac{1}{2\pi}\int_0^{2\pi} \Delta y(\varphi') \cot\frac{\varphi'-\varphi}{2}\,d\varphi' \tag{A6}$$

488

$$\Delta y(\varphi) = \frac{1}{2\pi}\int_0^{2\pi} \Delta x(\varphi') \cot\frac{\varphi'-\varphi}{2}\,d\varphi' \tag{A7}$$

Given the airfoil coordinates x and y, equations (A4), (A5), and (A6) can be solved for the mapping function $\Delta x(\varphi) + i\Delta y(\varphi)$ by the following method of successive approximation: The upper surface of the airfoil is drawn with its leading- and trailing-edge chordwise extremities at the points $(\pi\sigma, 0)$, $(-\pi\sigma, 0)$, respectively, where σ is the solidity c/h. This form of the airfoil is referred to as the normal form. For a conveniently chosen set of values of the variable φ from 0° to 180° the airfoil ordinates $\Delta y(\varphi)$ are measured at the chordwise stations x (equation (A4)) corresponding to some appropriate initial abscissa function $\Delta x(\varphi)$, such as that of the previous approximation, or $\Delta x(\varphi) \equiv 0$, if there is no previous approximation. The function $\Delta x(\varphi)$ is computed from this $\Delta y(\varphi)$ by equation (A6). (See appendix C.) The constants K and τ are next determined from the $\Delta x(\varphi)$ function by means of the equations

$$\sinh K = \frac{1}{\sinh\left[\frac{\pi\sigma}{2}\,\frac{\Delta x(\pi) - \Delta x(0)}{4}\right]} \tag{A8}$$

$$\tau = -\frac{1}{2}\left[\Delta x(0) + \Delta x(\pi)\right] \tag{A9}$$

The constants K and τ so determined, together with the corresponding mapping function $\Delta x(\varphi) + i\Delta y(\varphi)$, yield a derived airfoil contour by equations (A4) and (A5), which is in the normal form and can be compared with the given airfoil. If the agreement is not sufficiently close, the foregoing procedure is repeated.

After the mapping function relating the circle and airfoil planes has been found, the velocity in the airfoil planes can be determined from the general equation

$$v_c = V\left|\frac{d\zeta}{dz}\right| \tag{A10}$$

488

The resulting formula for the velocity distribution on the airfoil itself is

$$\frac{v_c}{V} = \frac{2\cosh K\ |\sin\varphi|}{(\sin^2\varphi + \sinh^2 K)\sqrt{\left(\left[\frac{d\zeta}{dp}\right] - \frac{d\Delta x}{d\varphi}\right)^2 + \left(\frac{d\Delta y}{d\varphi}\right)^2}} \tag{A11}$$

where

$$\left[\frac{d\zeta}{dp}\right] = \frac{2\cosh K\sin\varphi}{\sin^2\varphi + \sinh^2 K} \tag{A12}$$

The details of the calculation of the conjugate derivatives $d\Delta x/d\varphi$ and $d\Delta y/d\varphi$ from the known functions $\Delta x(\varphi)$ and $\Delta y(\varphi)$ are given in appendix C.

For the limiting case of the isolated airfoil, three of the six calculating equations (A4), (A5), (A6), (A8), (A9), and (A11) must be changed, namely, (A4), (A8), and (A11). The corresponding equations are, respectively,

$$x = \tau + r\cos\varphi + \Delta x(\varphi) \tag{A4'}$$

$$r = 1 + \frac{\Delta x(\pi) - \Delta x(0)}{2} \tag{A8'}$$

$$\frac{v_i}{V} = \frac{|\sin\varphi|}{\sqrt{\left(\sin\varphi - \frac{d\Delta x}{r\,d\varphi}\right)^2 + \left(\frac{d\Delta y}{r\,d\varphi}\right)^2}} \tag{A11'}$$

The quantity r is the diameter of the circle to which the isolated airfoil is conformally related.

The calculations by the method of finite chord were for the most part based on the set of 12 evenly spaced φ values, 0°, 15°, . . ., 180°. The leading edge of the airfoil corresponded to

488

$\varphi = 0^{\circ}$ and the trailing edge to 180°. The symmetry of the airfoil and its position has a corresponding symmetry in the mapping function and its derivatives; namely,

$$\left.\begin{array}{l} \Delta x(\varphi) \\ \Delta y(\varphi) \\ d\Delta x/d\varphi \\ d\Delta y/d\varphi \end{array}\right\} \text{is an} \left\{\begin{array}{l} \text{even} \\ \text{odd} \\ \text{odd} \\ \text{even} \end{array}\right\} \begin{array}{l} \text{function with respect to} \\ \text{the station } \varphi = \pi. \end{array}$$

APPENDIX B

CONFORMAL MAPPING: METHOD OF SEMI-INFINITE CHORD

In this method the flow through the unstaggered cascade of airfoils is determined by the conformal transformation relating the cascade of shapes consisting of the airfoils and their zero streamline prolongation in one direction, z-plane, the cascade of semi-infinite straight chord lines, ζ-plane, and the unit circle, p-plane.

The essential difference between this method and the method of finite chord lies in the relation between the ζ- and p-planes. In this case the relation is

$$\zeta = \frac{h}{2\pi} \log_e \left[1 - \left(\frac{p+1}{p-1}\right)^2\right] - 1 \tag{B1}$$

This function transforms the unit circle in the p-plane into an unstaggered cascade of semi-infinite straight lines of which the abscissas range from -1 to $+\infty$. The term $(p+1)/(p-1)$ transforms the unit circle into an infinite straight line; squaring the term yields a semi-infinite straight line; and the logarithm transforms the straight line into a cascade of straight lines. The vertical distance between two consecutive lines is h. On the unit circle

$$p = e^{i\varphi}$$

$$x = \frac{-2}{\pi\sigma} \log\left|\sin\frac{\varphi}{2}\right| - 1 + \Delta x(\varphi) - \Delta x(180^\circ) \tag{B2}$$

$$y = \Delta y(\varphi) \tag{B3}$$

where all lengths are expressed as fractions of airfoil chord c, which was taken as c = 2, and the term $\Delta x(180^\circ)$ has been inserted in order to locate the airfoils of the successive approximations with one extremity at the point (-1, 0).

The velocity distribution on the airfoil given by equation (A10) now becomes

$$\frac{v_c}{V} = \frac{\frac{1}{\pi\sigma}\cot\frac{\varphi}{2}}{\sqrt{\left(\frac{1}{\pi\sigma}\cot\frac{\varphi}{2} - \frac{d\Delta x}{d\varphi}\right)^2 + \left(\frac{d\Delta y}{d\varphi}\right)^2}} \tag{B4}$$

No intermediate adjustment such as is represented by equation (A8) is required; hence the solution by successive approximation outlined in appendix A is reduced to little more than the calculation of conjugates.

The chordwise stations for an evenly spaced set of φ-points tend to cluster around $x = -1$ with the transformation (B2). Consequently, in order to obtain a sufficiently even distribution of points over the airfoil, two devices were resorted to. The first was to perform the calculation twice for each case. The airfoil was first considered with the leading edge at $x = -1$ and the trailing edge at $x = 1$ and a solution obtained for the mapping function. The airfoil was then considered as reversed with respect to the y-axis and a solution obtained for another mapping function. The set of φ-points was the same in both solutions. The second device, which is applicable more generally in conformal-mapping problems, consisted in using a standard set of θ-points in a p'-plane related to the p-plane by the bilinear transformation

$$p = \frac{p' + \frac{n-1}{n+1}}{\frac{n-1}{n+1} p' + 1} \tag{B5}$$

The transformation (B5) is so chosen that (a) the unit circle $p = e^{i\varphi}$ goes into the unit circle $p' = e^{i\theta}$ with the points $p = \pm 1$ corresponding to $p' = \pm 1$ and the outside spaces corresponding, and (b) the derivative $\left(\frac{dp'}{dp}\right)_{p=1} = n$. By condition (a), the conjugate relation (A6) is valid in the p'-plane. Condition (b) causes a small range ϵ $(\epsilon = \varphi - \theta)$ of φ near $\varphi = 0$, which corresponds to $x = \infty$, to correspond, for $n > 1$, to a larger range $n\epsilon$ of θ near $\theta = 0$. Hence, for $n > 1$, an evenly spaced set of θ-points yields a more evenly distributed set of chordwise stations x than the same spacing of φ-points. The values of φ corresponding to the assumed θ-points are obtained from equation (B5) with $p = e^{i\varphi}$, $p' = e^{i\theta}$,

$$\tan \varphi = \frac{2n \sin \theta}{(n^2-1) + (n^2+1) \cos \theta} \tag{B6}$$

The conjugate derivatives in the velocity formula (B4) were obtained by

$$\left.\begin{aligned} \frac{d\Delta x}{d\varphi} &= \frac{d\Delta x}{d\theta}\frac{d\theta}{d\varphi} \\ \frac{d\Delta y}{d\varphi} &= \frac{d\Delta y}{d\theta}\frac{d\theta}{d\varphi} \end{aligned}\right\} \tag{B7}$$

with

$$\frac{d\theta}{d\varphi} = \frac{(n^2-1) \cos \theta + (n^2+1)}{2n} \tag{B8}$$

The derivatives $d\Delta x/d\theta$ and $d\Delta y/d\theta$, in the cases treated by the method of semi-infinite chord ($\sigma = 1.0, 1.5, 2.0$), were measured graphically by drawing tangents to the calculated curves $\Delta x(\theta)$ and $\Delta y(\theta)$. This procedure was found to be more accurate at high solidities than that of calculating the derivatives by the formulas given in appendix C.

A typical result obtained by the method of semi-infinite chord is illustrated in figure 8. The quantity n was so chosen that the points obtained for the front half of the airfoil overlapped the points obtained for the rear half of the airfoil. The resulting values of n ranged from 2 to 30 and are given for each case in tables II and III. The calculations were based in the case $\sigma = 1$ on the use of 12 evenly spaced values of $\theta = 0^\circ, 15^\circ, \ldots, 180^\circ$ and for the higher solidities on the 24 values $\theta = 0^\circ, 7.5^\circ, 15^\circ, \ldots, 180^\circ$.

It may be noted that the effect of boundary-layer development along and downstream of the airfoil can be taken into account quite simply in this method by considering as boundary contour the locus of the outer edge of the displacement boundary layer along and downstream of the airfoil.

The effect of boundary-layer development on the tunnel walls can be treated by so altering the mapping problem that the channel between the zero streamline of the airfoil and one tunnel wall is to be mapped into a uniform channel. The mapping methods for this problem are similar to those already described.

APPENDIX C

NUMERICAL EVALUATION OF CONJUGATE FUNCTIONS AND THEIR DERIVATIVES

The determination of the conjugate function $\Delta x(\varphi)$ and of the conjugate derivatives $d\Delta x/d\varphi$, $d\Delta y/d\varphi$ from a known function $\Delta y(\varphi)$ was based in this paper on numerical integration of equation (A6) and, for solidities of 0 and 0.5, integration of the respective derivatives of equations (A6) and (A7). After several trials with other methods of evaluation, including Fourier expansion, graphical methods, and various kinds of numerical integration, the following procedures were adopted as a compromise between accuracy and expenditure of effort.

In order to calculate $\Delta x(\varphi)$, the range of integration in equation (A6) was divided into an even number of equal intervals. The function $\Delta y(\varphi)$ was considered to be known numerically at the values of φ separating these intervals. In the region outside the intervals on either side of the singular point $\varphi = \varphi'$, the integral was evaluated by Simpson's rule. The contribution to the integral of the two intervals separated by the singular point φ' was obtained by representing $\Delta y(\varphi)$ in this range by the form

$$\Delta y(\varphi) = A \cos \varphi + B \sin \varphi + C \tag{C1}$$

The constants A, B, and C were so determined that equation (C1) was satisfied at the three φ-points bounding the two intervals. The final result for $\Delta x(\varphi)$ is an expression of the form

$$\Delta x(\varphi) = \sum_{k=0}^{2n-1} a_k \, \Delta y(\varphi + k\delta) \tag{C2}$$

where δ is the interval between two consecutive values of φ and $2n\delta = 2\pi$. The 24 coefficients a_k for $n = 12$ are listed in table VII.

The conjugate derivatives $d\Delta x/d\varphi$ and $d\Delta y/d\varphi$ were obtained in an analogous manner from the relations

$$\frac{d\Delta x(\varphi)}{d\varphi} = -\frac{1}{4\pi}\int_0^{2\pi} \frac{\Delta y(\varphi') - \Delta y(\varphi)}{\sin^2 \frac{\varphi' - \varphi}{2}} \, d\varphi' \tag{C3}$$

488.

$$\frac{d\Delta y(\varphi)}{d\varphi} = \frac{1}{4\pi}\int_0^{2\pi} \frac{\Delta x(\varphi') - \Delta x(\varphi)}{\sin^2 \frac{\varphi' - \varphi}{2}}\, d\varphi' \tag{C4}$$

These relations can be derived by differentiating equations (A6) and (A7) under the integral sign after subtracting $\Delta y(\varphi)$ and $\Delta x(\varphi)$ from the respective integrands to make this operation permissible. They can also be obtained by a limiting process in the complex plane similar to that of reference 1, appendix C. The numerical integration of equations (C3) and (C4) by Simpson's rule and a sinusoidal approximation over the singularity result as before in expressions of the form

$$\frac{d\Delta x}{d\varphi} = -\sum_{k=0}^{2n-1} b_k\, \Delta y(\varphi + k\delta) \tag{C5}$$

$$\frac{d\Delta y}{d\varphi} = \sum_{k=0}^{2n-1} b_k\, \Delta x(\varphi + k\delta) \tag{C6}$$

The b_k coefficients are listed in table VII for $n = 12$. The a_k and b_k coefficients were also calculated for 48 φ-points, and are listed in table VIII.

Explicit expressions for the coefficients for a $2n$-point scheme are $(2n\,\delta = 2\pi)$

$$\left.\begin{aligned}
a_0 &= 0\\
a_1 &= -\frac{\delta}{6\pi}\cot\frac{\delta}{2} - \frac{\delta + \sin\delta}{2\pi\sin\delta}\\
a_{2n-1} &= \frac{\delta}{6\pi}\cot\frac{\delta}{2} + \frac{\delta + \sin\delta}{2\pi\sin\delta}\\
a_k &= -\frac{\delta}{3\pi}\cot\frac{k\delta}{2} \qquad (k\ \text{odd})\\
a_k &= -\frac{2\delta}{3\pi}\cot\frac{k\delta}{2} \qquad (k\ \text{even})
\end{aligned}\right\} \tag{C7}$$

$$\left.\begin{aligned}
b_0 &= -\sum_{k=2}^{2n-2} b_k - \frac{\delta}{6\pi \sin^2 \frac{\delta}{2}} - \frac{\delta}{\pi(1 - \cos \delta)} \\
b_1 &= b_{2n-1} = \frac{\delta}{12\pi \sin^2 \frac{\delta}{2}} + \frac{\delta}{2\pi(1 - \cos \delta)} \\
b_k &= \frac{\delta}{3\pi \sin^2 \frac{k\delta}{2}} \qquad (k \text{ even}) \\
b_k &= \frac{\delta}{6\pi \sin^2 \frac{k\delta}{2}} \qquad (k \text{ odd})
\end{aligned}\right\} \quad \text{(C8)}$$

488

The accuracy of the 24- and 48-point schemes was checked on the function $\sin 2\varphi$. The 24-point scheme gave results for the conjugate accurate to 0.8 percent and for the derivatives accurate to 0.2 percent. The 48-point scheme resulted in 0.2-percent accuracy for the conjugate and 0.05-percent accuracy for the derivatives. These values for accuracy are given only as a reference with which to compare other methods. They do not give any direct indication of the accuracy of evaluation of the conjugate functions and derivatives of this paper.

488

APPENDIX D

FIRST-ORDER IMAGE THEORY

In this method of obtaining the constriction correction, the image airfoils (fig. 1) are replaced by equivalent doublets. The disturbance velocity produced in the region of the physical airfoil by these doublets is u and the resultant velocity is therefore $V + u$. The tunnel velocity distribution of the airfoil v_c is assumed to be given by its nondimensional isolated-airfoil velocity distribution v_i/V multiplied by the velocity $V + u$; that is,

$$\frac{v_c}{V + u} = \frac{v_i}{V} \tag{D1}$$

so that the constriction correction is

$$\frac{\Delta v}{V} = \frac{v_c - v_i}{V} = \frac{v_i}{V}\frac{u}{V} \tag{D2}$$

According to Glauert (reference 3, p. 53), the disturbance velocity u is given by

$$\frac{u}{V} = \frac{\pi^2}{12}\lambda\left(\frac{t}{h}\right)^2 \tag{D3}$$

where the factor λ is given by

$$\lambda = \frac{4}{\pi}\frac{c}{t}\int\frac{v_c}{V}\frac{y}{t}\,d\left(\frac{s}{c}\right) \tag{D4}$$

(reference 3, p. 55; Glauert does not explicitly indicate the chord c and his q is here v_c in accordance with his explanation of the evaluation of λ). The integral in equation (D4) is taken with respect to surface distance s along the upper surface of the airfoil from leading to trailing edge. Its form indicates that λ is approximately inversely proportional to t/c (see also reference 3, equation (17.10)), and thus u/V is proportional to the parameter tc/h^2. The values of λ calculated from equation (D4) for the various cases are given in table X.

The constriction correction given by equation (D2) represents a refinement of the usually given first-order constriction correction u/V, which is a constant along the chord. This procedure is used in order to be consistent with the constriction correction derived from Goldstein's theory as discussed in appendix E.

It may be noted that in calculating the strength of a doublet that is to replace an isolated airfoil, v_i rather than v_c should be used in equation (D4). However, inasmuch as the strength of the doublet must be increased when it is used to replace the same airfoil in a cascade, the use of v_c, which is greater than v_i, will change the value of λ in the right direction. For the low values of the solidity for which the doublet correction is used, however, there is no appreciable difference in the correction.

APPENDIX E

SECOND-ORDER IMAGE THEORY

Goldstein (reference 4) first replaces the image airfoils (fig. 1) by the doublet and higher-order singularities given by the potential function of the airfoil in a uniform free stream. The nonuniform disturbance velocity produced by these singularities in the physical region, in particular at the location of the physical airfoil, is calculated. This first-approximation nonuniform disturbance velocity (a) changes the velocity distribution of the airfoil from its isolated free-stream value and (b) changes the values of the singularities that are to be imaged. Change (b) is evaluated and a second-approximation nonuniform disturbance velocity is calculated, etc., to higher approximations. Lastly, the velocity distribution of the airfoil in the final nonuniform stream is calculated.

In principle, Goldstein's method is capable of yielding to any degree of accuracy the effect of a tunnel on the two-dimensional velocity distribution of an arbitrary airfoil, arbitrarily situated. The successive approximations, however, become increasingly laborious. Goldstein gives the formulas to the second approximation; that is, to the order tc^3/h^4, t^2c^2/h^4, t^3c/h^4. These formulas are quoted here as used in, and in the notation of, this paper.

The fundamental formula for the symmetrical constriction correction is obtained as the ratio of tunnel to free-stream velocity distribution:

$$\frac{v_c}{v_i} = \frac{U}{V}\left(1 + \frac{P(\theta)}{\sin\theta}\right) \tag{E1}$$

so that

$$\frac{\Delta v}{V} = \frac{v_c - v_i}{V} = \frac{v_i}{V}\left(\frac{v_c}{v_i} - 1\right) \tag{E2}$$

where

$$\frac{U}{V} = 1 + \frac{4}{3}S^2d_1 + \frac{2}{9}S^4\left(8d_1{}^2 - \frac{24}{5}d_3\right) \tag{E3}$$

$$\begin{aligned} P(\theta) = {} & \lambda_2'\,(R\sin 2\theta - A_0\sin\theta) \\ & + \lambda_3'\,(R^2\sin 3\theta - 2RA_0\sin 2\theta + A_0{}^2\sin\theta - A_1\sin\theta) \end{aligned} \tag{E4}$$

$$S = \frac{\pi}{2h} \tag{E5}$$

$$\left.\begin{aligned} \lambda_2' &= \frac{2\pi^4}{15c^4}\left(\frac{c}{h}\right)^4 d_2 \\ \lambda_3' &= -\frac{\pi^4}{15c^4}\left(\frac{c}{h}\right)^4 d_1 \end{aligned}\right\} \tag{E6}$$

$$\left.\begin{aligned} R &= \frac{c}{4}(1 + C_0) \\ A_n &= B_n \\ B_0 &= -\frac{c}{4} C_1 \\ B_1 &= -\frac{c^2}{16}(1 + C_2) \\ B_2 &= -\frac{c^3}{64} C_3 \end{aligned}\right\} \tag{E7}$$

$$\left.\begin{aligned} d_1 &= \frac{c^2}{16}(2C_0 - C_2) \\ d_3 &= -\frac{c^4}{256} C_4 \end{aligned}\right\} \tag{E8}$$

$$\left.\begin{aligned} C_0 &= \frac{2}{\pi c}\int_0^\pi \frac{y(\theta)}{\sin\theta}\,d\theta \\ C_n &= \frac{4}{\pi c}\int_0^\pi \frac{y(\theta)\cos n\theta}{\sin\theta}\,d\theta, \quad n > 0 \end{aligned}\right\} \tag{E9}$$

where $y(\theta)$ is the airfoil ordinate corresponding to the abscissa and $\theta = 0$ corresponds to the leading edge of the airfoil.

$$x = \frac{c}{2}\cos\theta \tag{E10}$$

Equation (E1) corresponds to Goldstein's equation (97) (p. 48) of reference 4. The factor U/V has been inserted to reduce the isolated-airfoil velocity, Goldstein's q_1, from U to V as the free-stream velocity. Equations (E3) to (E6) correspond respectively to Goldstein's equations (40) (p. 37), (99) (p. 48), (21) (p. 34), and (100) (p. 48). Equations (E7) to (E10) correspond to those of appendix 5 (p. 21).

The basic constants C_n calculated in this paper are given in table X on the basis that the airfoil chord be 2.

The velocity distribution by conformal mapping was used for v_i/V in equations (E2) and (D2) because it had already been calculated. It would have been somewhat more consistent to use the velocity distributions derived by thin-airfoil theory inasmuch as the constants C_n (equation (E9)) were so derived. The differences between the two distributions, being of the orders $(t/c)^2$, $(t/c)^3$, . . ., do not affect the main contribution to the second order of Goldstein's results, namely, the contribution of the order tc^3/h^4.

It is noted that in applying equation (E3) to thin airfoils, Goldstein in his equation (75) (p. 45) neglects the term d_1^2. This term was not found to be negligible in the calculations of this paper and was retained.

APPENDIX F

STREAM-FILAMENT THEORY

The irrotational motion of an ideal incompressible fluid is completely determined by the equations of irrotationality and continuity of mass and by the boundary conditions. Consider the equation of irrotationality in the form (reference 6, equation (41))

$$\frac{\partial v}{\partial n} + \frac{v}{R} = 0 \tag{F1}$$

where

n distance along potential line at point of flow field

R radius of curvature of streamline at same point of flow field; positive if streamline is convex in positive n direction.

Introduce the approximations (a) that the potential lines are straight lines perpendicular to the x-axis, or

$$n = y \tag{F2}$$

and (b) that the curvature of the streamlines at any chordwise location varies linearly from its known value at the airfoil to the known value, 0, at the wall, or

$$1/R = C = C_a \frac{(h/2) - y}{(h/2) - Y} \qquad Y < y < h/2 \tag{F3}$$

where

C curvature of streamline at chordwise station X

C_a curvature of airfoil surface at chordwise station X

Y ordinate of airfoil at chordwise station X

The boundary condition that the boundaries be streamlines is satisfied by equation (F3). Substitution of equations (F2) and (F3) into (F1) and integration yields

$$v = F(x)e^{\frac{C_a}{2}\frac{(h/2-y)^2}{(h/2-Y)}}$$

where $F(x)$ is an arbitrary function fixed by the condition of continuity. Integrating equation (F4) with respect to y from Y to $h/2$ gives the flow quantity $(h/2)V$ to the approximation underlying equations (2) and (3); that is,

488

$$V \frac{h}{2} = \int_{Y}^{h/2} v dy = F(x) \int_{Y}^{h/2} e^{\frac{C_a}{2} \frac{(h/2-y)^2}{(h/2-Y)}} dy \qquad \text{(F5)}$$

When this equation is solved for $F(x)$ and substituted in equation (F4), there results for the velocity at any point of the flow field

$$\frac{v}{V} = \frac{h/2 \; e^{\frac{C_a}{2} \frac{(h/2-y)^2}{(h/2-Y)}}}{\int_{Y}^{h/2} e^{\frac{C_a}{2} \frac{(h/2-y)^2}{(h/2-Y)}} dy} \qquad \text{(F6)}$$

Expressing all lengths, including the radius of curvature, as fractions of airfoil chord c and making the substitutions

$$t = \sqrt{\frac{C_a}{4\sigma} \frac{(1-2\sigma y)^2}{1-2\sigma Y}} \qquad \text{(F7)}$$

and

$$T = \sqrt{\frac{C_a}{4\sigma} (1-2\sigma Y)} \qquad \text{(F8)}$$

where

$$\sigma = c/h$$

and

$$C_a = C_a(X) = \frac{d^2Y/dX^2}{\left[1 + \left(\frac{dY}{dX}\right)^2\right]^{3/2}} \qquad \text{(F9)}$$

equation (F6) becomes

488

$$\frac{v}{V} = \frac{Te^{T^2\left(\frac{1-2\sigma y}{1-2\sigma Y}\right)^2}}{(1 - 2\ Y)\int_0^T e^{t^2}dt} \tag{F10}$$

At the airfoil, equation (F10) gives finally

$$\left(\frac{v}{V}\right)_a = \frac{Te^{T^2}}{(1 - 2\sigma Y)\int_0^T e^{t^2}dt} \tag{F11}$$

If $C_a = 0$, equation (F6) reduces to the simplest form of stream-filament theory, namely

$$\frac{v}{V} = \frac{h/2}{h/2 - Y} \tag{F12}$$

Equations (F8), (F9), and (F11) were used for the calculation of the velocity distributions of the airfoil in the tunnel by the stream-filament theory. The integral in equation (F11) is tabulated in reference 7 (p. 32).

This method may be useful in determining the influence of compressibility. For an ideal compressible fluid, the only change required in equation (F10) or (F11) is the insertion of the factor ρ/ρ_o under the integral sign, where ρ is the density of the fluid and ρ_o is the ultimate upstream density.

REFERENCES

1. Mutterperl, William: The Conformal Transformation of an Airfoil into a Straight Line and Its Application to the Inverse Problem of Airfoil Theory. NACA ARR No. L4K22a, 1944.

2. Mutterperl, William: A Solution of the Direct and Inverse Potential Problems for Arbitrary Cascades of Airfoils. NACA ARR No. L4K22b, 1944.

3. Glauert, H.: Wind Tunnel Interference on Wings, Bodies, and Airscrews. R. & M. No. 1566, A.R.C., 1933.

4. Goldstein, S.: Steady Two-Dimensional Flow past a Solid Cylinder in a Non-Uniform Stream and Two-Dimensional Wind-Tunnel Interference. R. & M. No. 1902, M.A.P., 1942.

5. Kaplan, Carl: The Flow of a Compressible Fluid Past a Curved Surface. NACA ARR No. 3K02, 1943.

6. von Kármán, Th.: Compressibility Effects in Aerodynamics. Jour. Aero. Sci., vol. 8, no. 9, July 1941, pp. 337-356.

7. Jahnke, Eugene, and Emde, Fritz: Tables of Functions with Formulae and Curves. Dover Publications (New York), 1943.

488

TABLE I. - ORDINATES OF AIRFOILS

Station (percent chord from nose)	Ordinate of 12-percent-thick airfoil	Ordinate of 24-percent-thick airfoil	Station (percent chord from nose)	Ordinate of 12-percent-thick airfoil	Ordinate of 24-percent-thick airfoil
0	0	0	50	5.880	11.810
1.25	1.425	2.250	55	5.540	11.380
2.5	1.900	3.285	60	5.025	10.665
5	2.585	4.620	65	4.415	9.735
10	3.540	6.455	70	3.750	8.575
15	4.250	7.890	75	3.060	7.250
20	4.820	9.050	80	2.350	5.825
25	5.295	10.070	85	1.685	4.365
30	5.655	10.885	90	1.060	2.925
35	5.900	11.495	95	.510	1.605
40	6.000	11.855	97.5	.260	.950
45	6.010	11.980	100	0	0

TABLE II. - VELOCITY DISTRIBUTIONS AND CARTESIAN MAPPING

FUNCTIONS FOR 12-PERCENT-THICK AIRFOIL

(a) c/h, 0; method of finite chord; r, 1.0896; τ, 0.0243

φ (deg)	Percent chord	$\frac{v_i}{V}$	x	Δy	Δx	$\frac{d\Delta x}{d\varphi}$	$\frac{d\Delta y}{d\varphi}$
0 × 15	0	0	1.0000	0	-0.1139	0	0.1200
1	1.625	1.0436	.9675	.0312	-.1093	.0363	.1121
2	6.480	1.0834	.8704	.0578	-.0976	.0521	.1005
3	14.24	1.1136	.7151	.0837	-.0797	.0845	.0908
4	24.24	1.1303	.5151	.1045	-.0540	.1117	.0695
5	35.70	1.1574	.2861	.1186	-.0202	.1436	.0305
6	47.80	1.1690	.0441	.1195	.1098	.1582	-.0347
7	60.06	1.1191	-.2012	.1008	.0565	.1183	-.0999
8	72.11	1.0422	-.4422	.0693	.0783	.0465	-.1233
9	83.15	.9821	-.6630	.0389	.0832	-.0072	-.1032
10	92.08	.9400	-.8416	.0168	.0777	-.0309	-.0660
11	97.94	.8996	-.9588	.0042	.0694	-.0301	-.0300
12	100.00	0	-1.0000	0	.0653	0	-.0127

(b) c/h, 0.5; method of finite chord; cosh k, 1.43094; τ, 0.04158

φ (deg)	Percent chord	$\frac{v_c}{V}$	$\frac{x}{0.5\pi}$	$\frac{\Delta y}{0.5\pi}$	Δx	$\frac{d\Delta x}{d\varphi}$	$\frac{d\Delta y}{d\varphi}$
0 × 15	0	0	1.0000	0	-0.2008	0	0.2331
1	2.515	1.0792	.9497	.0381	-.1897	.0850	.2081
2	9.190	1.1087	.8162	.0682	-.1623	.1218	.1644
3	18.20	1.1284	.6360	.0925	-.1256	.1558	.1269
4	28.02	1.1543	.4396	.1103	-.0806	.1872	.0830
5	37.96	1.1714	.2409	.1195	-.0290	.2046	.0291
6	47.82	1.1843	.0436	.1195	.0269	.2182	-.0411
7	57.76	1.1485	-.1552	.1059	.0805	.1865	-.1205
8	68.08	1.0789	-.3616	.0805	.1200	.1123	-.1713
9	78.74	1.0150	-.5747	.0507	.1387	.0314	-.1762
10	88.94	.9614	-.7789	.0236	.1376	-.0362	-.1360
11	96.90	.9207	-.9379	.0062	.1250	-.0541	-.0675
12	100.00	0	-1.0000	0	.1177	0	-.0311

TABLE II. - VELOCITY DISTRIBUTIONS AND CARTESIAN MAPPING

FUNCTIONS FOR 12-PERCENT-THICK AIRFOIL - Continued

(c) c/h, 1.0; method of semi-infinite chord; c, 2; h, 2; n, 4

θ (deg)	Percent chord	$\frac{v_c}{V}$	x	φ (deg)	Δy	Δx	$\frac{d\Delta x}{d\varphi}$	$\frac{d\Delta y}{d\varphi}$
Front half of airfoil								
0 × 15	∞	1.0000	∞	0	0	-0.1088	0	0
1	95.70	.9607	0.9139	3.770	.0086	-.1214	-.3324	1.1276
2	73.04	1.0742	.4608	7.665	.0667	-.1232	.3682	.5940
3	60.81	1.1637	.2162	11.824	.0988	-.0924	.4510	.3130
4	52.16	1.2215	.0431	16.426	.1151	-.0573	.4040	.1207
5	44.92	1.2192	-.1015	21.718	.1203	-.0258	.2984	.0162
6	38.34	1.2117	-.2333	28.072	.1197	.0032	.2227	-.0212
7	31.88	1.2043	-.3625	36.092	.1153	.0299	.1668	-.0413
8	25.27	1.1842	-.4946	46.826	.1064	.0563	.1165	-.0519
9	18.16	1.1595	-.6367	62.226	.0924	.0814	.0756	-.0523
10	10.56	1.1398	-.7888	86.030	.0726	.1061	.0452	-.0446
11	3.390	1.1275	-.9322	124.456	.0434	.1283	.0251	-.0424
12	0	0	-1.0000	180.000	0	.1384	0	-.0473
Rear half of airfoil								
0 × 15	-∞	1.0000	∞	0	0	-0.1442	0	0
1	2.350	[a].9668	0.9530	3.770	.0368	-.1442	0	2.5559
2	23.64	[a]1.1938	.5273	7.665	.1039	-.1186	.7898	.3835
3	34.90	[a]1.2359	.3020	11.824	.1180	-.0686	.5881	.0842
4	43.40	1.2265	.1321	16.426	.1204	-.0302	.4073	-.0075
5	50.64	1.2145	-.0129	21.718	.1169	.0009	.2950	-.0731
6	57.26	1.1872	-.1453	28.072	.1065	.0293	.2061	-.1062
7	63.94	1.1367	-.2787	36.092	.0909	.0517	.1254	-.1092
8	70.98	1.0845	-.4197	46.826	.0721	.0692	.0636	-.0926
9	78.80	1.0382	-.5759	62.226	.0503	.0802	.0240	-.0679
10	87.44	.9922	-.7488	86.030	.0277	.0842	0	-.0428
11	95.94	.9591	-.9187	124.456	.0084	.0799	-.0063	-.0175
12	100.00	0	-1.0000	180.000	0	.0765	0	0

[a]Rejected points.

TABLE II. - VELOCITY DISTRIBUTIONS AND CARTESIAN MAPPING

FUNCTIONS FOR 12-PERCENT-THICK AIRFOIL - Continued

(d) c/h, 1.5; method of semi-infinite chord; c, 2; h, 4/3; n, 8

θ (deg)	Per cent chord	$\frac{v_c}{V}$	x	φ (deg)	Δy	Δx	$\frac{d\Delta x}{d\varphi}$	$\frac{d\Delta y}{d\varphi}$
Front half of airfoil								
0 × $7\frac{1}{2}$	∞	1.0000	∞	0	0	-0.1819	0	0
1	84.68	[a]1.0101	0.6936	.939	.0340	-.1785	.4875	3.4182
2	70.72	[a]1.1157	.4145	1.886	.0732	-.1623	1.4512	1.6175
3	63.24	[a]1.1943	.2647	2.849	.0929	-.1363	1.4400	.8547
4	58.09	1.2407	.1618	3.837	.1048	-.1130	1.2561	.5231
5	54.10	1.2699	.0820	4.859	.1123	-.0928	1.0758	.3162
6	50.82	1.2851	.0163	5.928	.1169	-.0744	.9134	.1643
7	47.93	1.2842	-.0414	7.055	.1191	-.0580	.7629	.0769
8	45.34	1.2747	-.0931	8.256	.1201	-.0432	.6339	.0332
9	42.93	1.2707	-.1414	9.549	.1203	-.0300	.5413	.0067
10	40.64	1.2717	-.1872	10.958	.1202	-.0175	.4726	-.0078
11	38.43	1.2731	-.2314	12.512	.1198	-.0055	.4155	-.0270
12	36.28	1.2736	-.2745	14.250	.1189	.0064	.3652	-.0360
13	34.12	1.2694	-.3175	16.224	.1175	.0181	.3169	-.0467
14	31.94	1.2640	-.3612	18.505	.1152	.0298	.2733	-.0502
15	29.68	1.2556	-.4064	21.192	.1129	.0415	.2326	-.0549
16	27.31	1.2443	-.4538	24.433	.1096	.0537	.1945	-.0573
17	24.75	1.2339	-.5050	28.447	.1053	.0660	.1611	-.0571
18	21.98	1.2245	-.5605	33.585	.1006	.0791	.1317	-.0566
19	18.87	1.2119	-.6226	40.431	.0939	.0930	.1038	-.0536
20	15.32	1.1960	-.6935	50.019	.0854	.1077	.0776	-.0481
21	11.25	1.1792	-.7750	64.292	.0748	.1238	.0544	-.0420
22	6.656	1.1658	-.8669	87.030	.0588	.1414	.0355	-.0376
23	2.175	1.1432	-.9565	124.660	.0359	.1586	.0202	-.0344
24	0	0	-1.0000	180.000	0	.1666	0	-.0404
Rear half of airfoil								
0 × $7\frac{1}{2}$	-∞	1.0000	∞	0	0	-0.2335	0	0
1	12.90	[a]1.1409	0.7420	.939	.0793	-.2066	3.3265	2.3963
2	25.22	[a]1.2399	.4955	1.886	.1064	-.1571	2.5341	.8991
3	32.14	[a]1.2787	.3571	2.849	.1156	-.1204	1.8673	.3051
4	37.14	1.2787	.2573	3.837	.1192	-.0938	1.3824	.1196
5	41.07	1.2631	.1786	4.859	.1203	-.0723	1.0420	.0359
6	44.38	1.2774	.1124	5.928	.1204	-.0543	.8901	-.0246
7	47.25	1.2879	.0550	7.055	.1198	-.0379	.7706	-.0716
8	49.84	1.2868	.0033	8.256	.1179	-.0229	.6580	-.1092
9	52.24	1.2776	-.0447	9.549	.1150	-.0093	.5564	-.1320
10	54.53	1.2604	-.0906	10.958	.1115	.0030	.4629	-.1433
11	56.76	1.2421	-.1352	12.512	.1075	.0146	.3844	-.1482
12	58.97	1.2257	-.1794	14.250	.1029	.0253	.3205	-.1487
13	61.20	1.2078	-.2241	16.224	.0976	.0353	.2647	-.1451
14	63.51	1.1891	-.2702	18.505	.0920	.0446	.2158	-.1373
15	65.90	1.1682	-.3181	21.192	.0861	.0537	.1717	-.1278
16	68.46	1.1466	-.3691	24.433	.0790	.0623	.1331	-.1152
17	71.22	1.1247	-.4245	28.447	.0715	.0703	.0998	-.1016
18	74.28	1.1028	-.4856	33.585	.0632	.0780	.0716	-.0876
19	77.72	1.0816	-.5545	40.431	.0534	.0850	.0485	-.0731
20	81.72	1.0504	-.6343	50.019	.0425	.0908	.0257	-.0579
21	86.40	1.0153	-.7279	64.292	.0300	.0948	.0076	-.0412
22	91.83	.9822	-.8366	87.030	.0170	.0956	-.0026	-.0256
23	97.31	.9559	-.9462	124.660	.0055	.0928	-.0046	-.0114
24	100.00	0	-1.0000	180.000	0	.0905	0	0

[a]Rejected points.

NACA

TABLE II. - VELOCITY DISTRIBUTIONS AND CARTESIAN MAPPING

FUNCTIONS FOR 12-PERCENT-THICK AIRFOIL - Concluded

(e) c/h, 2.0; method of semi-infinite chord; c, 2; h, 1; n, 15

θ (deg)	Percent chord	$\frac{v_c}{V}$	x	φ (deg)	Δy	Δx	$\frac{d\Delta x}{d\varphi}$	$\frac{d\Delta y}{d\varphi}$
	Front half of airfoil							
0 x $7\frac{1}{2}$	∞	1.0000	∞	0	0	-0.2458	0	0
1	66.28	[a]1.1998	0.3255	.501	.0849	-.2152	6.4838	5.0200
2	57.80	[a]1.3457	.1560	1.006	.1055	-.1626	4.7171	1.2607
3	52.94	[a]1.3765	.0588	1.520	.1140	-.1285	3.3077	.6595
4	49.44	1.3710	-.0112	2.047	.1181	-.1037	2.4177	.2982
5	46.71	1.3692	-.0658	2.593	.1200	-.0830	1.8974	.0902
6	44.39	1.3742	-.1122	3.164	.1203	-.0662	1.5696	.0308
7	42.35	1.3647	-.1530	3.766	.1204	-.0515	1.2936	-.0036
8	40.50	1.3537	-.1901	4.408	.1202	-.0385	1.0805	-.0315
9	38.78	1.3443	-.2244	5.101	.1199	-.0263	.9154	-.0426
10	37.16	1.3501	-.2568	5.857	.1193	-.0148	.8074	-.0521
11	35.60	1.3446	-.2880	6.692	.1185	-.0036	.6985	-.0579
12	34.06	1.3484	-.3188	7.628	.1174	.0072	.6185	-.0768
13	32.52	1.3525	-.3496	8.694	.1160	.0180	.5477	-.0813
14	30.94	1.3439	-.3811	9.931	.1143	.0287	.4710	-.0773
15	29.31	1.3340	-.4138	11.396	.1123	.0397	.4017	-.0739
16	27.58	1.3216	-.4485	13.174	.1100	.0510	.3386	-.0813
17	25.70	1.3118	-.4860	15.398	.1070	.0629	.2830	-.0750
18	23.62	1.2931	-.5275	18.286	.1036	.0757	.2272	-.0676
19	21.26	1.2871	-.5749	22.222	.0990	.0898	.1838	-.0620
20	18.46	1.2642	-.6309	27.943	.0939	.1055	.1368	-.0560
21	15.00	1.2476	-.7001	37.058	.0849	.1237	.0974	-.0485
22	10.52	1.2381	-.7896	53.714	.0722	.1462	.0636	-.0399
23	4.645	1.1758	-.9071	90.974	.0500	.1740	.0271	-.0314
24	0	0	-1.0000	180.000	0	.1887	0	-.0344
	Rear half of airfoil							
0 x $7\frac{1}{2}$	$-\infty$	1.0000	∞	0	0	-0.2660	0	0
1	29.70	[a]1.3950	0.4061	.501	.1127	-.2194	10.3834	1.9169
2	37.16	[a]1.3927	.2567	1.006	.1192	-.1468	5.1175	.3331
3	41.90	[a]1.3449	.1621	1.520	.1204	-.1100	3.0781	.0306
4	45.42	1.3684	.0916	2.047	.1201	-.0857	2.3995	-.0963
5	48.14	1.3756	.0372	2.593	.1192	-.0649	1.9233	-.1709
6	50.47	1.3689	-.0094	3.164	.1171	-.0481	1.5591	-.2245
7	52.50	1.3469	-.0499	3.766	.1147	-.0332	1.2544	-.2347
8	54.36	1.3365	-.0872	4.408	.1119	-.0204	1.0506	-.2437
9	56.09	1.3193	-.1218	5.101	.1089	-.0085	.8769	-.2580
10	57.76	1.3013	-.1551	5.857	.1054	.0021	.7338	-.2531
11	59.38	1.2876	-.1875	6.692	.1020	.0121	.6218	-.2409
12	61.00	1.2764	-.2199	7.628	.0981	.0213	.5303	-.2237
13	62.63	1.2499	-.2526	8.694	.0942	.0302	.4312	-.2048
14	64.32	1.2362	-.2863	9.931	.0900	.0387	.3618	-.1864
15	66.08	1.2182	-.3215	11.396	.0854	.0472	.2965	-.1677
16	67.96	1.2010	-.3592	13.174	.0805	.0555	.2415	-.1569
17	70.01	1.1830	-.4002	15.398	.0748	.0639	.1919	-.1388
18	72.32	1.1624	-.4464	18.286	.0684	.0720	.1459	-.1148
19	74.96	1.1336	-.4992	22.222	.0613	.0806	.1024	-.0988
20	78.13	1.1045	-.5626	27.943	.0523	.0890	.0662	-.0813
21	82.10	1.0737	-.6420	37.058	.0413	.0971	.0364	-.0578
22	87.38	1.0321	-.7476	53.714	.0278	.1034	.0120	-.0367
23	94.57	.9826	-.8914	90.974	.0111	.1049	-.0018	-.0173
24	100.00	0	-1.0000	180.000	0	.1039	0	0

[a]Rejected points.

NACA

TABLE III. - VELOCITY DISTRIBUTIONS AND CARTESIAN MAPPING

FUNCTIONS FOR 24-PERCENT-THICK AIRFOIL

(a) c/h, 0; method of finite chord; r, 1.1855; τ, 0.0317

488

φ (deg)	Percent chord	$\frac{v_i}{V}$	x	Δy	Δx	$\frac{d\Delta x}{d\varphi}$	$\frac{d\Delta y}{d\varphi}$
0 × 15	0	0	1.0000	0	-0.2172	0	0.2103
1	1.720	.9233	.9656	.0542	-.2112	.0460	.2059
2	6.735	1.1013	.8653	.1067	-.1931	.0922	.1977
3	14.64	1.1634	.7071	.1564	-.1629	.1412	.1825
4	24.64	1.2297	.5071	.2002	-.1173	.2055	.1509
5	35.84	1.2962	.2832	.2314	-.0553	.2654	.0818
6	47.42	1.3361	.0517	.2388	.0200	.2986	-.0267
7	59.10	1.2682	-.1820	.2164	.0931	.2531	-.1400
8	70.60	1.1594	-.4119	.1683	.1491	.1682	-.2174
9	81.49	1.0178	-.6298	.1078	.1768	.0477	-.2308
10	90.92	.9019	-.8184	.0536	.1766	-.0406	-.1756
11	97.54	.8217	-.9508	.0188	.1626	-.0546	-.0939
12	100.00	0	-1.0000	0	.1538	0	-.0569

(b) c/h, 0.5; method of finite chord; cosh k, 1.34708; τ, 0.05243

φ (deg)	Percent chord	$\frac{v_c}{V}$	$\frac{x}{0.5\pi}$	$\frac{\Delta y}{0.5\pi}$	Δx	$\frac{d\Delta x}{d\varphi}$	$\frac{d\Delta y}{d\varphi}$
0 × 15	0	0	1.0000	0	-0.3930	0	0.4310
1	2.855	1.0375	.9429	.0705	-.3744	.1396	.3961
2	10.14	1.1600	.7972	.1302	-.3263	.2248	.3276
3	19.42	1.2225	.6115	.1787	-.2581	.2918	.2566
4	29.04	1.2954	.4193	.2151	-.1733	.3530	.1721
5	38.38	1.3442	.2325	.2353	-.0763	.3837	.0719
6	47.50	1.3602	.0500	.2386	.0261	.3938	-.0362
7	56.68	1.2302	-.1335	.2232	.1270	.3713	-.1506
8	66.24	1.2304	-.3248	.1888	.2169	.3085	-.2645
9	76.46	1.1082	-.5291	.1370	.2826	.1893	-.3504
10	87.08	.9768	-.7415	.0757	.3090	.0157	-.3411
11	96.20	.8790	-.9240	.0262	.2992	-.0807	-.2236
12	100.00	0	-1.0000	0	.2882	0	-.1468

NACA

TABLE II. - VELOCITY DISTRIBUTIONS AND CARTESIAN MAPPING FUNCTIONS FOR 24-PERCENT-THICK AIRFOIL - Continued

(c) c/h, 1.0; method of semi-infinite chord; c, 2; h, 2; n, 6

θ (deg)	Percent chord	$\frac{v_c}{V}$	x	φ (deg)	Δy	Δx	$\frac{d\Delta x}{d\varphi}$	$\frac{d\Delta y}{d\varphi}$
Front half of airfoil								
$0 \times 7\frac{1}{2}$	∞	1.0000	∞	0	0	-0.2370	0	0
1	115.6	[a].9661	1.3125	1.252	0	-.2574	-1.0231	0
2	92.24	[a].8895	.8449	2.514	.0471	-.2811	-1.0200	4.9886
3	79.28	[a]1.1239	.5856	3.798	.1221	-.2778	1.4057	2.4101
4	71.70	[a]1.2656	.4340	5.114	.1640	-.2400	1.6663	1.3743
5	66.07	1.3231	.3214	6.476	.1899	-.2025	1.4736	.9146
6	61.44	1.3662	.2289	7.898	.2081	-.1687	1.2873	.5854
7	57.54	1.4146	.1509	9.397	.2208	-.1363	1.1610	.3766
8	54.09	1.4469	.0818	10.993	.2297	-.1059	1.0337	.2339
9	50.94	1.4652	.0188	12.709	.2350	-.0768	.9129	.1458
10	47.98	1.4733	-.0405	14.576	.2383	-.0493	.8010	.0684
11	45.14	1.4769	-.0971	16.631	.2396	-.0224	.7032	.0104
12	42.37	1.4745	-.1526	18.925	.2389	.0037	.6148	-.0277
13	39.60	1.4674	-.2079	21.521	.2368	.0294	.5351	-.0608
14	36.80	1.4554	-.2640	24.509	.2330	.0549	.4620	-.0827
15	33.91	1.4346	-.3218	28.012	.2276	.0806	.3921	-.0984
16	30.87	1.4059	-.3826	32.204	.2201	.1066	.3258	-.1078
17	27.62	1.3730	-.4475	37.347	.2104	.1332	.2651	-.1121
18	24.10	1.3468	-.5180	43.837	.1980	.1603	.2142	-.1102
19	20.20	1.3152	-.5961	52.301	.1819	.1880	.1669	-.1060
20	15.85	1.2832	-.6830	63.764	.1621	.2163	.1246	-.0958
21	11.09	1.2482	-.7782	79.919	.1365	.2456	.0879	-.0858
22	6.130	1.1717	-.8774	103.388	.1018	.2739	.0526	-.0806
23	1.835	1.0333	-.9633	137.064	.0561	.2966	.0306	-.0758
24	0	0	-1.0000	180.000	0	.3056	0	-.0738
Rear half of airfoil								
$0 \times 7\frac{1}{2}$	-∞	1.0000	∞	0	0	-0.2733	0	0
1	-17.43	[a].9558	1.3486	1.252	0	-.3040	-1.3465	0
2	5.740	[a].9243	.8852	2.514	.1001	-.3234	0	5.9909
3	16.71	[a]1.3396	.6658	3.798	.1677	-.2803	2.6010	1.5367
4	23.56	[a]1.3535	.5287	5.114	.1959	-.2281	1.9476	.9475
5	29.04	[a]1.3767	.4193	6.476	.2144	-.1872	1.5893	.6356
6	33.48	[a]1.4015	.3303	7.898	.2264	-.1500	1.3419	.3701
7	37.32	[a]1.4374	.2537	9.397	.2338	-.1162	1.1847	.1831
8	40.72	[a]1.4570	.1856	10.993	.2378	-.0848	1.0391	.0856
9	43.86	[a]1.4662	.1227	12.709	.2395	-.0556	.9090	.0225
10	46.81	[a]1.4634	.0638	14.576	.2391	-.0276	.7888	-.0406
11	49.65	1.4686	.0070	16.631	.2368	-.0010	.6973	-.0843
12	52.44	1.4596	-.0487	18.925	.2328	.0249	.6066	-.1162
13	55.22	1.4439	-.1045	21.521	.2272	.0501	.5230	-.1371
14	58.06	1.4202	-.1612	24.509	.2197	.0751	.4447	-.1512
15	61.01	1.3814	-.2202	28.012	.2100	.0996	.3679	-.1690
16	64.13	1.3430	-.2826	32.204	.1982	.1239	.2984	-.1653
17	67.50	1.3070	-.3501	37.347	.1833	.1478	.2398	-.1626
18	71.21	1.2558	-.4242	43.837	.1656	.1714	.1817	-.1594
19	75.38	1.1933	-.5076	52.301	.1429	.1937	.1250	-.1462
20	80.18	1.1161	-.6036	63.764	.1153	.2130	.0715	-.1282
21	85.72	1.0334	-.7145	79.919	.0832	.2265	.0257	-.0985
22	91.88	.9658	-.8377	103.388	.0480	.2309	0	-.0675
23	97.54	.8979	-.9507	137.064	.0189	.2265	-.0092	-.0371
24	100.00	0	-1.0000	180.000	0	.2230	0	0

[a]Rejected points.

TABLE III. - VELOCITY DISTRIBUTIONS AND CARTESIAN MAPPING FUNCTIONS FOR 24-PERCENT-THICK AIRFOIL - Continued

(d) c/h, 1.5; method of semi-infinite chord; c, 2; h, 4/3; n, 8

θ (deg)	Percent chord	$\frac{V_c}{V}$	x	φ (deg)	Δy	Δx	$\frac{d\Delta x}{d\varphi}$	$\frac{d\Delta y}{d\varphi}$
Front half of airfoil								
$0 \times 7\frac{1}{2}$	∞	1.0000	∞	0	0	-0.4634	0	0
1	74.50	[a]1.2438	0.4900	.626	.1477	-.4140	8.7854	8.4772
2	63.92	[a]1.5358	.2784	1.257	.1997	-.3236	7.0656	2.8107
3	58.32	[a]1.5987	.1664	1.899	.2189	-.2569	4.8956	1.2701
4	54.29	[a]1.6524	.0858	2.558	.2292	-.2086	3.7931	.6855
5	51.17	[a]1.6718	.0234	3.241	.2348	-.1686	3.0286	.3554
6	48.56	[a]1.6763	-.0289	3.954	.2379	-.1348	2.4837	.1598
7	46.29	1.6684	-.0742	4.706	.2393	-.1046	2.0691	.0510
8	44.23	1.6617	-.1154	5.509	.2395	-.0776	1.7564	-.0144
9	42.34	1.6654	-.1533	6.374	.2389	-.0525	1.5237	-.0673
10	40.52	1.6613	-.1896	7.318	.2375	-.0290	1.3234	-.0986
11	38.76	1.6633	-.2247	8.360	.2356	-.0065	1.1618	-.1159
12	37.04	1.6600	-.2593	9.527	.2334	.0154	1.0180	-.1299
13	35.30	1.6441	-.2939	10.856	.2303	.0371	.8818	-.1369
14	33.53	1.6197	-.3294	12.396	.2267	.0589	.7562	-.1436
15	31.68	1.6023	-.3664	14.218	.2221	.0810	.6494	-.1441
16	29.71	1.5813	-.4058	16.426	.2168	.1038	.5515	-.1426
17	27.57	1.5582	-.4486	19.183	.2102	.1276	.4619	-.1388
18	25.20	1.5281	-.4960	22.750	.2022	.1532	.3769	-.1304
19	22.48	1.4856	-.5505	27.586	.1916	.1809	.2953	-.1209
20	19.24	1.4333	-.6151	34.552	.1777	.2114	.2182	-.1058
21	15.27	1.3815	-.6946	45.462	.1590	.2459	.1513	-.0907
22	10.26	1.3382	-.7949	64.666	.1309	.2864	.0962	-.0750
23	4.130	1.2114	-.9174	103.629	.0840	.3306	.0444	-.0631
24	0	0	-1.0000	180.000	0	.3524	0	-.0664
Rear half of airfoil								
$0 \times 7\frac{1}{2}$	$-\infty$	1.0000	∞	0	0	-0.5031	0	0
1	21.64	[a]1.4721	0.5672	.626	.1879	-.4314	13.2430	6.3899
2	30.83	[a]1.7148	.3834	1.257	.2200	-.3132	8.1650	1.5171
3	36.26	[a]1.6763	.2749	1.899	.2320	-.2431	5.1959	.6839
4	40.26	[a]1.6823	.1948	2.558	.2372	-.1942	3.8646	.3391
5	43.32	[a]1.6921	.1335	3.241	.2394	-.1530	3.0691	.0925
6	45.94	1.6674	.0812	3.954	.2394	-.1192	2.4612	-.0549
7	48.19	1.6621	.0362	4.706	.2382	-.0889	2.0595	-.1218
8	50.26	1.6608	-.0053	5.509	.2361	-.0622	1.7591	-.1478
9	52.18	1.6477	-.0435	6.374	.2333	-.0373	1.5062	-.1939
10	54.02	1.6361	-.0803	7.318	.2300	-.0143	1.3015	-.2123
11	55.78	1.6222	-.1155	8.360	.2261	.0080	1.1275	-.2216
12	57.54	1.6049	-.1507	9.527	.2213	.0293	.9759	-.2254
13	59.30	1.5798	-.1861	10.856	.2160	.0503	.8382	-.2285
14	61.14	1.5539	-.2228	12.396	.2097	.0709	.7170	-.2263
15	63.05	1.5252	-.2610	14.218	.2027	.0918	.6086	-.2238
16	65.10	1.4869	-.3021	16.426	.1943	.1129	.5056	-.2174
17	67.34	1.4427	-.3468	19.183	.1843	.1347	.4105	-.2076
18	69.87	1.3967	-.3974	22.750	.1723	.1572	.3239	-.1900
19	72.78	1.3566	-.4557	27.586	.1572	.1811	.2507	-.1714
20	76.32	1.2716	-.5265	34.552	.1376	.2054	.1662	-.1468
21	80.80	1.1723	-.6160	45.462	.1117	.2299	.0916	-.1205
22	86.82	1.0763	-.7365	64.666	.0770	.2502	.0360	-.0863
23	94.77	.9593	-.8954	103.629	.0333	.2580	0	-.0491
24	100.00	0	-1.0000	180.000	0	.2577	0	0

[a]Rejected points.

NACA

TABLE III. - VELOCITY DISTRIBUTIONS AND CARTESIAN MAPPING FUNCTIONS FOR 24-PERCENT-THICK AIRFOIL - Concluded

(e) c/h, 2.0; method of semi-infinite chord; c, 2; h, 1; n, 30

θ (deg)	Percent chord	$\frac{v_c}{V}$	x	φ (deg)	Δy	Δx	$\frac{d\Delta x}{d\varphi}$	$\frac{d\Delta y}{d\varphi}$
Front half of airfoil								
0 × 7½	∞	1.0000	∞	0	0	-0.5528	0	0
1	54.02	[a]2.9318	0.0805	.250	.2298	-.4566	48.0667	1.9118
2	50.26	[a]2.4921	.0053	.503	.2361	-.3098	21.7485	1.0144
3	47.18	2.0095	-.0564	.760	.2389	-.2401	12.0661	.4444
4	44.74	2.0103	-.1052	1.024	.2396	-.1941	8.9548	.0168
5	42.93	2.0025	-.1414	1.297	.2391	-.1550	7.0434	-.1671
6	41.30	1.9859	-.1739	1.582	.2381	-.1242	5.7267	-.2203
7	39.94	1.9569	-.2012	1.884	.2370	-.0960	4.7407	-.2510
8	38.65	1.9564	-.2270	2.205	.2355	-.0716	4.0515	-.2701
9	37.48	1.9472	-.2503	2.552	.2340	-.0485	3.4861	-.2747
10	36.35	1.9430	-.2730	2.930	.2322	-.0272	3.0307	-.2645
11	35.27	1.9505	-.2946	3.349	.2303	-.0063	2.6647	-.2546
12	34.18	1.9379	-.3165	3.818	.2280	.0136	2.3231	-.2463
13	33.09	1.9070	-.3382	4.354	.2258	.0336	2.0049	-.2429
14	31.97	1.8601	-.3606	4.975	.2230	.0536	1.7098	-.2479
15	30.80	1.8257	-.3840	5.712	.2200	.0742	1.4593	-.2395
16	29.55	1.8080	-.4090	6.609	.2166	.0956	1.2492	-.2288
17	28.19	1.7828	-.4362	7.734	.2123	.1184	1.0517	-.2164
18	26.66	1.7531	-.4667	9.202	.2074	.1431	.8667	-.1959
19	24.88	1.7156	-.5023	11.217	.2010	.1704	.6916	-.1709
20	22.76	1.6762	-.5448	14.182	.1928	.2022	.5312	-.1510
21	19.97	1.6100	-.6006	19.026	.1810	.2393	.3754	-.1347
22	16.14	1.5680	-.6771	28.416	.1632	.2887	.2396	-.0971
23	10.28	1.4955	-.7944	53.913	.1309	.3667	.1118	-.0576
24	0	0	-1.0000	180.000	0	.4129	0	-.1019
Rear half of airfoil								
0 × 7½	-∞	1.0000	∞	0	0	-0.5504	0	0
1	40.56	[a]6.4445	0.1887	.250	.2377	-.4492	61.6136	1.3365
2	44.00	[a]2.4479	.1199	.503	.2396	-.2960	21.4506	0
3	47.02	2.0071	.0597	.760	.2389	-.2249	12.0523	-.4346
4	49.48	1.9861	.0105	1.024	.2368	-.1793	8.8597	-.4759
5	51.30	1.9730	-.0260	1.297	.2345	-.1405	6.9538	-.5004
6	52.95	1.9658	-.0590	1.582	.2318	-.1102	5.6857	-.5122
7	54.34	1.9234	-.0869	1.884	.2290	-.0825	4.6755	-.5214
8	55.66	1.8777	-.1132	2.205	.2262	-.0588	3.8962	-.5177
9	56.86	1.8665	-.1372	2.552	.2229	-.0362	3.3512	-.5084
10	58.04	1.8667	-.1608	2.930	.2197	-.0158	2.9249	-.4875
11	59.16	1.8613	-.1833	3.349	.2162	.0042	2.5560	-.4616
12	60.31	1.8437	-.2062	3.818	.2126	.0230	2.2225	-.4400
13	61.44	1.8095	-.2289	4.354	.2086	.0421	1.9108	-.4153
14	62.64	1.7660	-.2528	4.975	.2041	.0606	1.6263	-.3910
15	63.88	1.7268	-.2776	5.712	.1994	.0798	1.3804	-.3713
16	65.21	1.6881	-.3042	6.609	.1940	.0995	1.1604	-.3446
17	66.67	1.6515	-.3334	7.734	.1873	.1203	.9645	-.3166
18	68.34	1.6074	-.3667	9.202	.1797	.1422	.7827	-.2932
19	70.27	1.5614	-.4054	11.217	.1701	.1664	.6165	-.2629
20	72.65	1.5014	-.4530	14.182	.1580	.1931	.4565	-.2214
21	75.74	1.4235	-.5147	19.026	.1410	.2243	.3065	-.1772
22	80.21	1.2813	-.6042	28.416	.1150	.2607	.1560	-.1318
23	88.20	1.0860	-.7639	53.913	.0690	.2963	.0362	-.0803
24	100.00	0	-1.0000	180.000	0	.3120	0	0

[a]Rejected points.

TABLE IV. - LOCAL CONSTRICTION CORRECTIONS $\Delta v/V$ FOR 12-PERCENT-THICK AIRFOIL

Percent chord	Conformal-mapping correction, c/h				First-order image correction, c/h				Percent chord	Second-order image correction, c/h			
	0.5	1.0	1.5	2.0	0.5	1.0	1.5	2.0		0.5	1.0	1.5	2.0
0	0	0	0	0	0	0	0	0	0	0	0	0	0
5.0	.020	.058	.085	.118	.0124	.0516	.1193	.2183	.7595	.0094	.0249	.0029	-.1475
10.0	.012	.040	.075	.137	.0128	.0529	.1224	.2240	3.016	.0098	.0277	.0140	-.1141
15.0	.009	.038	.080	.133	.0129	.0536	.1241	.2270	6.698	.0103	.0316	.0315	-.0584
20.0	.010	.043	.091	.151	.0130	.0540	.1250	.2286	11.70	.0108	.0362	.0534	.0130
25.0	.014	.050	.103	.173	.0131	.0544	.1260	.2305	17.86	.0111	.0409	.0764	.0899
30.0	.013	.055	.112	.193	.0133	.0550	.1272	.2327	25.00	.0115	.0451	.0978	.1611
35.0	.010	.053	.116	.194	.0134	.0556	.1287	.2354	32.90	.0118	.0488	.1152	.2180
40.0	.008	.047	.102	.182	.0135	.0562	.1300	.2378	41.32	.0122	.0513	.1259	.2514
45.0	.011	.048	.104	.199	.0136	.0563	.1303	.2384	50.00	.0121	.0510	.1250	.2493
50.0	.016	.055	.121	.204	.0135	.0560	.1297	.2372	58.68	.0116	.0478	.1120	.2099
55.0	.018	.054	.113	.183	.0133	.0552	.1277	.2335	67.10	.0109	.0422	.0896	.1419
60.0	.014	.047	.099	.160	.0130	.0539	.1247	.2280	75.00	.0101	.0362	.0634	.0601
65.0	.014	.043	.088	.145	.0126	.0523	.1210	.2213	82.14	.0095	.0302	.0363	-.0270
70.0	.014	.040	.080	.128	.0122	.0507	.1174	.2148	88.30	.0089	.0247	.0103	-.1117
75.0	.014	.038	.073	.112	.0119	.0492	.1139	.2083	93.30	.0084	.0198	-.0124	-.1852
80.0	.012	.033	.062	.093	.0116	.0480	.1110	.2030	96.98	.0080	.0159	-.0297	-.2405
85.0	.010	.027	.049	.075	.0113	.0469	.1085	.1985	-------	------	------	------	------
90.0	.005	.030	.042	.061	.0110	.0457	.1057	.1934	-------	------	------	------	------
95.0	.009	.041	.045	.059	.0107	.0443	.1025	.1875	-------	------	------	------	------

TABLE V. - LOCAL CONSTRICTION CORRECTIONS $\Delta v/V$ FOR 24-PERCENT-THICK AIRFOILS

Percent chord	Conformal-mapping correction				First-order image correction				Percent chord	Second-order image correction			
	c/h				c/h					c/h			
	0.5	1.0	1.5	2.0	0.5	1.0	1.5	2.0		0.5	1.0	1.5	2.0
0	0	0	0	0	0	0	0	0	0	0	0	0	0
5.0	.030	.067	.175	------	.0291	.1251	.3057	.5859	.7595	.0136	.0303	-.0429	-.4470
10.0	.029	.108	.206	.363	.0306	.1314	.3211	.6153	3.016	.0190	.0467	-.0293	-.5020
15.0	.027	.113	.214	.386	.0316	.1356	.3313	.6349	6.698	.0211	.0593	.0170	-.3633
20.0	.028	.115	.245	.430	.0325	.1397	.3413	.6540	11.70	.0225	.0724	.0794	-.1458
25.0	.033	.122	.289	.488	.0334	.1434	.3504	.6714	17.86	.0241	.0871	.1501	.1012
30.0	.038	.136	.323	.558	.0342	.1469	.3589	.6878	25.00	.0257	.1020	.2212	.3482
35.0	.038	.150	.348	.650	.0350	.1503	.3672	.7036	32.90	.0272	.1153	.2831	.5612
40.0	.032	.151	.347	.645	.0357	.1534	.3748	.7183	41.32	.0286	.1254	.3268	.7067
45.0	.024	.140	.330	.675	.0362	.1555	.3800	.7281	50.00	.0287	.1268	.3344	.7341
50.0	.029	.144	.334	.656	.0359	.1543	.3771	.7227	58.68	.0273	.1179	.3002	.6282
55.0	.034	.146	.331	.596	.0352	.1512	.3694	.7080	67.10	.0252	.1034	.2398	.4322
60.0	.032	.138	.311	.590	.0341	.1467	.3583	.6867	75.00	.0227	.0856	.1650	.1877
65.0	.027	.122	.275	.480	.0329	.1414	.3455	.6622	82.14	.0201	.0673	.0887	-.0602
70.0	.020	.105	.230	.404	.0316	.1356	.3313	.6349	88.30	.0180	.0516	.0218	-.2804
75.0	.020	.091	.194	.335	.0299	.1286	.3143	.6022	93.30	.0163	.0390	-.0322	-.4591
80.0	.023	.082	.163	.265	.0281	.1208	.2952	.5657	96.98	.0150	.0299	-.0709	-.5858
85.0	.030	.077	.137	.194	.0263	.1131	.2764	.5297	-------	------	------	------	------
90.0	.031	.072	.116	.135	.0247	.1062	.2594	.4970	-------	------	------	------	------
95.0	.037	.074	.103	------	.0231	.0992	.2423	.4643	-------	------	------	------	------

NACA

TABLE VI. - AVERAGE CONSTRICTION CORRECTIONS

Method	c/h	12-percent-thick airfoil	24-percent-thick airfoil	10-percent Kaplan section
Conformal-mapping correction	0.5	0.0123	0.0294	0.0085
	1.0	.0444	.1199	.0305
	1.5	.0907	.2642	----------
	2.0	.1511	.4731	.1033
First-order image correction	0.5	0.0131	0.0324	----------
	1.0	.0534	.1397	----------
	1.5	.1226	.3406	----------
	2.0	.2250	.6538	----------
Second-order image correction	0.5	0.0110	0.0252	----------
	1.0	.0426	.0994	----------
	1.5	.0877	.2186	----------
	2.0	.1330	.3555	----------

TABLE VII. - CONJUGATE AND DERIVATIVE COEFFICIENTS FOR 24-POINT SCHEME

k	Conjugate coefficients a_k	Derivative coefficients b_k	k	Conjugate coefficients a_k	Derivative coefficients b_k
0	0	-4.95445	12	0	0.02778
1	-.42564	1.63040	13	.00366	.01413
2	-.20734	.41467	14	.01489	.02977
3	-.06706	.09484	15	.01151	.01627
4	-.09623	.11111	16	.03208	.03704
5	-.03620	.03748	17	.02131	.02207
6	-.05556	.05556	18	.05556	.05556
7	-.02131	.02207	19	.03620	.03748
8	-.03208	.03704	20	.09623	.11111
9	-.01151	.01627	21	.06706	.09484
10	-.01489	.02977	22	.20734	.41467
11	-.00366	.01413	23	.42564	1.63040

TABLE VIII. - CONJUGATE AND DERIVATIVE COEFFICIENTS FOR 48-POINT SCHEME

k	Conjugate coefficients a_k	Derivative coefficients b_k	k	Conjugate coefficients a_k	Derivative coefficients b_k
0	0	-9.90891	24	0	0.01389
1	-.42470	3.24694	25	.00091	.00697
2	-.21099	.81517	26	.00366	.01413
3	-.06982	.18246	27	.00276	.00722
4	-.10367	.20733	28	.00744	.01489
5	-.04092	.06721	29	.00472	.00774
6	-.06706	.09484	30	.01151	.01627
7	-.02816	.03550	31	.00685	.00863
8	-.04811	.05556	32	.01604	.01852
9	-.02079	.02250	33	.00928	.01004
10	-.03620	.03748	34	.02132	.02207
11	-.01584	.01597	35	.01218	.01229
12	-.02778	.02778	36	.02778	.02778
13	-.01218	.01229	37	.01584	.01597
14	-.02132	.02207	38	.03620	.03748
15	-.00928	.01004	39	.02079	.02250
16	-.01604	.01852	40	.04811	.05556
17	-.00685	.00863	41	.02816	.03550
18	-.01151	.01627	42	.06706	.09484
19	-.00472	.00774	43	.04092	.06721
20	-.00744	.01489	44	.10367	.20733
21	-.00276	.00722	45	.06982	.18246
22	-.00366	.01413	46	.21099	.81517
23	-.00091	.00697	47	.42470	3.24694

TABLE IX. - CRITICAL MACH NUMBER OF ISOLATED AIRFOIL
[By equation (65), fig. 13, reference 7]

Method	t/h	c/h	$\frac{tc}{h^2}$	Critical Mach number: 12-percent-thick airfoil	Critical Mach number: 24-percent-thick airfoil
First-order image correction	0.06	0.5	0.03	0.74	0.63
	.12	1.0	.12	.75	.63
	.18	1.5	.27	.76	.65
	.24	2.0	.48	.78	.65
Second-order image correction	0.12	0.5	0.06	0.74	0.62
	.24	1.0	.24	.74	.61
	.36	1.5	.54	.75	.62
	.48	2.0	.96	.79	.68
Conformal-mapping correction-------------------				0.74	0.62

NACA

488

TABLE X. - CONSTANTS USED IN FIRST- AND SECOND-ORDER IMAGE CORRECTIONS

(a) Constants λ used in the first-order corrections

c/h	λ	
	12-percent-thick airfoil	24-percent-thick airfoil
0	3.89	2.24
.5	3.93	2.29
1.0	4.06	2.45
1.5	4.18	2.67
2.0	4.30	2.88

(b) Constants C_n used in second-order correction, c = 2

	C_n	
	12-percent-thick airfoil	24-percent-thick airfoil
C_0	0.08722	0.17157
C_1	.05534	.07177
C_2	-.02401	-.06306
C_3	.00455	.00158
C_4	.00475	-.00224

NACA

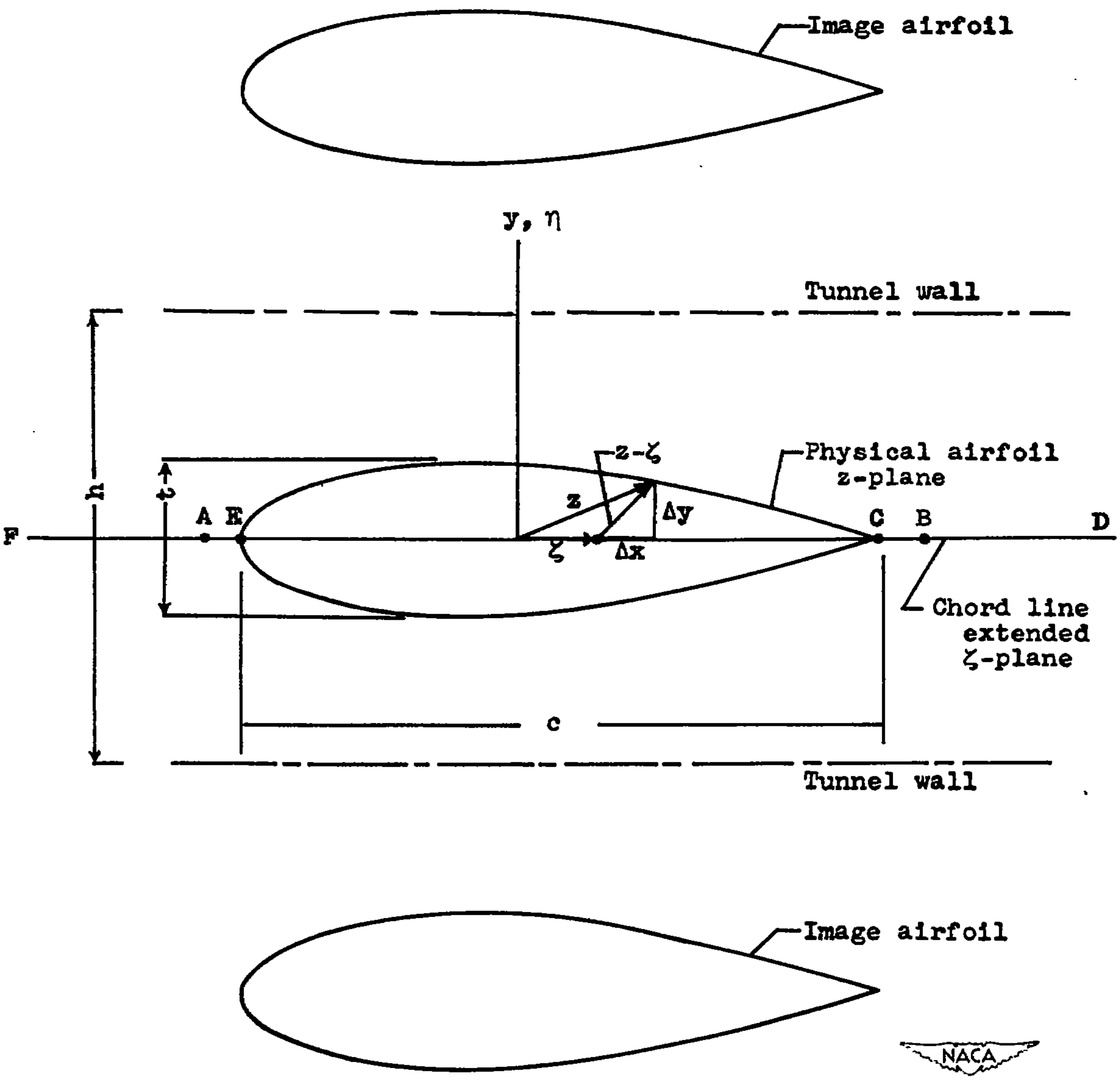

Figure 1.- Representation of symmetrical airfoil in two-dimensional tunnel as unstaggered cascade of airfoils; only three airfoils of cascade shown.

488

488

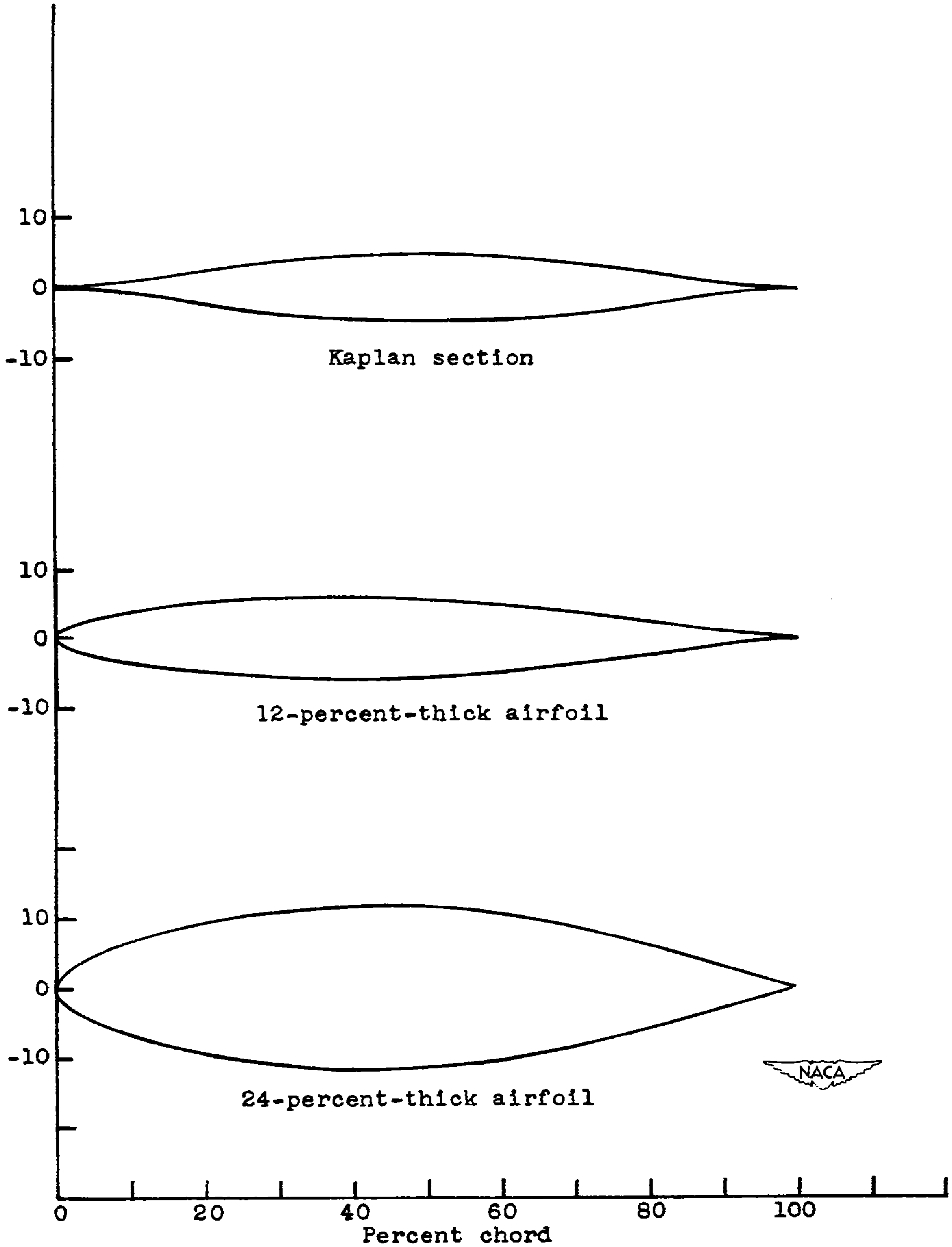

Figure 2.- Airfoil sections for which calculations were made.

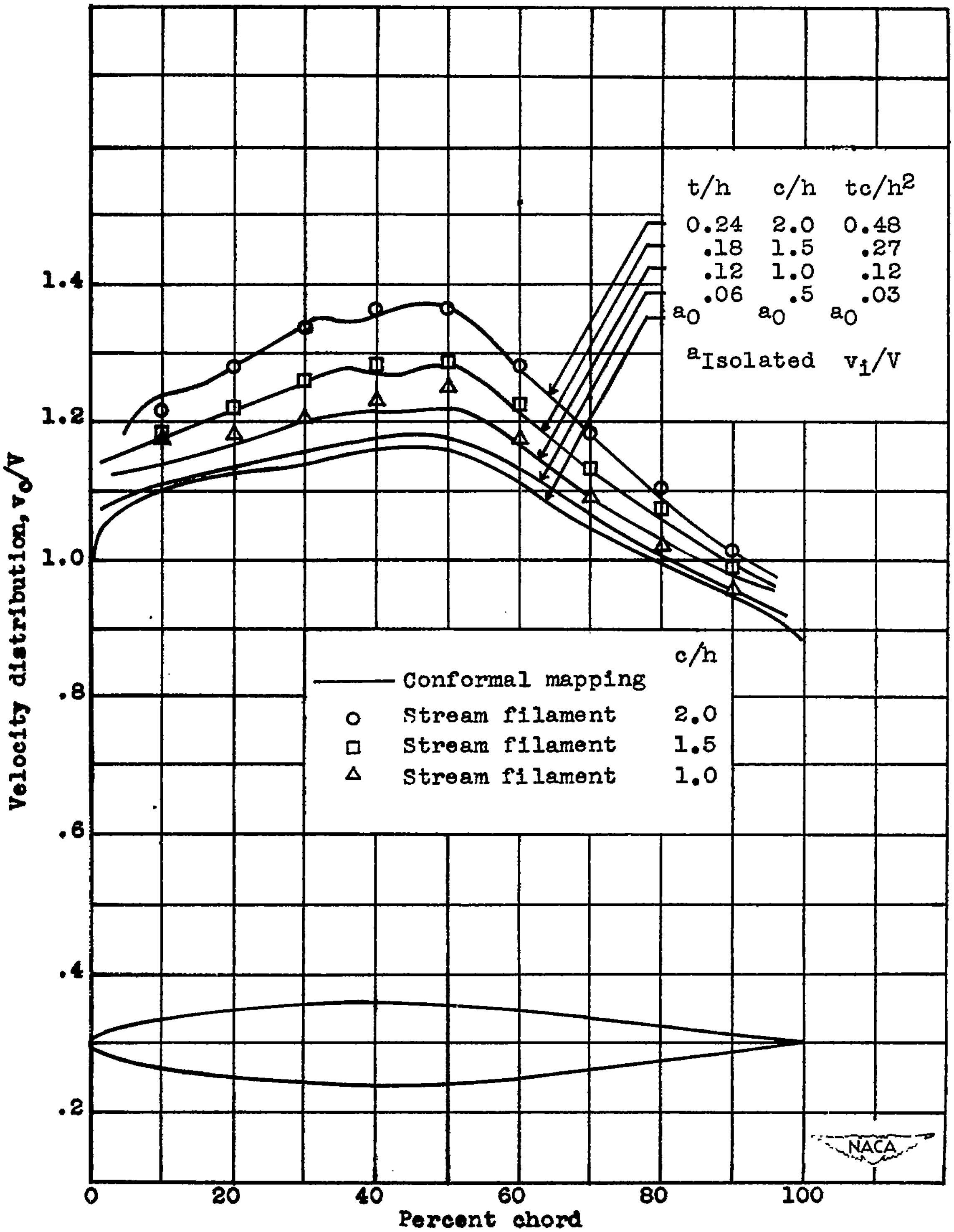

(a) 12-percent-thick airfoil.

Figure 3. - Velocity distributions on airfoils by mapping and stream-filament theory. c, chord of airfoil; h, height of tunnel; t, maximum thickness of airfoil.

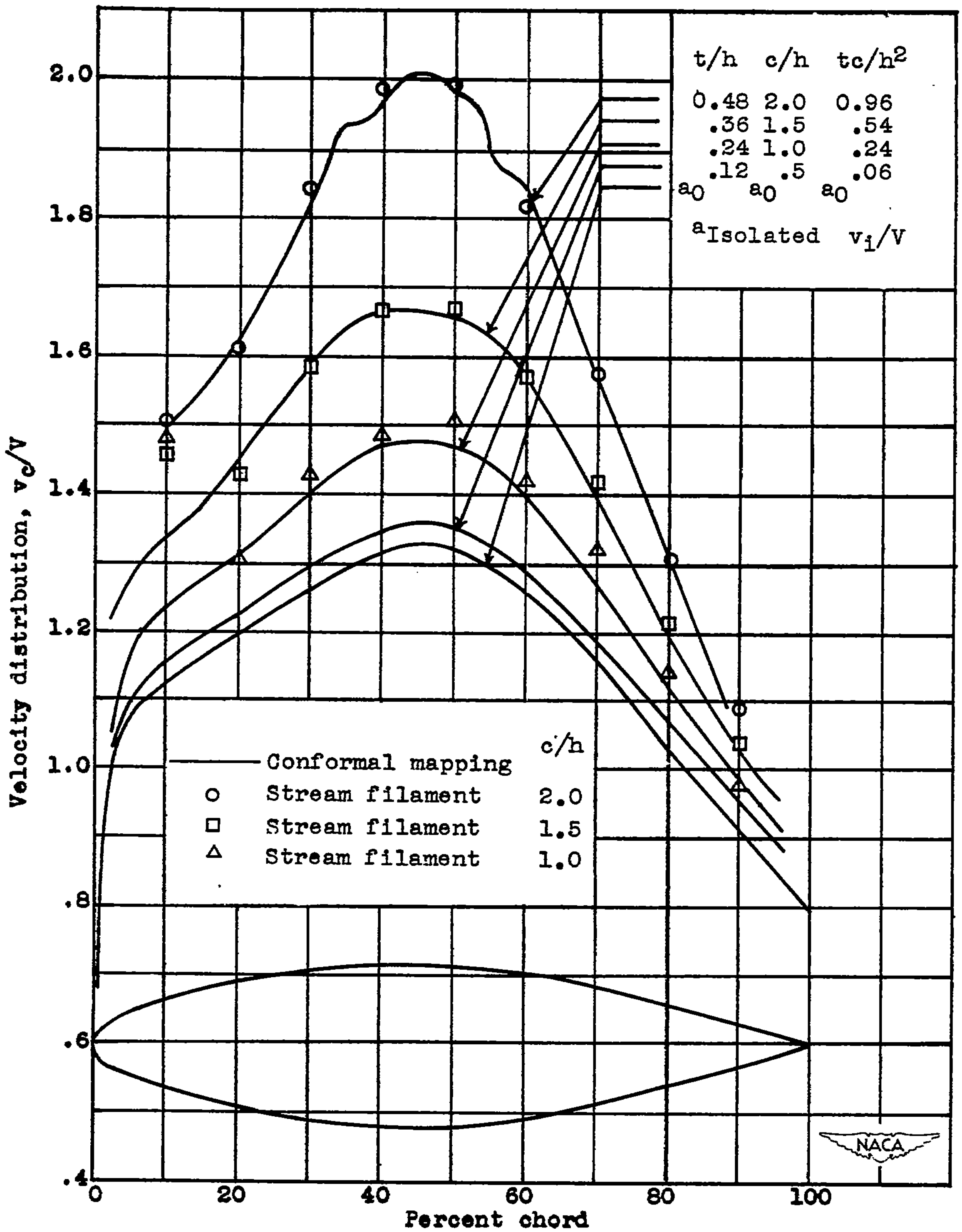

(b) 24-percent-thick airfoil.

Figure 3. - Concluded. Velocity distributions on airfoils by mapping and stream-filament theory. c, chord of airfoil; h, height of tunnel; t, maximum thickness of airfoil.

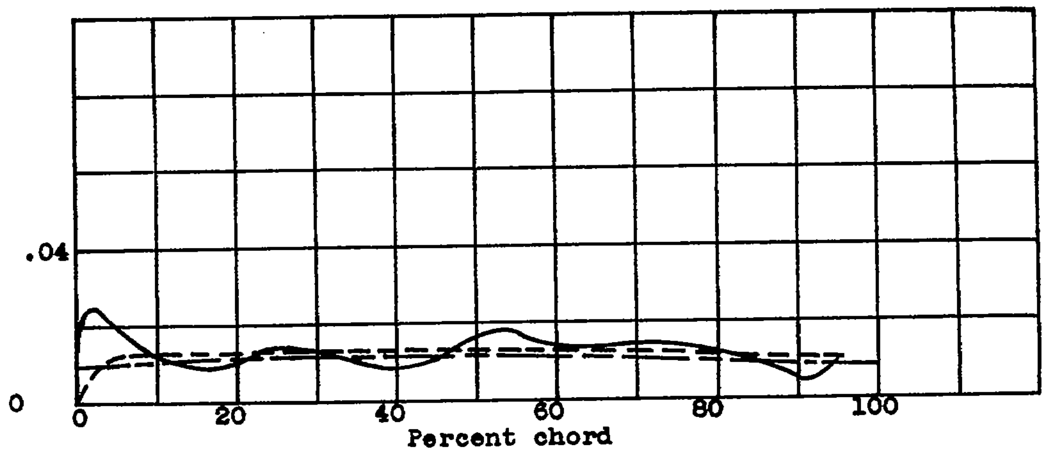

(a) Ratio of chord of airfoil to height of tunnel c/h, 0.5.

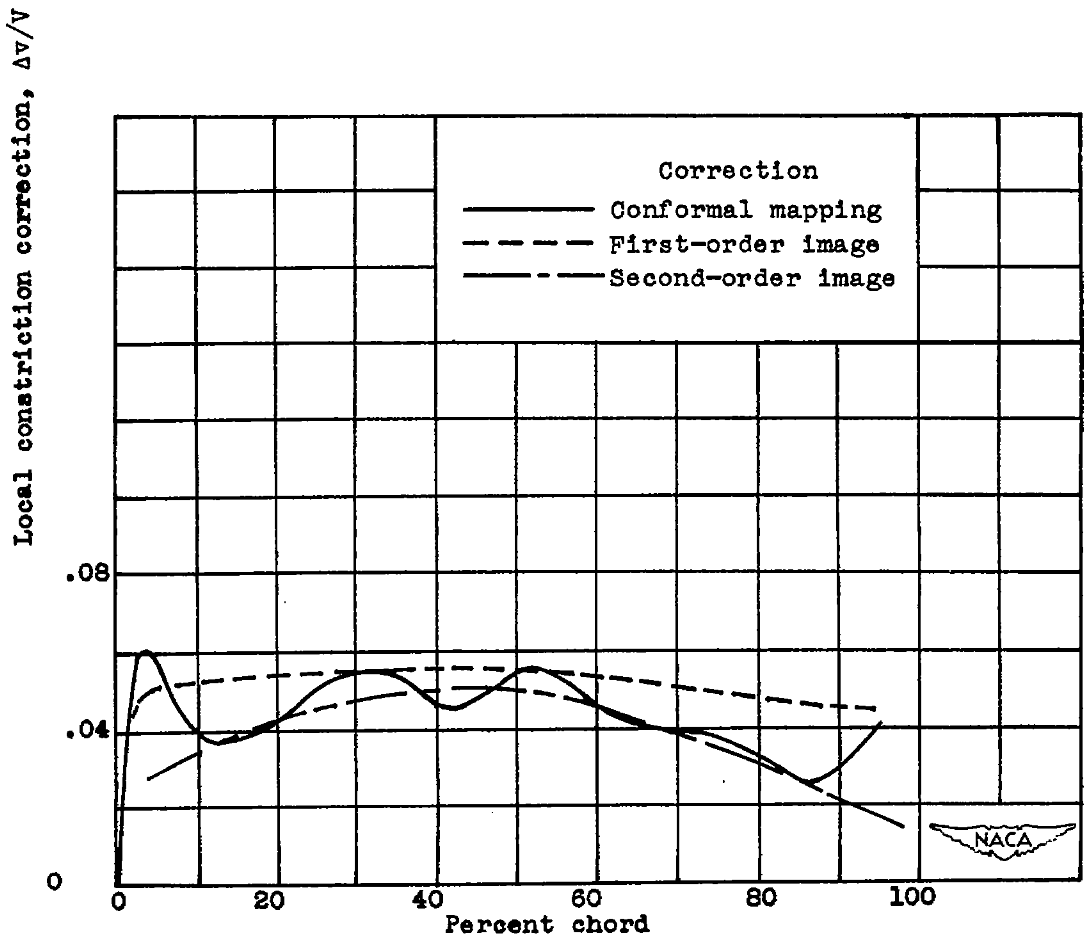

(b) Ratio of chord of airfoil to height of tunnel c/h, 1.0.

Figure 4. - Local constriction corrections for 12-percent-thick airfoil.

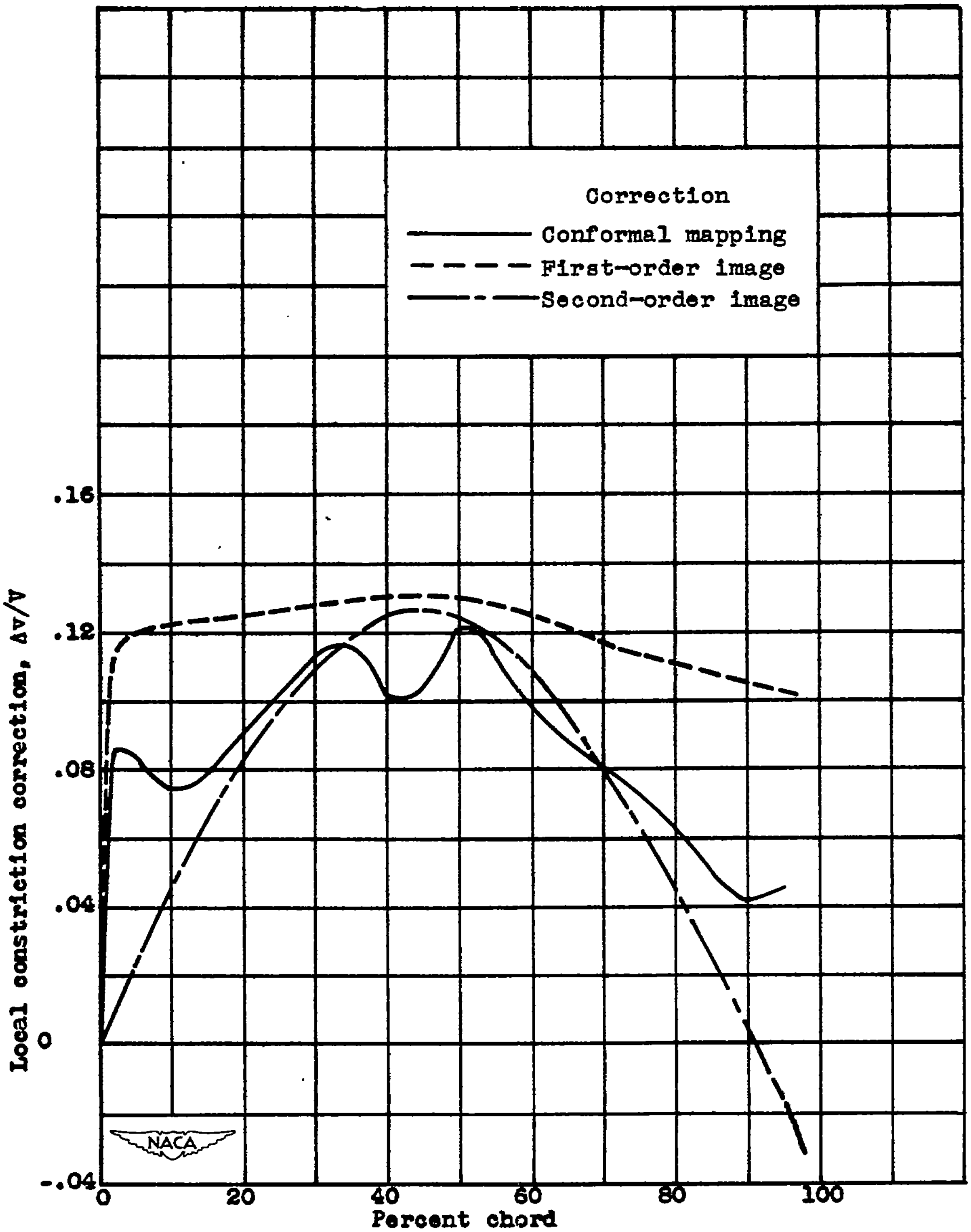

(c) Ratio of chord of airfoil to height of tunnel c/h, 1.5.

Figure 4. - Continued. Local constriction corrections for 12-percent-thick airfoil.

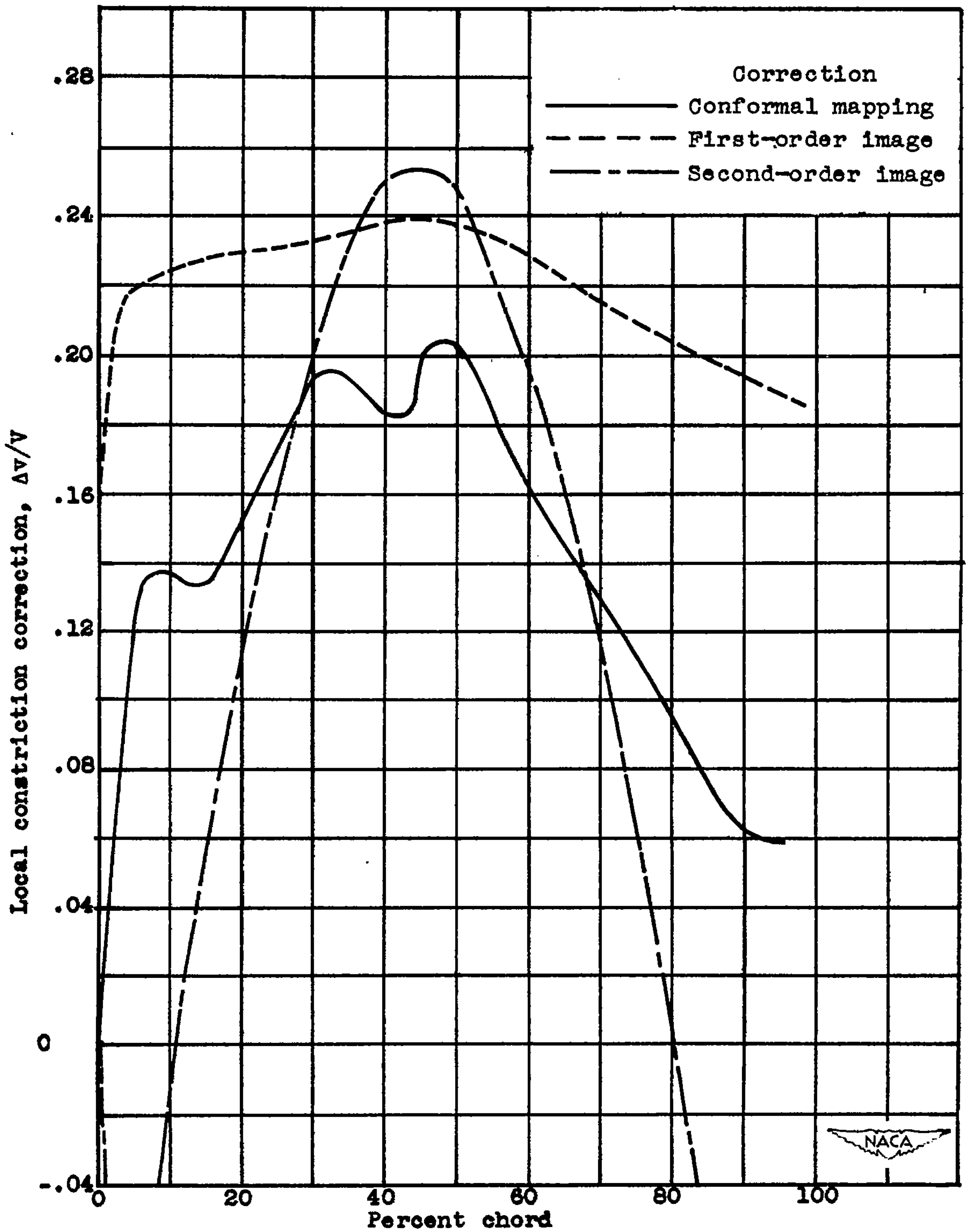

(d) Ratio of chord of airfoil to height of tunnel c/h, 2.0.

Figure 4. - Concluded. Local constriction corrections for 12-percent-thick airfoil.

488

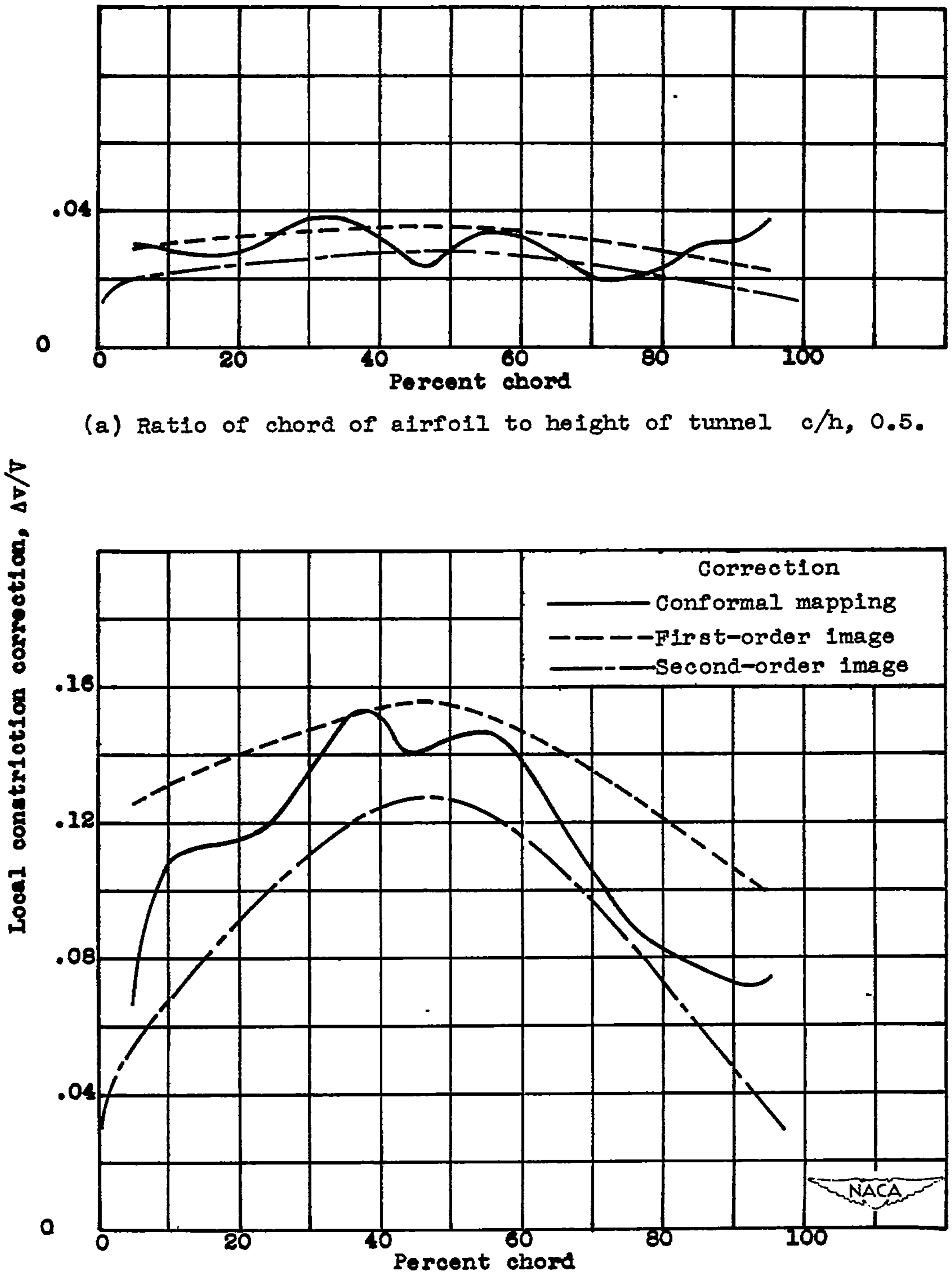

(a) Ratio of chord of airfoil to height of tunnel c/h, 0.5.

(b) Ratio of chord of airfoil to height of tunnel c/h, 1.0.

Figure 5. - Local constriction corrections for 24-percent-thick airfoil.

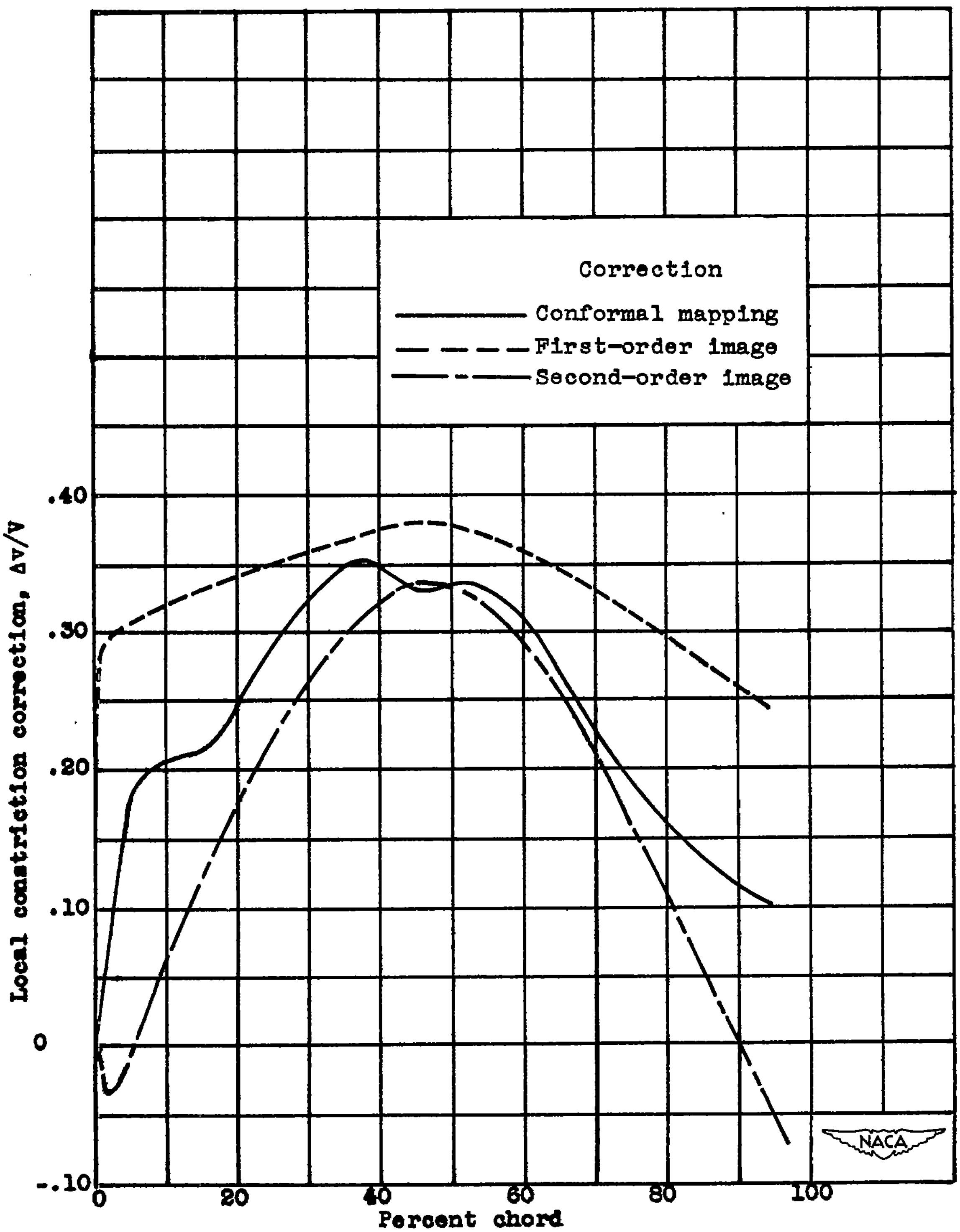

(c) Ratio of chord of airfoil to height of tunnel c/h, 1.5.

Figure 5. - Continued. Local constriction corrections for 24-percent-thick airfoil.

488

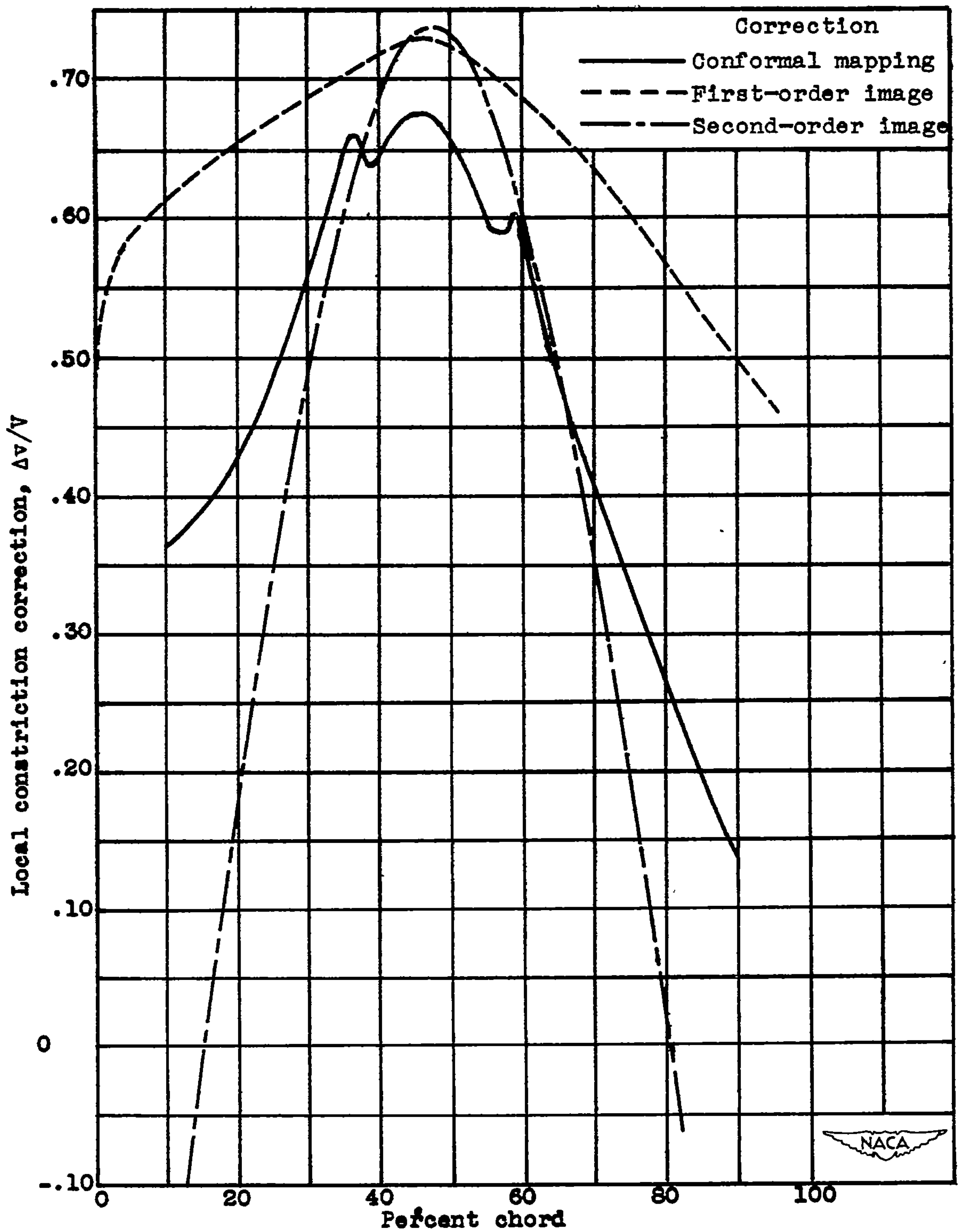

(d) Ratio of chord of airfoil to height of tunnel c/h, 2.0.

Figure 5. - Concluded. Local constriction corrections for 24-percent-thick airfoil.

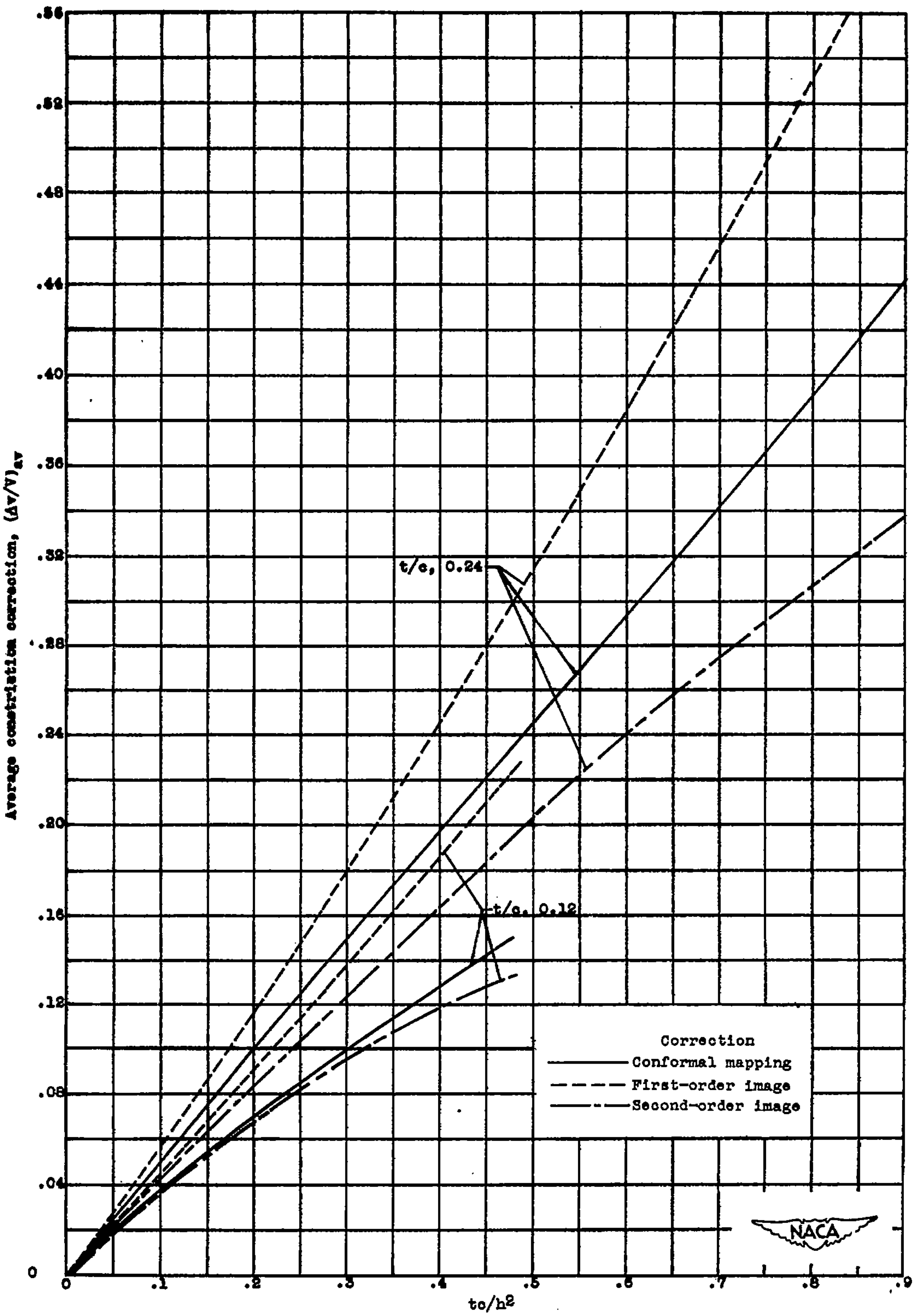

Figure 6.- Comparison of average constriction corrections by different methods. c, chord of airfoil; h, height of tunnel; t, maximum thickness of airfoil.

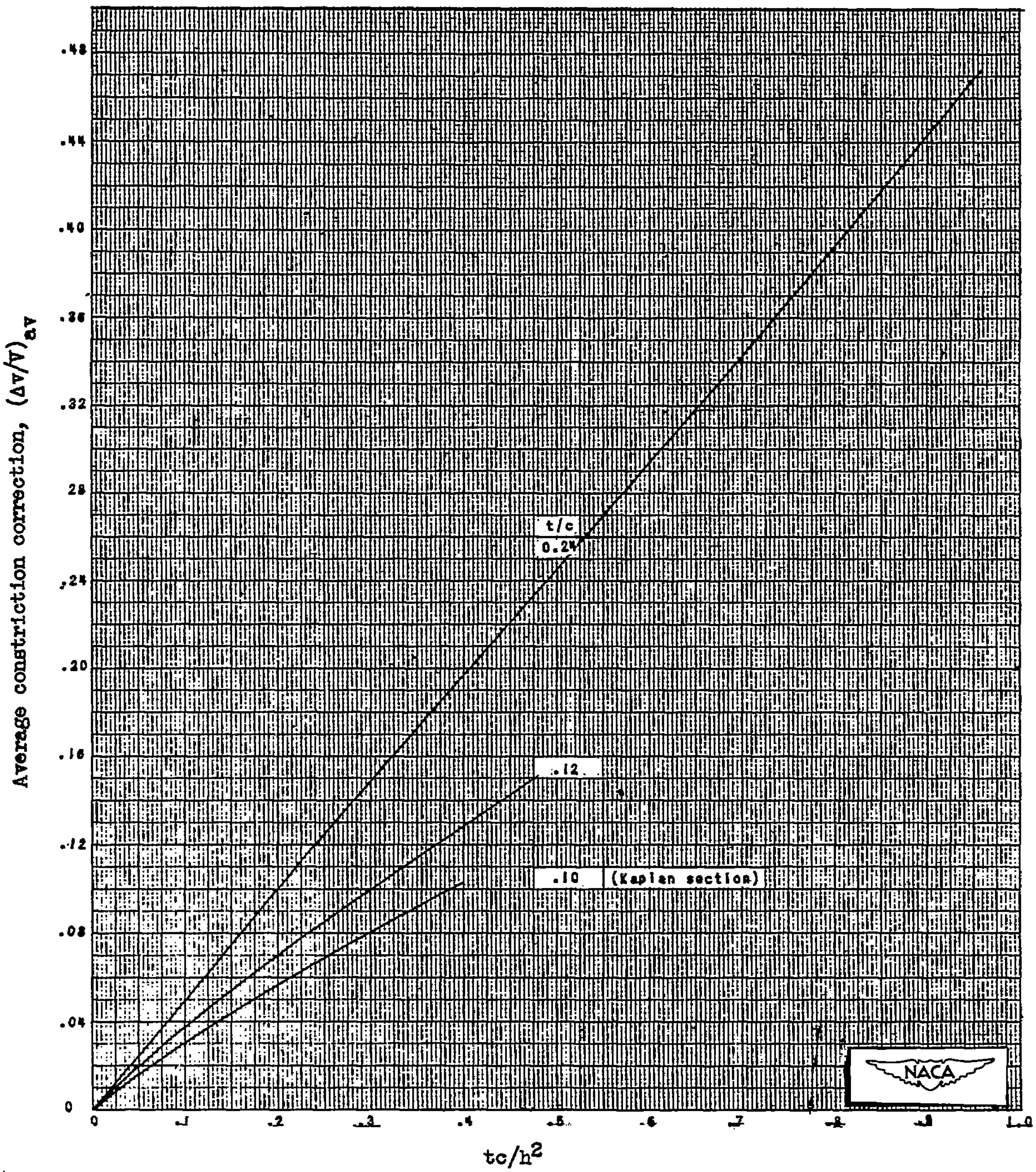

(a) As a function of tc/h^2.

Figure 7. - Constriction correction by mapping averaged along chord for airfoils of 12-percent and 24-percent thickness and a Kaplan section of 10-percent thickness. c, chord of airfoil; h, height of tunnel; t, maximum thickness of airfoil.

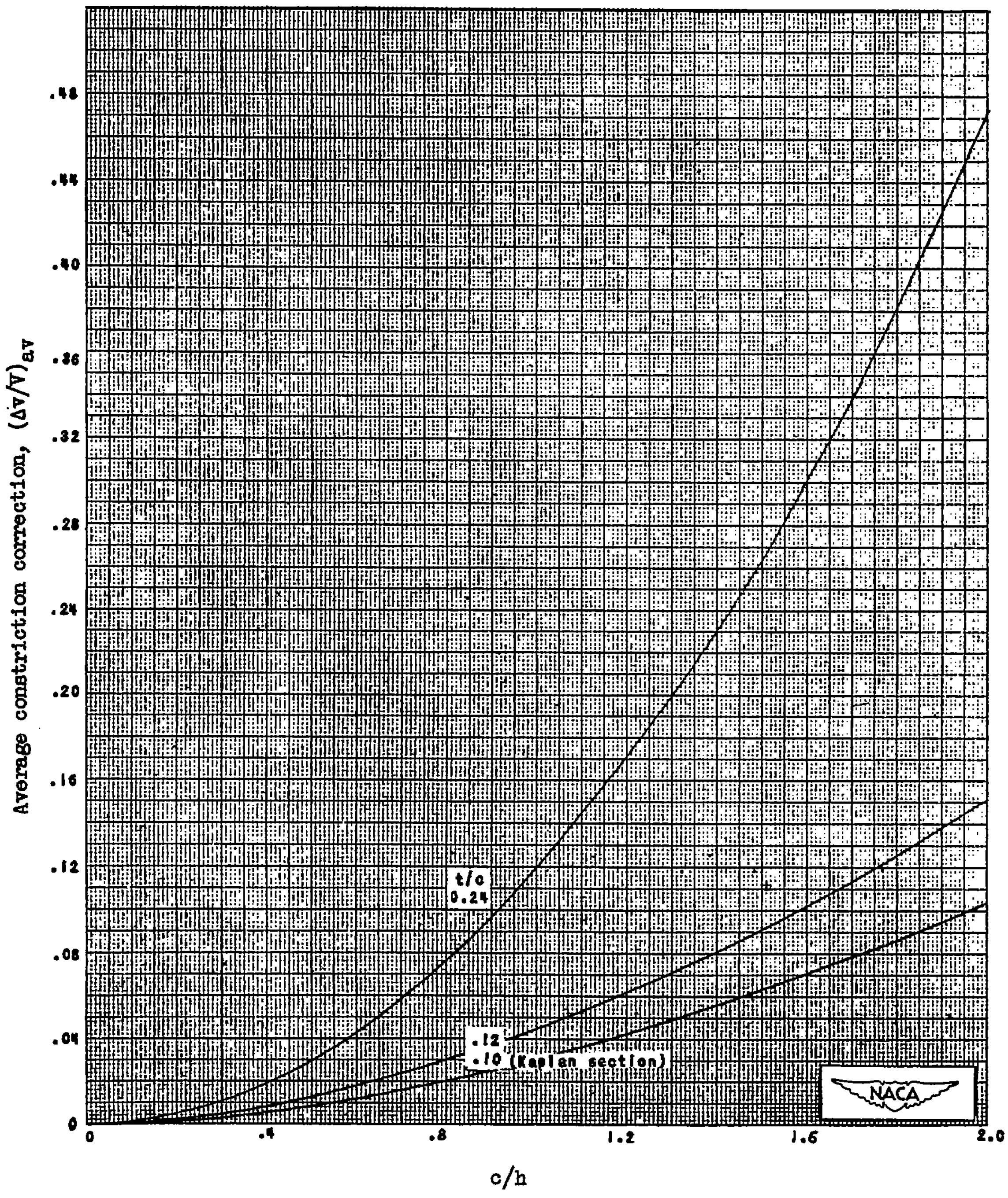

(b) As a function of c/h.

Figure 7. - Continued. Constriction correction by mapping averaged along chord for airfoils of 12-percent and 24-percent thickness and a Kaplan section of 10-percent thickness. c, chord of airfoil; h, height of tunnel; t, maximum thickness of airfoil.

488

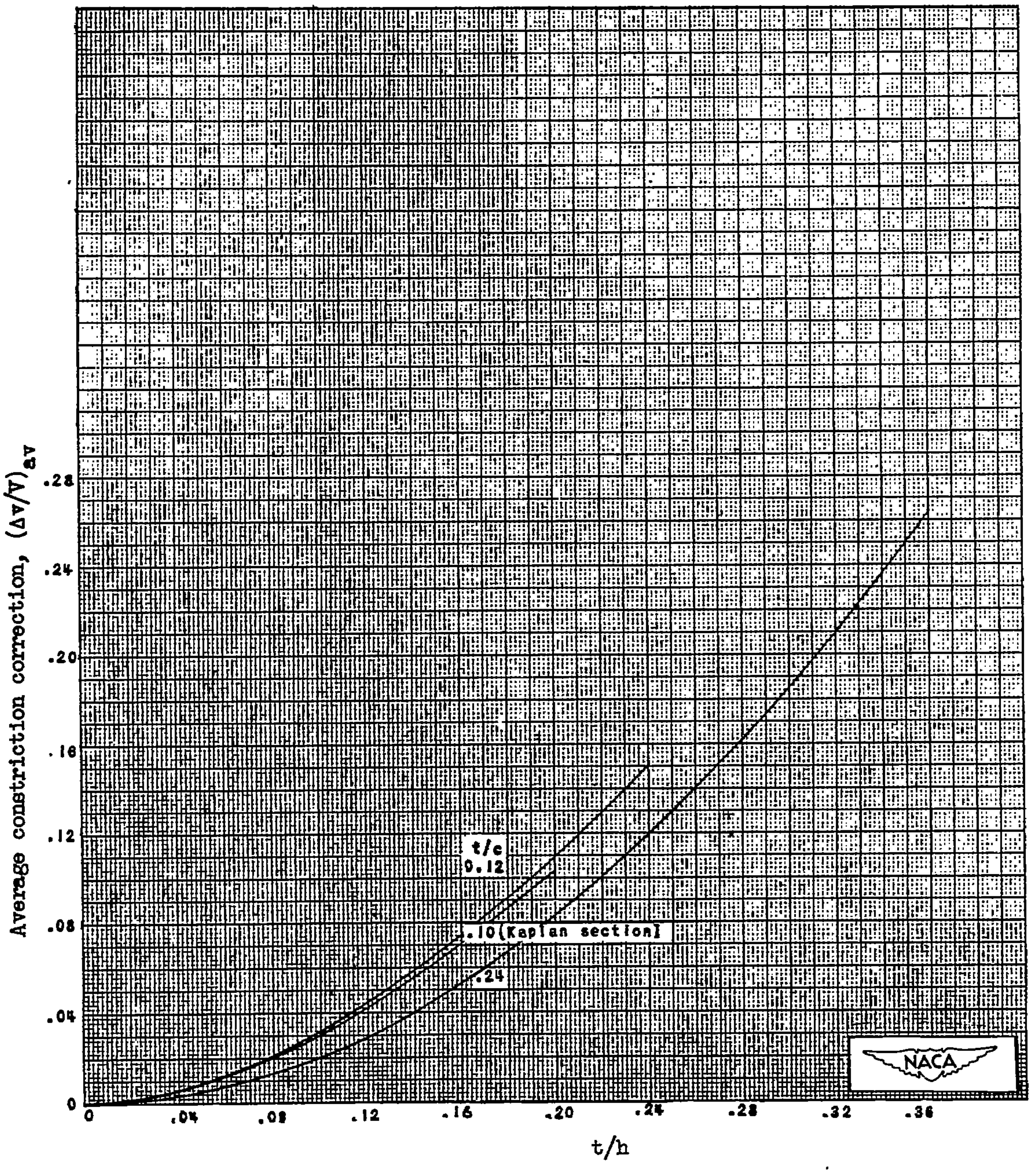

(c) As a function of t/h.

Figure 7. - Concluded. Constriction correction by mapping averaged along chord for airfoils of 12-percent and 24-percent thickness and a Kaplan section of 10-percent thickness. c, chord of airfoil; h, height of tunnel; t, maximum thickness of airfoil.

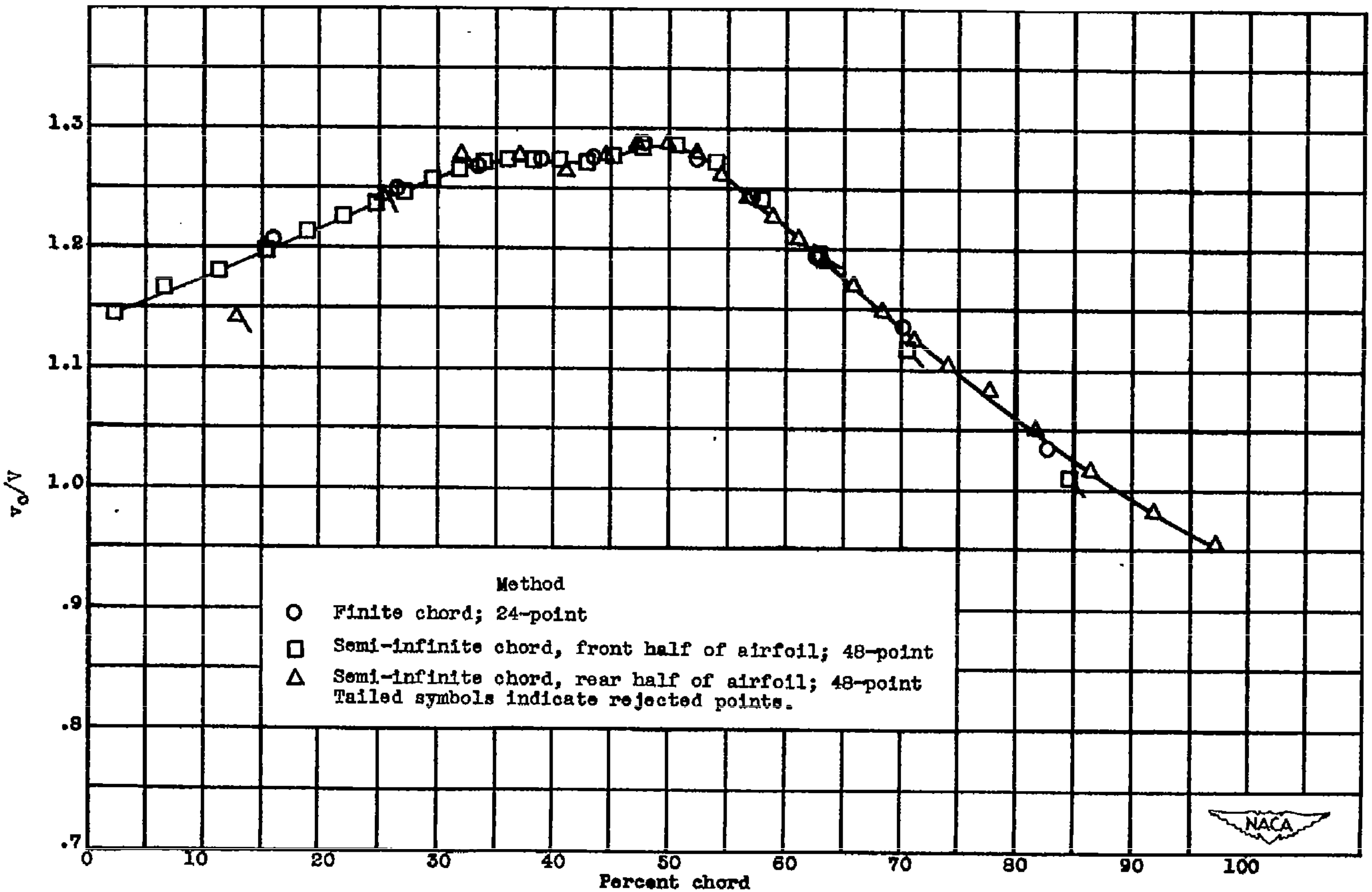

Figure 8. - Comparison of velocity distributions by the two conformal-mapping methods. 12-percent-thick airfoil; $\sigma = 1.5$; v_c, velocity on airfoil in tunnel or equivalent cascades; V, undisturbed stream velocity.

order to determine the starting characteristics of a commercial 220-pound-thrust rocket engine using crude monoethylaniline and other fuels with mixed acid.

The freezing points and low-temperature fuel-igniting properties of fuming nitric acids are of current interest because of a demand to extend the use of these oxidants to rockets operating at low temperature. The interrelated effects of water, from 0 to 10 percent by weight, and nitrogen tetroxide, from 0 to 25 percent by weight, in fuming nitric acid were studied with respect to the freezing points of the acid and the ignition delays with several fuels. Several possible chemical causes for the opposing effects of water and nitrogen tetroxide on ignition have been proposed.

Ignition delays of several propellant combinations obtained with a modified open-cup apparatus and a small-scale rocket engine of approximately 50 pounds thrust were compared to study any correlations that might exist between the two methods of ignition-delay determination. The results were used in determining the relative utility of each apparatus.

The literature pertaining to the preparation, physical properties, corrosiveness, thermal stability, constitution, and analysis of various nitric acids has been reviewed primarily with respect to their use as rocket oxidants. Conflicting data are evaluated and recommendations for additional experimental work are indicated.

Numerous studies have been made of the vapor pressure of essentially pure nitric acid and of the binary system, nitric acid-water. Data for the ternary system, nitric acid-water-nitrogen dioxide, are for the most part lacking. Work was therefore undertaken to provide more complete vapor-pressure data for the ternary system at physical equilibrium. Mixtures containing 71 to 97 weight-percent nitric acid, 0 to 20 percent nitrogen dioxide, and 0 to 15 percent water were used.[24]

Because the storage of fuming nitric acids presents a serious operating problem, means for improving the storage properties of this acid were sought. The storage properties of fuming nitric acids, with and without additives, were studied at a temperature of 170° F in closed containers of approximately 100-milliliter capacity; the containers had aluminum bodies and stainless-steel caps.

Among the storage properties of fuming nitric acid, corrosion and decomposition are of foremost concern. Additional information concerning the effectiveness of fluorides as corrosion inhibitors in fuming nitric acid was therefore obtained. It was found that for acids containing no fluorides, the weight loss of aluminum was approximately one-fifth that of stainless steel. Addition of 1-percent fluoride ion to the acid reduced the weight loss of both metals to practically zero even after 26 days of exposure to the acid at 170° F. Additional information concerning the effect of fluorides on corrosion was obtained by measuring the electrode potentials of the metals against a platinum reference electrode.

[24] See paper by McKeown and Belles listed on p. 78.

Rocket Combustion

Ignition-delay determinations of several fuels with nitric-acid oxidants were made at simulated altitude conditions from sea level to 100,000 feet utilizing a small-scale rocket engine of approximately 50 pounds thrust. Included in the fuels were aniline, hydrazine hydrate, furfuryl alcohol, furfuryl mercaptan, turpentine, and mixtures of triethylamine with mixed xylidines and diallylaniline. Red-fuming, white-fuming, and anhydrous nitric acids were used with and without additives.

The rocket phenomenon known as screaming often causes chamber, injector, or nozzle burnout failures and has been observed to increase the specific impulse. Rocket-engine screaming is a type of combustion-driven oscillation, with frequencies from 1,000 to 10,000 cycles per second, and is characterized by an audible wailing exhaust sound, by a bluish almost-invisible exhaust jet in which the shock positions oscillate (making the shock pattern appear fuzzy to the eye) and by increased heat transfer to the chamber surfaces. The high-frequency oscillations have been attributed to a combustion-reinforced pressure wave passing through the chamber and reflecting from the chamber surfaces to trigger the succeeding combustion surge. The frequency would therefore be governed by the velocity of wave propagation and the geometry of the chamber. A simplified analysis, based on the concept of acoustical resonance, has been developed to correlate scream frequencies with chamber geometry in terms of experimentally measurable quantities. The derived parameter is substantially independent of propellant combination or operating conditions.

The application of radiation-measurement techniques to the determination of gas temperatures in the flame resulting from liquid propellant reactions has recently been investigated. Such techniques are desirable in rocket combustion and injector design studies because they permit the study of conditions in a flame zone without disturbing the flow and without the necessity of maintaining a probe in the chamber. Radiation-temperature measurements were made throughout the flame developed within an open-tube combustor using liquid oxygen and a heptane-turpentine mixture as the reactants.[25] The temperature measurement utilizes carbon radiation from the flame.

[25] See paper by Auble and Heidmann listed on p. 76.

AIRCRAFT CONSTRUCTION

Problems associated with the structural integrity of aircraft in the subsonic and lower supersonic range are many and complex. Aerodynamic heating resulting from greater speeds continues to add a host of new problems and to complicate those of a long standing nature further. The need for increased research in the field of aircraft construction is evident.

The NACA, during the past year, has continued its efforts on the important problems associated with structural strength, efficiency, loading, flutter, fatigue, and materials under normal temperatures. It has also developed research tools and techniques for investigating aircraft under the elevated-temperature conditions encountered in high-speed flight. Further, it has succeeded in defining and exposing new thermal problems which future high-speed aircraft will encounter and has found solutions to certain of these problems.

Most of this research has been performed at the NACA laboratories with additional assistance provided by educational and other nonprofit institutions under contract to the NACA. A description of the Committee's recent unclassified research in the field of aircraft construction is given in the following pages and is divided into four sections: (1) Aircraft Structures; (2) Aircraft Loads; (3) Vibration and Flutter; and (4) Aircraft Structural Materials.

AIRCRAFT STRUCTURES

Static Properties

The use of integrally stiffened skins on aircraft is increasing because of the possibilities of saving weight and eliminating rivets and bolts. Compared with riveted-on stiffeners, integral stiffeners participate more fully with the skin in resisting external loads but, because of this action, may lead to an undesirable coupling of plate distortions for certain proportions and loading conditions. The nature of this problem is discussed in Technical Note 3646 where the modifications to the equations for stress distribution and deflection are made to account for the effects of coupling. Conditions under which the effects of coupling are significant are given in this paper.

Because engineering beam theory fails for deflection analysis of thin low-aspect-ratio wings, the development of efficient methods of analysis has become a problem. A matrix method based on energy principles for obtaining influence coefficients is presented in Technical Note 3640. The required matrices may be set directly from the data of the wing design. The necessary calculations have been arranged to take full advantage of automatic computing machines.

The thick-skin multiweb box beam is representative of wings of high-speed aircraft. Experimental data and strength analysis of this component are presented in Technical Note 3633. The combinations of design parameters which lead to minimum structural weight for various values of a loading index are given. The results are presented in such a manner that the lightest weight structure which satisfies wing-stiffness requirements can be found.

Classical theories of the structural strength and stability of plates assume that the plate deflections experienced are small in comparison with the plate thickness. In order to evaluate the inaccuracies resulting when this assumption is not fulfilled, Columbia University has developed a nonlinear plate theory of motion and solved the equations for certain dynamic cases. Underlying assumptions of various plate equations have also been studied. The results of this study are presented in Technical Note 3578.

Comparisons between the results of a theory for calculating stresses around cutouts in stiffened cylinders and the results of experiment are presented in Technical Note 3544. The data and the theory were previously published and coefficients for use with the theory have been calculated and published in Technical Note 3460. The theory takes into account the bending flexibility of the ring stiffeners. The comparisons show that good agreement is obtained if this factor is correctly accounted for.

New York University has conducted, under NACA sponsorship, a critical review of the literature published since 1940 on buckling and failure of plate elements. The results of this review, including a compilation of existing theories and experimental data, are presented in Technical Note 3781. A similar review has also been made at New York University of the existing literature on buckling of composite elements. The results of this review are presented in Technical Note 3782. During these reviews, general equations for the plastic buckling of cylinders were derived. These equations were then used to obtain solutions for the compressive and torsional buckling of long cylinders in the plastic region. These results, as well as comparisons between computed and test data, are presented in Technical Note 3726.

An analysis of the stresses in the plastic range around a circular hole in a plate was made both to explore means for solving stress problems in the plastic range and to obtain the solution of this basic problem. The results are presented in Technical Note 3542. Calculations were made for four different materials and the resulting stress-concentration factors are compared with those derived from a previously developed approximate formula.

Dynamic Properties

The major role that flutter plays in the design of high-performance aircraft requires that methods for computing accurate vibration modes and frequencies be obtained. In Technical Note 3636, the investigation of the usefulness of the substitute-stringer method for including the effects of shear lag in the calculation of the transverse modes and frequencies of box beams is continued. Box beams, the covers of which consist of normal-stress-carrying stringers on sheets carrying not only shear but also normal stress, are analyzed exactly. Frequencies of beams with various numbers of stringers, obtained by means of this exact analysis, serve to determine the possible accuracy of the frequencies obtained by the substitute-stringer approach. A combined experimental and theoretical investigation of the modes and frequencies of a large-scale built-up box beam is reported in Technical Note 3618. For bending vibrations, frequencies obtained from an analysis of a substitute-stringer structure which includes the influence of transverse shear deformation and shear lag were found to agree very well with those obtained experimentally. In the case of torsional vibrations, the frequencies obtained from either an elementary or a four-flange beam analysis which includes the effects of restraint of warping were found to be in satisfactory agreement with the experimental frequencies.

The vibration characteristics of hollow thin-walled rectangular beams have been investigated to obtain insight into the factors affecting the modes and frequencies of wings. The experimental results from this study are presented in Technical Note 3463 and indicate that the effect of shear deformation of the cross section on the torsional frequencies can be large. Further evaluation of this effect has been made and is presented in Technical Note 3464.

Thermal Properties

Rapid changes in temperature of the surface of an aircraft can induce thermal loads in the primary structure which may have serious aerodynamic and structural consequences. The nature of this problem was investigated by subjecting box beams which simulate high-speed-wing structure to a high-intensity heat source. These tests are reported in Technical Note 3474. It was found that the internal structure of the beams provided enough restraint against expansion of the heated skin surfaces to cause severe buckling of the skin. Buckling of the shear webs occurred during the cooling phase of the test when the temperature of the internal structure exceeded that of the skin. Measured strains were used to determine distortions and stresses which were found to agree with a thermal stress analysis of the test conditions.

One of the most important structural problems resulting from aerodynamic heating is the deterioration of material properties at elevated temperatures. This deterioration of material properties produces loss of strength and creep of structures and can lead to weight increases that adversely affect the performance of high-speed aircraft. A study has been made of the strength and creep behavior of aircraft structural elements at elevated temperatures to obtain methods for predicting structural behavior from material characteristics. One of these studies, reported in Technical Note 3552, was concerned with the elevated-temperature compressive strength and creep lifetime of simply supported plates. A similar study on the compressive strength and creep lifetime of skin-stringer panels is reported in Technical Note 3647. Both studies indicate that elevated-temperature strength of structural elements can be predicted from methods available for determining room-temperature strength provided that the appropriate stress-strain curve for elevated-temperature material is used. Previously reported studies of the elevated-temperature buckling strength of structural components have indicated similar results. The present studies also show that creep lifetime of structural elements may be determined from methods used to determine structural strength if the compressive creep properties of the material are substituted for the material stress-strain curve. The results make it possible to estimate the effect of creep on the weight of structures that are designed to operate at elevated temperatures.

The transient thermal stresses produced by aerodynamic heating of supersonic aircraft depend upon the temperature distribution within the structure, which, in turn, can be markedly influenced by the thermal conductivity of any joints present. In order to investigate the effects of joint conductivity on the thermal stresses in aerodynamically heated skin-stiffener combinations under various aerodynamic conditions, a theoretical study was made. In this study an aerodynamic heat-transfer parameter (called the Biot number), a joint-conductivity parameter, and geometrical proportions were varied. The results, presented in Technical Note 3699, indicate that increasing the joint conductivity beyond a certain value results in almost no change in the maximum skin or stiffener stresses; but, as the joint conductivity approaches zero, the maximum skin and stiffener stresses increase appreciably. Increasing the Biot number, an index of the rate of transfer of external heat to internal heat, can also cause a considerable increase in the maximum skin and stiffener stresses. However, when the Biot number is large (high rate of external heating), the value of the joint conductivity is relatively unimportant since the structure is heated so fast that there is no time for heat to be conducted into the interior of the structure; the joint conductivity thus affects the thermal stresses most significantly when the external heating rate is low. Changing the geometric characteristics produces results which are essentially independent of the joint conductivity and the Biot number.

In the design of aircraft structures, where aerodynamic heating is encountered, knowledge of the temperature distribution within the structure is of considerable importance. Because interior elements of the structure are heated by conduction through joints, the influence of various joint properties on thermal conductance has been investigated previously and reported by Syracuse University. Before extending this investigation, Syracuse University explored the influence of joint conductance on the transient temperature distribution in composite aircraft joints. Fabricated specimens representative of typical skin-stringer cross sections, as well as geometrically similar specimens without joints, were tested under aerodynamic heating conditions and the results from the two sets of joints were compared. The results, which are presented in Technical Note 3824, indicate that, in the practical case, joint conductance must be taken into account if temperature distributions throughout composite structures are to be predicted accurately.

Aircraft structures for high-speed flight must be designed so that excessive creep deformation and creep rupture does not occur during the design lifetime of the structure. An understanding of the creep behavior of structures is therefore necessary in order to eliminate such failures. A previously reported investigation by the National Bureau of Standards indicated that creep deformations within joints may be responsible for a considerable portion of the overall deformation of structures. However, no correlation was obtained between the creep of a riveted joint and the creep of its component materials. This study has now been extended and creep-test results of a number of additional joints are reported in Technical Note 3842. Methods are presented by which the time to rupture, the mode of rupture, and the deformation of structural joints in creep may be predicted. These methods are based upon the creep properties of the materials of the joint in tension, shear and bearing.

Aircraft structural elements subjected to long periods of heating and compressive loadings can buckle even though the applied load is less than the critical load of the element at the elevated temperature. This phenomenon is called creep buckling. Research equipment and techniques have been developed at the Polytechnic Institute of Brooklyn and are presented in Technical Note 3493. Additional creep-buckling tests of 2024T–4 aluminum alloy columns besides those published in this report have been conducted and the results correlated with theory.

The aircraft designer at the present time must deal with a multiplicity of materials and material properties which vary with temperature. It is essential, therefore, that speedy and accurate methods for predicting the influence of changes in material properties on structural strength be available. Such methods are given in Technical Note 3553 and Technical Note 3600 for various types of structural components which fail by compressive crippling. The methods utilize the concept of crippling-strength moduli which are readily calculated from the compressive properties of the material in the structure. Accuracy of the methods is illustrated with experimental data obtained in various materials and under different temperature conditions.

The transient temperature distributions produced by aerodynamic heating of thin solid wings induce thermal stresses that may effectively reduce the stiffness of the wing. This is a new problem that can be a significant factor in the aero-elastic behavior of aircraft structures. Such reductions in stiffness have been investigated experimentally by rapidly heating the edges of a cantilever plate. The midplane thermal stresses imposed by the nonuniform temperature distribution caused the plate to buckle torsionally, increased the deformations of the plate under a constant applied torque, and reduced the frequency of the first two natural modes of vibration. Small-deflection plate theory, employing energy methods, predicted the general effects of the thermal stresses but became inadequate when plate deflections were large. Additional studies have been initiated to investigate these effects.

AIRCRAFT LOADS

Basic Load Distribution

Extensive flight investigations have been made with the X–5 variable-wing-sweep research airplane at Mach numbers up to 1.0 to determine the effects on the wing and horizontal tail loads of varying the angle of wing sweep without modifying the other characteristics of the airplane. Up to a Mach number of 0.85, the balancing horizontal-tail loads measured in flight show a consistent variation as the wing sweep angle is increased from 20° to 59° with the greatest down tail load occurring at sweep angles of about 36°. The wing loads were found to have a nonlinear variation with airplane angle of attack and to reflect the changes that occurred in the wing characteristics. In another flight investigation, pressure measurements over the midspan station of the 8-percent-thick wing on the X–1 airplane in the transonic speed range showed a rearward movement of the chordwise load center with increasing Mach number with a particularly rapid and large movement in the Mach number range of 0.82 to 0.88. In the Mach number range 0.95 to 1.25 at high normal force coefficients, upper surface pressure distributions approached a rectangular slope.

In Technical Note 3476, spanwise lift distributions have been calculated for 61 swept wings with various aspect and taper ratios and a variety of angle-of-attack distributions including flap and aileron deflections. The information presented can be used both in the analysis of untwisted wings or wings with known twist distributions and in aeroelastic calculations involving

435875—57——5

initially unknown twist distributions. The information presented in Technical Note 3476 supplements similar information previously given in Technical Note 3014 for unswept wings so that the two papers cover all practical plan forms.

A method for computing the span loads and the resulting rolling moments for sideslipping wings of arbitrary plan form in incompressible flow is presented in Technical Note 3605. The basic method requires mechanical differentiation and integration to obtain the rolling moment for a wing of arbitrary plan form in sideslip when the span load at zero sideslip is known The mechanical differentiation and integration can be avoided, however, by use of a step-load method which is also derived. A comparison of the calculated span loads and rolling-moment parameters with available experimental data shows good agreement.

The development of new-type control devices requires that structural design data be provided. The effects, therefore, on the chordwise pressures and section forces and moment coefficients near midspan of deflecting various plain spoilers and a flap-type control with and without an attached tab on a swept wing have been investigated at Mach numbers from 0.60 to 0.93.

In order to design aircraft one must have a knowledge of body effects on the wing spanwise load distribution at all speeds. Although methods exist for predicting such body effects on sweptback wings at low speeds, practically no direct experimental verifications have been available. In a recent investigation, detailed wing pressure-distribution data that permit the desired comparison were obtained. The data, reported in Technical Note 3730, indicated that, although previous methods did not satisfactorily predict body effects on the unflapped uncambered wing, a swept-wing method employing 19 spanwise lifting elements and control points gave good agreement except when the wing had deflected trailing-edge flaps or was cambered and twisted.

Normal-force and normal-pressure distributions for an ogive-cylinder body of revolution of fineness ratio 10 are reported in Technical Note 3716 for a free-stream Mach number of 1.98 and an angle-of-attack range from 0° to 20°. Comparisons of experimental and theoretical normal-force and normal-pressure distributions indicate that available theoretical methods can be used to predict experimental results with good accuracy for angles of attack to about only 5°. At greater angles of attack, the normal-force distributions differ significantly from those calculated in accordance with theories which include methods of estimating the effects of viscosity on the forces and moments for inclined bodies. Analysis of the data shows that these differences are, in general, attributable to inadequate estimates of the magnitude and distribution of the cross forces resulting from flow separation. A correlation curve for the longitudinal distribution of the cross-flow drag coefficient for laminar boundary-layer flow has been developed and is based upon the assumption that the distribution depends primarily upon the body shape. It is believed that use of this curve for the viscous cross-force contribution in conjunction with first-order linear theory for the potential cross force provides a satisfactory method for estimating normal-force and pitching-moment characteristics for similarly shaped bodies with laminar-boundary-layer flow.

In Technical Note 3479, horizontal-tail loads measured in gradual and abrupt longitudinal maneuvers on two configurations of a four-engine jet bomber are presented. The least-squares procedures were used to determine aerodynamic loads from strain-gage measurements of structural loads. The results are anolyzed to determine the flight values of the aerodynamic coefficients which are important in calculations of horizontal-tail loads for comparison with wind-tunnel results. The effects of fuselage flexibility on the loads are determined and some calculations of critical horizontal-tail loads beyond the range of the tests are compared with the design loads.

Some indication of the importance of the directional-stability characteristics of present-day high-speed airplanes with increasing angle of attack and Mach number has become apparent from recent wind-tunnel tests. An analysis of wind-tunnel data has shown that the vorticity shed from the nose of the fuselage and directed by the wing to strategic locations in the vicinity of the vertical tail markedly affects the load on the vertical tail in sideslip at high angles of attack and supersonic Mach numbers. For such conditions, the directional stability of the airplane may become negative.

Gust Loads

The collection of data with NACA VG and VGH recorders to determine the magnitude and frequency of occurrence of the gusts and gust loads and the operating air speeds and altitudes of commercial transport airplanes has been continued. The VGH data covering about 3,000 hours of operation from two types of four-engine transport airplanes currently in use on transcontinental and eastern United States routes are presented in Technical Notes 3475 and 3483. The analysis of these data indicates that the more severe gust loads occurred for operations over the eastern portion of the United States, a result attributable to the higher operating speeds in rough air for these operations. A related study of approximately 70,000 hours of VG data from six different operations of twin-engine transport airplanes over the past eight or nine years, presented in Technical Note 3621, indicates that the loads and gusts were comparable with those experienced in previous operations of the same type of airplane.

The information available on the spectrum of atmospheric turbulence is briefly reviewed in Technical Note

3540 and a method is presented for converting available gust statistics normally given in terms of counts of gust peaks into a form appropriate for use in spectral calculations. The fundamental quantity for this purpose appears to be the probability distribution of the root-mean-square gust velocity. Estimates of the variation of this distribution with altitude and weather condition are also derived from available gust statistics. A critical problem in connection with the design and operation of missiles and airplanes capable of high-speed vertical flight arises from the loads and motions experienced when intense layers of wind shear are encountered. As a consequence, data on the magnitude and frequency of occurrence of the shear layers at different altitudes and seasons were determined from U. S. Weather Bureau rawinsonde data and are reported in Technical Note 3732. These data indicate that maximum shear intensities of about 120 feet per second per 1,000 feet occur at altitudes of about 50,000 feet during the spring and winter seasons but occur in relatively thin layers having thicknesses not greater than about 3,000 feet.

A method for obtaining a power spectrum of vertical gust velocity over a wide range of wave length has been devised and test results are published in Technical Note 3702. A spectrum of vertical gust velocity was measured at low altitude in clear-air turbulence having a root-mean-square intensity of 5 feet per second for wave lengths from 10 feet to 60,000 feet. At the higher frequencies (short wave lengths), the power spectral density varied at a rate which was approximately predicted by theory. The spectrum which was obtained tended to flatten out for the longest test wave lengths. The break frequency which provides an indication of the scale of the turbulence occurred at a wave length of approximately 6,000 feet.

Calculated unsteady-lift functions and spanwise lift distributions for delta, rectangular, and elliptical wings undergoing a sudden change in sinking speed are presented in Technical Note 3639. These data indicate that the normalized unsteady-lift functions are substantially independent of the plan form for elliptical, rectangular, or moderately tapered wings, but for delta wings the increase of lift toward the steady-state value is much more rapid. The results in this report corroborate the results of other investigations which show that the rate of growth of lift tends to increase with a decrease in aspect ratio and that spanwise distributions of the indicial lift seem to be independent of time for rectangular and elliptical wings. In Technical Note 3748, reciprocal relations for unsteady flow are used to calculate total-lift responses of wings to sinusoidal gusts and to sinusoidal vertical oscillations. A variety of plan forms are considered for incompressible, subsonic compressible, sonic, and supersonic flow. A theory is presented in Technical Note 3805 for calculating the variation with frequency of the lateral-force and yawing-moment coefficients due to sinusoidal side gusts passing over the profile of a simple fuselage combined with a vertical fin. Since slender-body theory is used, the results are applicable to both subsonic and supersonic airspeeds, provided the local flow angles between the profile and the airstream are small.

An investigation to determine the gust-alleviation capabilities of fixed spoilers and deflectors on a transport-airplane model incorporating a straight wing is reported in Technical Note 3705. The results indicate about equal effectiveness (from 20 to 40 percent) of spoilers or deflectors in reducing normal accelerations in rough air through reductions in lift-curve slope. Both devices were also equally effective in decreasing the airspeed through increased drag. In Technical Note 3746, the wing and horizontal-tail loads and spar strains measured on a twin-engine light transport airplane, modified by a gust-alleviating device for passenger comfort, were presented. The results presented are an initial analysis of samples of measurements obtained in clear-air turbulence with the alleviation system both off and on. Although the alleviation system was not optimum, the root-mean-square normal acceleration at the airplane center of gravity was reduced by 43 percent and the wing bending strains were reduced, but wing-shear strains and horizontal-tail shear and bending strains were increased.

Landing Loads

In Technical Note 3541, a method is presented for statistically deriving contact vertical velocities of airplanes from measurements of maximum incremental center-of-gravity acceleration at contact. Probability curves of derived velocities for a test airplane when compared with curves of measured velocities show a difference of less than 0.2 foot per second throughout the velocity range covered in the investigation. A statistical comparison of the landing-impact velocities of the first and second wheel to touch ground from about 350 transport landings is reported in Technical Note 3610. The comparison indicates that the mean vertical velocity at the instant of contact was about the same for either wheel but that the probability of a high value of vertical velocity was somewhat greater for the second wheel to touch than for the first. The effect of the rolling velocity of the airplanes at the instant of initial contact was to increase the vertical velocity of impact of the wheel toward which the airplane was rolling regardless of whether it was the first or second wheel to touch. There appeared to be no definite influence of the ratio of landing-gear tread to radius of gyration of the airplanes on the relative vertical velocities of the first and second wheels to touch, as would be expected from theoretical considerations.

Technical Note 3604 reports results of tests made to determine the lateral or cornering force, drag force, torsional moment or self-alining torque, pneumatic caster, vertical tire deflection, lateral tire deflection, wheel torsion or yaw angle, rolling radius, relaxation length, tire footprint area, and variation of unloaded tire radius with inflation pressure for two 26- by 6.6-inch, type VII, 12-ply-rating tires. Data were recorded for conditions of rectilinear-yawed rolling over a range of inflation pressures and yaw angles at the rated vertical load and at twice the rated vertical load. Vibration tests were made to determine the dynamic lateral elastic characteristics of the tires. During rectilinear-yawed rolling, the normal force generally increased with increasing yaw angle within the test range, the variation of normal force with yaw angle differed for the two vertical loads tested, the pneumatic caster was a maximum at small yaw angles and tended to decrease with increasing yaw angle, and the sliding drag coefficient of friction tended to decrease with increasing bearing pressure.

A comprehensive correlation, evaluation, and extension of linearized theories for tire motion and wheel shimmy has been made and is reported in Technical Note 3632. It is demonstrated that most of the previously published theories represent varying degrees of approximation to a summary theory developed therein which is a minor modification of the basic theory of Von Schlippe and Dietrich. In most cases where strong differences exist between the previously published theories and the summary theory, the previously published theories are shown to possess certain deficiencies. Comparison of the existing experimental data with the predictions of the summary theory provides a fair substantiation. Some discrepancies exist however, which may be due to tire hysteresis effects or other unknown influences.

Theory indicates a sharp increase in the hydrodynamic load as the dead-rise angle approaches zero. There have been, however, few experimental data available for verifying the loads predicted by theory for angles of dead rise below 20°. Results of a brief investigation of the loads in smooth water for 10° angle of dead rise are reported in Technical Note 3608 and are compared with theory for immersed hydrodynamic impact of nonchine bodies. The trend of the experimental variation of load-factor coefficient, draft coefficient, time coefficient and velocity ratio is in good agreement with the theoretical variation.

Technical Note 3619 presents data showing the effect of horizontal restraint of carriage mass in experimental testing facilities upon the general theoretical equations of motion for the prismatic body during a hydrodynamic impact. The data indicate that the carriage mass has little effect for the low trims, since at this condition the resisting water force has only a small component in the horizontal direction, but for the higher trims the effect is appreciable. For the more usual seaplane-design conditions, that is, approach parameters larger than 1.0 and trims up to 15°, the maximum correction for any of the coefficients is 10 percent or less.

Research Techniques

It is frequently desirable to predict the loads that would be experienced with more hazardous control motions or flight conditions than those for which test data exist. Accordingly, considerable effort has been expended in developing and comparing various methods by which such predictions can be made. Fourier and Laplace transforms and the type of analyses used in studies of servomechanisms have been used extensively in this development. It appears from the work accomplished that the concept and use of a unit impulse as a research technique has considerable merit. Simple and rapid methods for determining the time response to a unit impulse from frequency-response data and for evaluating the Fourier transform as a function of time have been derived and are presented in Technical Note 3598. These methods are applicable to linear functions for which Fourier transforms exist, which is usually the case in the treatment of airplane maneuvers. In Technical Note 3701, the method developed in Technical Note 3598 is compared with several other methods of obtaining the time response of linear systems to either a unit impulse or to an arbitrary input from frequency-response data. The comparisons indicate that most methods gave good accuracy when applied to a second-order system; the main difference is in the computing time. In general, the method of Technical Note 3598 was advantageous in all respects, since it was more accurate and required less time.

VIBRATION AND FLUTTER

Flutter

The sonic and supersonic speeds of modern aircraft plus their use of relatively flexible thin wings and stabilizers have caused flutter to assume a more important role in aircraft design. In addition to research on the flutter characteristics of typical aircraft configurations, research is also being carried out to understand better the aerodynamic, structural, and inertial considerations inherent in flutter.

On the basis of an analysis of a large quantity of flutter data taken from subsonic, transonic, and supersonic wind tunnels and from rocket- and bomb-drop tests for a wide variety of wing plan forms, a criterion was derived which permits a rapid estimate of the probability of flutter for lifting surfaces. This criterion groups the significant parameters into simple geometric dimensions and structural properties. Another simple criterion was developed for stall flutter.

A number of swept wings having systematic variations in plan form and structural characteristics have been flutter tested in transonic and supersonic wind tunnels to establish the effect of various parameters on flutter and to serve as a basis for evaluating analytical procedures. Because of the large number of parameters involved, this is a large test program and is still underway.

An alternative to the testing of a systematic series of wind-tunnel models in order to establish the influence on flutter of elastic and inertial structural characteristics is to employ an analog computer whose electrical elements and behavior approximate the elements and dynamic behavior of the structure. Such an analog study has been carried out at the California Institute of Technology and is discussed in Technical Note 3780. Four wings representative of those of current aircraft were considered and the effects of changes in bending and torsional stiffnesses, mass distribution and angle of sweep on the flutter characteristics were determined. A sufficient number of cases were treated to establish the trend over a sizeable range for each parameter.

As reported in the Forty-First Annual Report, 1955, a theoretical study of the flutter of two-dimensional panels was reported in Technical Note 3465. More recently, flutter of panels mounted on the wall of a supersonic wind tunnel was obtained at a Mach number of 1.3. It was found that, at the flow conditions of these tests, increasing the tensile forces in the panel was effective in eliminating flutter, as was shortening the panels or increasing their bending stiffness. No apparent systematic trends in the flutter modes or frequencies could be observed, and it is significant that the panel flutter sometimes involved higher modes and frequencies. The presence of a pressure differential between the two surfaces of a panel was observed to have a stabilizing effect. Initially buckled panels were more susceptible to flutter than panels without buckling. Buckled panels with all four edges clamped were less liable to flutter than buckled panels clamped only on the front and rear edges.

In Technical Note 3638, a preliminary theoretical investigation of the panel flutter and divergence of infinitely long, unstiffened and ring-stiffened, thin-walled, circular cylinders is described. Linearized unsteady potential-flow theory was utilized in conjunction with Donnell's cylinder theory to obtain equilibrium equations for panel flutter. Where necessary, a simplified version of Flügge's cylinder theory was used to obtain greater accuracy. By applying Nyquist diagram techniques, analytical criteria for the location of stability boundaries were derived. This report also includes a limited number of computed results.

One of the most troublesome types of flutter is that involving oscillations of a control surface at transonic speeds, commonly referred to as buzz. In Technical Note 3687, results of wind-tunnel tests of three wing models are presented and it is shown that a large range of change in density of the test medium had little effect on the initial magnitude and initial Mach number of buzz. The buzz frequency decreased somewhat with decrease in density. The Mach number corresponding to the onset of buzz decreased as the wing angle of attack was increased. Mass balance and changes in spring stiffness changed only the oscillation frequency. The test results indicated that placing the aileron at the wing tip delayed the onset of buzz to higher Mach numbers. A comparison of the experimental results with two published empirical analyses showed only qualitative agreement.

Designers of thin aircraft wings must consider the possibility of wing torsion flutter at high angles of attack, which is referred to as stall flutter. The results of an exploratory, analytical, and experimental study of some of the factors which might be of importance in the stall-flutter characteristics of thin wings are presented in Technical Note 3622. The factors considered were Mach number, Reynolds number, density, aspect ratio, sweepback, structural damping, location of the torsion node line, and presence of concentrated tip weights. The importance of aerodynamic torsional damping on the stall flutter of thin wings was demonstrated by comparison of the regions of negative torsional damping measured on a spring-mounted model with the regions of flutter. The results of a series of experiments on a thin wing tested at various spans indicated that compressibility alters the stall-flutter characteristics and that these effects depend upon aspect ratio. A brief study of the inertia effects of concentrated weights at the tip indicated that such effects can be important. An approximate analysis is presented for such configurations.

Aerodynamics of Flutter

It has been demonstrated that generalized forces for a harmonically oscillating wing in pure supersonic flow may be expressed in terms of certain integrals commonly referred to as f_λ functions. These functions have been tabulated on a large computer for a wide range of parameters important to flutter and the tabulated results are presented in Technical Note 3606.

A fundamental study of the aerodynamic forces on an oscillating wing is presented in Technical Note 3643. This report presents the magnitude and phase angle of the components of normal force and pitching moment acting on an airfoil oscillating in pitch about the midchord at both high and low mean angles of attack and for Mach numbers of 0.35 and 0.70. The magnitudes of normal-force and pitching-moment coefficients were much higher at high mean angles of attack than at low angles of attack for some conditions. Large regions of angle of attack and reduced frequency were found wherein one-degree-of-freedom torsion flutter is possible. It was shown that the effect of increasing the Mach number from 0.35 to 0.70 was to decrease the initial angle of attack at which unstable damping occurred. In addition, the aerodynamic damping in essentially the first bending mode was measured for two finite-span, 3- and 10-percent-thick wings for a range of mean angles of attack and reduced frequencies. No regions of negative damping were found for this motion, and it was found that the damping measured at high angles of attack was generally larger than that at low angles of attack.

An experimental study of the lift and moment about the quarter chord of an oscillating wing at high subsonic Mach numbers is presented in Technical Note 3686. A comparison of the experimental magnitude of the lift vector with the theory as given by Dietze showed good agreement. Comparisons with theory of the moments and the out-of-phase component of lift indicated that some refinements in the testing technique are necessary for the experimental determination of these quantities in the transonic speed range.

An experimental wind-tunnel investigation was carried out of the forces, moments, and phase angles on a two-dimensional wing equipped with an oscillating circular-arc spoiler. Schlieren photographs were obtained which showed the flow over and behind the spoiler while it was oscillating. The forces and moments on the wing were obtained from instantaneous pressure-distribution measurements. The results indicated that the effects of Reynolds number on the normal-force and moment coefficients and their phase angles were very small and somewhat erratic. An increase in Mach number increased the normal-force coefficient and had no consistent effect on the moment coefficient, while the phase lag of both the normal force and moment decreased. There was little effect of reduced frequency on the normal-force coefficient; however, increasing the reduced frequency produced an essentially linear increase in the phase lag of the normal force.

Buffeting

Several studies have been made of the available transonic Mach number data on wing dropping, low-lift buffeting, buffet boundaries, and changes in the angle of zero lift for symmetrical airfoils and various airplane configurations. These phenomena are indicated to be allied and are probably the result of shock-induced separated flow. It was found that unswept wings which have airfoil sections 9 percent thick or thicker are susceptible to wing dropping at transonic speeds. Wing dropping may occur even for thin wings, however, if the airfoil contour is not fair. Sweepback only partially relieves the wing dropping and buffeting problem for thick wings. The studies have also indicated that there are combinations of airfoil-thickness ratio, aspect ratio, and sweep angle which may allow flight through the transonic speed range without either wing dropping or buffeting at low lift. Decreases in aspect ratio and thickness ratio and increases in sweepback all tend to alleviate high-speed buffeting. Low-lift buffeting, however, may be induced by the interference effects of thin intersecting surfaces such as a tail arrangement in which the horizontal tail is mounted above the fuselage on the vertical tail. Such a tail arrangement may also be partially responsible for large transonic trim changes and may exhibit an increase in drag over that for a comparable tail arrangement where the horizontal tail is mounted on the fuselage.

An analysis of some statistical properties of the buffet loads measured on the unswept wing and tail of a fighter airplane has indicated that buffeting can be considered as a random process. Buffet loads measured on the wing and tail in both the stall and shock regimes indicated that the wing loads in buffeting can be treated as the response of a simple elastic system to a random input. The wing buffet loads were normally distributed and the probability that a peak load would exceed a given level was in agreement with theoretical results. There was evidence that the tail buffet loads were not normally distributed as the wing loads but appeared to represent a more complicated process. The spectrum of the wing-root shear indicated that the buffet loads were primarily associated with response in first symmetrical bending. The spectrum for the tail-root shear indicated that the tail buffet loads were associated with the fuselage-torsion or tail-rocking mode. This study was reported in Technical Note 3733.

AIRCRAFT STRUCTURAL MATERIALS

Structural Materials at High Temperatures

Aerodynamic heating continues to be the source of the most perplexing and urgent problems in the field of aircraft structural materials. This is true in extreme cases such as long-range ballistic missiles where the severity of the requirements will clearly necessitate the development of new kinds of structural materials and new kinds of test facilities. In addition, it is true for less severe applications such as manned airplanes, where the effects of high temperatures on the common engineering properties of existing materials are so inadequately known that the designer lacks the handbook data he needs to arrive at an efficient, yet safe, design. In effect, heat has introduced a new dimension in all material problems; strain-rate effects, changes in modulus, creep, stress rupture, thermal stress, thermal conductivity, and many other temperature-linked characteristics, which heretofore could be ignored, will have to be taken into consideration in the future. Some of these problems are under attack on several fronts.

The tensile properties of a number of structural materials under rapid-heating conditions were determined by means of a new type of test (a so-called rapid-heating test) in which the material is first loaded and then heated at various heating rates until yield and failure occur. Sheet materials used in this investigation included 7075–T6 and 2024–T3 aluminum alloys (Technical Note 3462, reported in the Forty-first, 1955, Annual Report), Inconel and RS–120 titanium alloy (Technical Note 3731), HK31XA–H24 magnesium alloy (Technical Note 3742), and AZ31A–O magnesium alloy (Technical Note 3752). In these tests, heating rates have been varied from 0.2° to 100°F per second. At the higher heating rates, the materials were found to be stronger, in general, than under constant-temperature conditions when loaded at a strain rate of 0.002 per minute. In most cases, yield stress, rupture stress, and temperature have been found to be correlated by means of a temperature-rate parameter. Some of the materials, such as the new high-temperature magnesium alloy HK31XA–H24, exhibited a marked increase in strength at high heating rates in the high-temperature region. Other materials, such as 2024–T3 aluminum alloy and RS–120 titanium alloy, behaved in a very complicated manner under rapid heating.

In an investigation, conducted at the University of Alabama under NACA sponsorship, the fatigue strengths at 10 million cycles of two of the more promising titanium alloys, 3Mn Complex and 3Al–5Cr, were determined at 200°, 400°, 600°, 800°, and 1,000°F. Data of this sort are needed for the evaluation of these new alloys of titanium before the role they can play in the solution of some phases of the high-temperature problem can be predicted.

The use of thermal insulation on the surface of structural materials is one of several possible methods of defeating the adverse effects of aerodynamically generated heat. However, there are many fundamental and technological difficulties, such as the realization of adequate strength of the coating-to-metal bond, which stand in the way of achieving practicable coatings. Results of an investigation conducted at the National Bureau of Standards and reported in Technical Note 3679 show that copper ions in the coating have the effect of producing a significant increase in the adhesion between the coating and the surface of stainless steel.

Laminates of nonmetallic materials possess characteristics which uniquely suit them for use in certain components of aircraft. The rate of deterioration of their mechanical properties with temperature, however, is a deterrent to their use in very fast aircraft. Future progress demands that improved materials be developed and further test data be obtained to enable the designer to gage the range of applicability of existing laminates. In an investigation conducted at the University of Illinois and reported in Technical Note 3414 the static-tension, static-compression, tension-creep, and time-to-fracture characteristics of melamine-resin glass-fabric laminates and silicone-resin glass-fabric laminates at temperatures up to 600°F were determined. In the analysis of the creep data an equation based on the activation-energy theory, which describes the effects of stress, time, and temperature is reported.

Fatigue

Failure by fatigue has always been and still is a potential hazard in aircraft structures and is therefore an important subject for research. Although steady and significant progress has been made in understanding the phenomena of fatigue and in designing structures that will incorporate characteristics that both lessen the likelihood of fatigue cracks and preserve the integrity of the structure when a crack does develop, there are still many aspects of the fatigue problem that require solution. Among these is the stress-concentration effect of geometrical discontinuities on fatigue properties of aircraft structural materials. Technical Note 3631 presents the results of axial-load fatigue tests on 2024–T3 and 7075–T6 aluminum-alloy sheet specimens with central holes. Specimens with various combinations of hole diameters and widths were tested to provide data suitable for study of the geometrical size effect.

In Technical Note 3293, which reports an investigation conducted at the National Bureau of Standards, the results of cumulative-damage tests of 7075S–T6 and 2024S–T3 aluminum-alloy sheets under various loading conditions are given. The cumulative damage ratio, which should be unity if the theory were absolutely correct, was found to vary from 0.568 to 1.440; however, 40 percent of the cumulative damage ratios were within 10 percent of unity.

At the University of California, a study (Technical Note 3495) was made of fatigue under combined repeated stresses with superimposed static stress. A comprehensive critical review of the literature where such tests were reported was made. In addition, tests were performed to determine the effects of static compression on alternating torsion, which was the only combination that had received no previous attention. The results were compared with the predictions of theory. It was shown that the Orowan theory of the effects of combined stress and cyclic stress on fatigue can be modified to predict the observed test results.

In an investigation conducted at the Battelle Memorial Institute, effects of notch severity on the initiation and propagation of fatigue cracks in ¼- and 2-inch-diameter notched bars were determined in rotating bending fatigue tests. These bars consisted of 2024S–T4 aluminum alloy with stress concentration factors of 5.2 and 13.9. The results reported in Technical Note 3685 indicate that cracks initiate in severely notched bars earlier than in unnotched or mildly notched bars. Discernible cracks occurred at 1,000 cycles at stress levels that would result in failure at 200,000 to 1,700,000 cycles. Differences in results of the tests of the ¼- and 2-inch-diameter bars indicated a size effect, which was attributed to residual stresses in the larger bars.

Fatigue stressing and the accumulation of damage have effects on the internal friction of metals and alloys.

Internal friction measurements are therefore useful in the study of the fundamentals of fatigue. In an investigation conducted at the California Institute of Technology and reported in Technical Note 3755, a correlation of internal friction and torsional fatigue was made at various temperatures. The results indicated the existence of a critical temperature at which fatigue life reached a minimum, and the effect of this temperature on internal friction was found to be substantial. In addition, the recovery of internal friction during periods of rest after fatigue stressing was observed. This recovery was found to be dependent on both stress level and temperature. Attempts were made to rationalize the relationship between the changes in the characteristics of internal friction and the inadequately understood phenomena of damage, recovery, and coaxing in fatigue.

Plastic Behavior of Metals

An understanding of the plasticity of metals is essential to the understanding of strength, ductility, resistance to brittle fracture, workability, and other properties of metals which account for their usefulness as aircraft structural materials. The NACA is conducting research in various areas of this field.

Technical Note 3681 reports results of an investigation conducted at the Battelle Memorial Institute on the plastic behavior of binary aluminum alloys by internal-friction methods. Effects of strain rate, amount of strain, heat treatment, temperature, and cyclic frequency on internal friction were determined, and the results were analyzed and rationalized in the framework of the dislocation theory of plasticity.

During plastic deformation of materials, distortions occur which are not predictable by the usual assumption of isotropy. Errors in strain of 50 percent and more resulting from anisotropy in the plastic range would not be uncommon for some of the materials used in aircraft construction. A series of tests, described in Technical Note 3736, are utilized to establish semi-empirical relationships between Poisson's ratio and the properties of the materials as shown by their stress-strain curves. The tests also show that there is no permanent change in volume of the metals tested after stressing into the plastic range.

In an investigation conducted at Battelle Memorial Institute and reported in Technical Note 3728, the structure of slip lines developed in single crystals of aluminum at various stages during tensile deformation were examined in an electron microscope. On the basis of experimental results from this work and others from the literature, a mechanism for slip-band formation based on dislocation theory was formulated. The possible effects of short-range ordering on deformation modes are discussed.

Non-Metallic Materials

Cotton fabric-phenolic laminates are useful structural materials for aircraft, but the knowledge of the effects of processing and manufacturing variables on their properties is inadequate. In an investigation conducted at the National Bureau of Standards and reported in Technical Note 2825, tests were conducted to determine strength properties of (1) several untreated commercial cotton fabric-phenolic sheet laminates, (2) the same materials after exposure to typical postforming heating cycles, (3) industrially postformed shapes made from one of these materials, (4) industrially-made and laboratory-molded shapes, and (5) flat panels postformed from the laboratory-molded shapes. It was shown that molding of phenolic laminates may or may not affect the strength, depending on the fabrication techniques used.

OPERATING PROBLEMS

During the past year, the NACA has continued to conduct research on various problems that are associated with the operation of today's modern high-speed aircraft. It is recognized that as the performance of the nation's aircraft is increased new problems are encountered and some old problems become more important in the day-to-day operation of these aircraft. Some of the most important current problems include the effect of aircraft noise on aircraft and people; atmospheric effects such as icing, turbulence, lightning, temperature, and density; and flight safety, which includes crash fire, survival, aircraft braking, visibility, engine reliability, foreign-object damage, and other problems. Working with the NACA Committee on Operating Problems are the Subcommittee on Aircraft Noise, the Subcommittee on Meteorology Problems, the Subcommittee on Icing Problems, and the Subcommittee on Flight Safety.

The effects of the intense noise from modern aircraft and missiles present one of the most serious problems which faces the civil and military aircraft operators today. This problem offers a great challenge to our technical ability to find a satisfactory solution. The NACA with the advice and active help of the Subcommittee on Aircraft Noise has expanded its research on noise with particular emphasis on understanding the mechanisms of noise production and noise suppression. The scope of the last several meetings of this Subcommittee has been expanded to be, in effect, limited conferences on aircraft noise and have had international participation. These meetings were arranged to provide a free and comprehensive discussion of the noise problems and research efforts of various groups active in this field. The results of such meetings have been profitable: A cooperative effort to utilize the intellectual resources and research facilities of all concerned with aircraft noise is essential to the solution of the noise problem.

As part of the constant NACA effort to summarize, discuss, and present recent NACA research results so that industry can best use these results for practical aircraft applications, technical conferences are held when appropriate for representatives of pertinent segments of the aircraft industry. On April 17, 1956, the NACA Conference on Airplane Crash-Impact Loads, Crash Injuries, and Principles of Seat Design for Crash Worthiness was held at the Lewis Flight Propulsion Laboratory. The NACA summarized the results of several years' work in the field of crash survival and proposed design criteria which, if applied, could improve aircraft seat design for crash survival. Civil and Military aircraft operators, manufacturers, and seat manufacturers now have the material presented at this conference as a guide for seat design. This material for the first time includes experimental data from actual dynamic-crash-load studies utilizing actual full-scale cargo, transport, and fighter-type aircraft.

A Summary of results of most of the recent unclassified investigations on operating problems is presented in the following paragraphs.

AIRCRAFT NOISE

The noises produced by current aircraft and missile power plants have increased to such intense levels that they affect the integrity of aircraft and missile structures, equipment, and control systems as well as present serious bioacoustic, efficiency, and annoyance problems for persons exposed to the noises. The effect of noises and related vibrations must now be considered as one of the principal elements of aircraft or missile design, and a specific NACA research program is directed toward obtaining full understanding and control of the production and effects of high-intensity noises.

While the noises produced by jet exhausts remain of primary concern to the NACA, research is also being conducted on boundary-layer and propeller noise, on the effects of noise on structures, and on propagation of noise through the atmosphere.

Jet Noise

NACA research has established that jet noise is produced by the turbulent mixing of the jet exhaust with the surrounding air; consequently, detailed investigations of the mixing phenomena are under way. One phase of this study consisted of measuring the turbulence in a subsonic jet by use of a hot-wire anemometer. The results are described in Technical Note 3561.

The studies begun last year of devices for altering the jet exhaust flow and thereby reducing jet noise are continuing. Tests on toothed and ejector nozzles are described in Technical Notes 3516 and 3573. Tests of the use of square, rectangular, and elliptical nozzles for subsonic jets, as reported in Technical Note 3590, showed that simple changes in jet-nozzle shape had very little effect on noise generation. It is shown in that report, however, that if the exiting flow is supersonic, a convergent-divergent nozzle operating near its design point will produce less noise than an ordinary convergent nozzle.

With the data presented in Technical Note 3591 for an investigation of the scaling parameters between various jet engines and model jets, it is possible to estimate the far noise field of a jet engine from its flow characteristics. Detailed data are also presented in that report for the noise field around a modern jet engine operating under static conditions with and without afterburner.

A method for limiting the noise received on the ground during takeoff of a jet aircraft is to control the operational techniques. A study of the effects of various climbing procedures, reported in Technical Note 3582, showed that lowest effective noise levels over the largest ground area will be obtained when the aircraft is climbing on the steepest flight path consistent with minimum safe airspeed.

Boundary Layer Noise

In addition to the noise problems caused by a jet exhaust, serious problems result from the noise produced by the boundary layer flow over the surface of the fuselage and wings. Preliminary flight tests have been made to determine the surface pressure fluctuations caused by a turbulent boundary layer. The relation of boundary-layer noise to Reynolds number, velocity, and altitude has been studied and further work is being done on flight at high subsonic velocities.

A study by the California Institute of Technology of subsonic and supersonic flow of air past rectangular cavities cut into a flat surface indicated that the cavities would emit a strong acoustic radiation. From that work as reported in Technical Note 3487 and the above NACA flight tests it appears that noise considerations may be a primary factor in establishing the limits for such items as surface finish and size and shape of surface cutouts or protuberances for high-speed aircraft.

As a part of its work on aerodynamic noises under NACA sponsorship, the California Institute of Technology developed an instrument of fairly simple design for measuring time correlation functions of two stationary random-input signals. The device and its use in determining auto-correlation functions are discussed in Technical Note 3682.

Propeller Noise

Instrumentation suitable for making flight measurements of the free-space sound pressures in the immedi-

435875—57——6

ate vicinity of a propeller in forward flight has been developed and successfully used on a fighter airplane up to a Mach number of 0.72. The sensing element is a capacity microphone housed in a streamlined probe and used in conjunction with an oscillator to convert the pressure pulses into a frequency-modulated signal which is telemetered to the ground. At the ground receiving station, the telemetered signal is detected and recorded on magnetic tape. Subsequently, the recorded signal is converted to a varying voltage which is fed into a heterodyne frequency analyzer. This instrumentation is reported in Technical Note 3534.

Effects of Noise on Structures

NACA research is continuing on the problems of designing and constructing structures that will be suitable for use in the intense-noise-pressure fields near propellers and jets. The response of various structural systems to acoustic inputs, the stresses encountered in the systems, the fatigue characteristics of the systems, and the effects of insulation and damping on the structure are all under study. Stress data has been obtained for panels exposed to discrete and random noise levels of over 160 decibels. The fatigue life of panels was noted to decrease markedly for further nominal increases in the noise intensity level.[26] [27]

Attenuation of Noise

The NACA has continued its sponsorship of research at the Massachusetts Institute of Technology to determine the effects of terrain and atmospheric conditions on the attenuation of noise. A theoretical and experimental investigation of the sound field about a point source over a plane boundary in the presence of a vertical temperature gradient is reported in Technical Note 3494. Methods are presented for analyzing the effects of temperature gradients on the attenuation of sound in the shadow zone of a sound field. A further study has produced a semiempirical method for the calculation of a sound field about a source over ground. This study considered the effects of vertical temperature as well as wind gradients and the scattering of sound by turbulence into the shadow zone (Technical Note 3779).

A theoretical study of the sound field from a random noise source above ground as measured by a receiver with finite band width is presented in Technical Note 3557. It is shown that the far sound field still contains two major regions so far as attenuation over ground is concerned. In the first region, the sound pressure level decreases approximately 6 decibels per doubling of distance. In the second region, however, beyond a certain distance from the source, the level decreases monotonically 12 decibels per doubling of distance.

[26] See Regler paper listed on p. 78.
[27] See Lassiter, Hess, and Hubbard paper listed on p. 78.

FLIGHT SAFETY

During this second year of its existence the NACA Subcommittee on Flight Safety has not only monitored research into problems directly related to safety, such as fire, ditching, engine reliability, crash loads, and crash survival, but also studied results of research in other specialized fields so that they could be channeled directly to aircraft designers and operators through their safety organizations for immediate consideration. The following information shows the results of varied research projects that are significant for particular phases of aircraft operation which are considered to be most important from a safety standpoint.

Landing Problems

Operating statistics indicate that the landing phase of flight is most important from the standpoint of safety. There is much to be learned about the many facets of the landing problem. The NACA is actively studying many parts of the problem and has during the past year reported the results obtained with respect to landing loads, landing statistics, runway roughness and aircraft braking. In addition, the NACA has given wide distribution to the results obtained by other organizations investigating specific phases of the problem, namely nose-wheel shimmy (Technical Memorandum 1391) and friction of aircraft tires (Technical Note 3294). In the first of these two reports, general concepts regarding the effects of the condition of the tire, the type of rolling motion, and the loading are discussed. In Technical Note 3294, the results of a systematic study to determine the effects of temperature and normal pressure on frictional resistance between tire-tread material and concrete are given. Although these data are only a small part of the overall problem, they do offer some insight into the problem of tire-to-runway friction coefficient problem which is being attacked through both experimental flight and laboratory studies at the NACA Langley Laboratory.

In recent years, propeller reversing has been employed very effectively to assist in braking the aircraft during the landing roll on modern propeller-driven aircraft. A similar reverse-thrust device for the modern jet aircraft would be equally useful and can be accomplished by the reversing of the direction of the propulsive jet during landing. The NACA has completed an experimental investigation in which three types of thrust reversers were studied. Models of a target type, a tailpipe cascade type, and a ring cascade type were tested and the effects of design variables on performance and reversed-flow boundaries were determined. This work was reported in Technical Note 3664 and the results indicate that reverse-thrust ratios of from 40 to 80 percent could be obtained and that all three types had satisfactory thrust-modulation characteristics. Performance and operational studies of a full-scale jet engine thrust reverser (Technical Note 3665) of the target type utilized on a turbojet engine were also conducted. This device was pylon mounted under the wing of a cargo airplane to simulate a jet transport. The thrust reverser was operated for both stationary and taxi conditions, but the airplane was not flown. In addition to obtaining the performance of the thrust reverser, heat-rise patterns and rates resulting from impingement of the reversed hot gases on a simulated lower wing were also measured during periods of thrust reversal. Reingestion of the reversed hot gases into the engine inlet constituted an additional operating problem in that the temperature levels were raised throughout the engine and the reversed-thrust ratio was reduced. Taxi tests indicated that at ground speeds of 62 knots, the free-stream velocity was sufficient to prevent the reversed gas flow from entering the engine inlet.

Fire

The NACA has continued its research with turbojet and turboprop types of engines into the problems of crash-fire inerting and, in addition, has been studying the problems of flight fires in jet aircraft. Effective fire-fighting methods are still an important aspect of the problem. At the heart of the problem is the need for potent fire-extinguishing agents which have properties that make them suitable for use on aircraft. In Technical Note 3565, the results of a study which explains the quenching action of halogenated agents in the fire-extinguishing process are given. It is concluded that the presence of halogen in an agent need not reduce its fire-fighting ability provided that there is enough halogen to make the agent noninflammable. The assumption that halogenated agents act merely by chain-breaking reactions with active particles is consistent with the experimental facts available and will help guide the selection of other halogenated agents for further tests of their fire-fighting properties.

Technical Note 3560 presents the results of an investigation conducted at the University of Cincinnati under the sponsorship of the NACA on the spontaneous ignition of lubricants of reduced inflammability. In the initial phase of the investigation, the spontaneous-ignition characteristics of approximately 50 organic compounds were investigated and observations were made on the effects of structure on ignition. In studying compounds of interest as lubricants, it was found that hydrogenated polyisobutylene showed remarkable resistance to spontaneous ignition. Results indicate that those esters possessing high autoignition temperatures have low molecular weights, while those having low molecular weights in the lubricant range show poor resistance to spontaneous ignition.

Gust Alleviation

Whenever rough air is encountered in flight, the recommended practice is to reduce the speed of the airplane to the design speed for maximum gust intensity. When encountering rough air, the pilot does not always have time or advanced warning so that he can reduce the airspeed to the design speed. In these cases, the distance and maneuvering required to reduce speed may have an important bearing on the loads imposed on the airframe. Technical Note 3613 presents the results of an investigation of the problem of reducing the speed of a jet transport in flight. It was found that the required distance was much greater for a jet transport than for a typical piston-engine transport at the same altitude. The distance was also found to increase with altitude up to the altitude for maximum true airspeed. The increased distance for the jet transport was primarily the result of increased kinetic energy and to a lesser extent that of lower drag coefficients. These results are believed to be qualitatively correct for high-speed transport aircraft. The use of aerodynamic brakes, thrust reversal, or a climbing maneuver has been shown to be effective in reducing the distance required to reach the rough-air speed.

The ability of the human pilot to fly a precision course in rough air has been questioned and compared with the ability of an airplane autopilot combination to do the same task. Although the NACA has not studied this question directly, it has conducted theoretical studies involving various types of autopilots in an attempt to learn the characteristics of airplane response to gusts. The results of two such investigations have been published in Technical Notes 3635 and 3603. The results given in the former report indicate that the response to side gusts can be noticeably reduced. In the latter report, when the airplane was flown by various autopilots, the increased yaw damping greatly reduced the resonance associated with Dutch-roll of the airplane. The addition of an autopilot supplied directional stability and roll stability and greatly reduced the yaw and roll responses to gusts. Autopilots that held side forces to low values and provided good course response to command signals allowed large roll response to side gusts.

The NACA has been studying various means of increasing the smoothness of flight through rough air, both theoretically and experimentally. One of the most promising methods utilizes an autocontrol system in which the flaps and elevators are operated in accordance with indications of changes in angle of attack to maintain constant lift and zero pitching moment of the airplane. A detailed analysis of this system and its various refinements is presented in Technical Note 3597, including a study of the transient response of the airplane for both gust disturbances and longitudinal control inputs. The aerodynamic characteristics necessary for optimum gust alleviation are derived and the response of this system is compared with that of the basic airplane. In order to study these analytical results in flight, an experimental investigation was conducted with a light transport airplane whose controls were modified to the extent necessary to provide gust alleviation. The results indicate that the gust alleviation system is at least capable of alleviating the normal acceleration due to gusts by 50 percent at a frequency of 0.6 cycle per second, the natural frequency of the airplane, and by 40 percent at a frequency of 2 cycles per second. The airplane can be controlled adequately when this gust alleviation system is operating.

Other devices that have been proposed for reducing the acceleration effects of rough air are spoilers, deflectors, and spoiler-deflector combinations. These devices have been investigated for both swept- and unswept-wing models. The results have been reported in Technical Note 3705 and it would appear from gust-tunnel and wind-tunnel tests that a forward-located fixed deflector would be a practical and effective alleviator of gust loads on an airplane having unswept wings. Preliminary results on a model having a 35°-swept-back wing have indicated that deflectors, in order to have the same effectiveness as reported for the unswept wing model, would have to be located more to the rearward on the swept wing and would possibly require larger projections if they are to have the same effectiveness they had on the unswept-wing airplane.

Optimum Flight Paths

The climb of turbojet aircraft, and the effects of tangential accelerations, have been analytically determined for minimum time of climb, climb with minimum fuel consumption, and steepest climb. For each flight condition, the optimum Mach number was obtained from the solution of a sixth-order equation whose coefficients are functions of two fundamental parameters: the ratio of minimum drag in level flight to the thrust and the Mach number which represents the flight at constant altitude and maximum lift-drag ratio. Diagrams have been prepared for the quick calculation of the optimum Mach numbers and the effect of acceleration on the rate of climb in tropospheric and stratospheric flight.

Airspeed Measuring Systems

Accurate determination of Mach number is fundamental to any detailed flight research and is of particular importance in the transonic speed range where many of the aerodynamic parameters vary markedly with Mach number. In order to conduct extensive research in this speed range, it was necessary that a suitable airspeed system be devised. Accordingly, calibrations of four airspeed systems installed in a turbojet fighter were determined in flight at Mach numbers up to 1.04 by the NACA radar-phototheodolite method (Technical Note 3526). The results indicate that, of the systems investigated (a nose boom, two different wing-tip booms, and a fuselage-mounted service system), the nose-boom installation is the most suitable for research use at transonic and low supersonic speeds. The static-pressure error of the nose-boom system is small and constant above a Mach number of 1.03 after passage of the fuselage bow shock wave over the airspeed head.

The need for design information to provide rigid tubes to measure total head pressures correctly at high angles of attack and at high speeds has arisen because of the development of airplanes having good maneuverability at supersonic speeds. Conventional tubes, both rigid and swiveling, are unsatisfactory under these conditions. In Technical Note 3641, the results of wind-tunnel tests of 54 total-pressure tubes have been summarized and data are presented on the effects of inclination of the airstream on measured pressures at subsonic, transonic, and supersonic speeds. These data are in a form which permits a more detailed comparison of the effects of pertinent design values.

Spin Hazards and Recovery

The pilot's loss of orientation during spins, especially during unintentional spins, is a rising problem and has apparently led to a number of recent accidents and near-accidents with both trainer and fighter aircraft during acrobatic maneuvers and after recovery from erect spins. In Technical Note 3531, the nature of inverted spins, the optimum control technique for recovery, and some of the apparent reasons for a pilot's loss of orientation are discussed. It is pointed out that a pilot in an inverted spin should attempt to orient himself with respect to direction of turn by referring to the airplane rate-of-turn indicator in order to determine properly the direction of the yawing component of the total spin rotation. Optimum recovery from the inverted spin should then be obtainable by rapidly reversing the rudder from full with this yawing rotation to full against it while the control stick is held full forward and laterally neutral and, shortly thereafter, the stick should be moved from full forward to full back while it is maintained laterally neutral.

The general policy for recovery from either intentional or accidental spins has been to cut off power as soon as possible after the spin is initiated, because of possible adverse effects. In some instances however, pilots have flown out of an otherwise uncontrollable spin by application of full power in a propeller-driven airplane. Such results from power-on spins may have been due to increased effectiveness of the controls in the slipstream. For a jet engine, however, the situation is different, and unpublished data indicate that thrust alone might be of little assistance. For both propeller-driven and jet-propelled airplanes, spin and spin-recovery characteristics may differ for power-on and power-off conditions, as well as for power-on spins to the right and to the left. These differences may at times have caused serious difficulty in recovering from spins in one direction, whereas recoveries from spins in the other direction could be readily achieved. The differences in spins and recoveries may have been due, in part, to the gyroscopic moments produced by rotating propellers or rotating parts of jet engines. For a jet-propelled airplane, the rotating parts of the engine may continue to rotate at nearly full speed for a long time after power is cut off. A preliminary investigation has been made and reported in Technical Note 3480 to determine the gyroscopic effects of jet-engine rotating parts on the erect spin and recovery characteristics of a model of a military attack airplane. Results indicate that rotating parts affected the spin characteristics differently depending on the type of mass load distribution and the direction of spin.

Control Device for Personal-Owner-Type Airplanes

Although most present-day personal-owner-type airplanes possess a slight degree of inherent spiral stability in cruising flight, they show unstable spiral tendencies under operational conditions. The main reasons for this apparent spiral instability are a lack of means for trimming the airplane laterally and directionally. A variation of lateral and directional trim with airspeed and control-system friction prevents the control surfaces from returning to trim position after control deflection. The specific problems facing the pilot of a personal-owner-type airplane are that of maintaining the airplane in wings-level position during times when there is no natural horizon reference and that of keeping, the airplane from diverging spirally while he may be preoccupied with navigational problems. It has been demonstrated that the pilot's sense of orientation is unreliable in the absence of a visual reference, as may be the case when inadvertently or unavoidably encountering instrument weather. Technical Note 3637 describes the results of a flight investigation to determine the effectiveness of an automatic aileron trim control device installed in a personal-owner-type airplane. The results indicate that the device is capable of maintaining the airplane in equilibrium over its operational speed range under directional out-of-trim conditions that would cause rapid divergence of the basic airplane. The device also prevents excessive heading wander and airplane gyration in turbulent air without pilot control. A means is provided for holding the airplane in a stabilized turn to facilitate mild maneuvering through the use of the automatic control.

Precision of Instrument Flight in Helicopters

Early studies of helicopter instrument flight indicated the need for improved handling qualities, particularly for low-speed flight and for precision maneuvers such as instrument approaches, sonar dipping, or hoist operations. Although a number of stability parameters affect the handling characteristics, damping about the principal axes appeared to be a worthwhile subject for initial study. Technical Note 3537 presents the results of a study of the effects of increased damping in roll, pitch, and yaw on the instrument flight-handling qualities of a single-rotor helicopter. Electronic components were used to vary the damping of the helicopter, and these variations were evaluated by performing precision maneuvers while flying on instruments. The studies indicated that, for a representative single-rotor helicopter, increased damping can improve the accuracy of the maneuvers and reduce the effort required of the pilot, particularly at low forward speeds. For the speed range considered (25 to 65 knots), increased damping in roll was found to be particularly effective, much more effective than corresponding changes in yaw and pitch.

AERONAUTICAL METEOROLOGY

Atmospheric Turbulence

Previously evaluated effective gust velocities, U_e, from the data available for both convective and frontal types of thunderstorms have been converted to the recently defined derived gust velocities, U_{de}, which take into account the variations with altitude of the airplane response to gusts. The results, given in Technical Note 3538, indicate that the intensities of the derived gust velocities are essentially constant for altitudes up to approximately 20,000 feet in thunderstorms and that an approximate 10-percent reduction in the intensity occurs as altitude is increased to 30,000 feet.

The NACA provided the Cambridge Research Center of the Air Force with a VGH recorder for measuring turbulence in a flight investigation of the jet stream and the Sierra Mountain Wave. Evaluation of the data showed that the turbulence encountered during the flights was generally light.

A review was made of available information concerning continuous operation of airplanes through rough air at low altitudes and high speeds. From the standpoints of crew efficiency and flight precision, it appears that reductions in the loads and motions due to turbulent air to about one-third of those for present operational airplanes may be required for low-altitude flight. A study of design features indicated that the major factors that effect such reductions are increased wing loadings and reduced lift-curve slopes. Reductions in lift-curve slopes accompany low-aspect-ratio, swept-back, and flexible wings. Changes in stability for airplanes with satisfactory stability characteristics were not significant when the loads were changed in rough air. For configurations with low damping, which causes amplification of the loads in continuous turbulence, the use of augmented damping can result in significant reductions in loads.

Characteristics of Icing Cloud

A statistical survey and a preliminary analysis were made of icing data collected from scheduled flights over the United States and Canada from November 1951 to June 1952 by airline aircraft equipped with NACA pressure-type icing-rate meters. Over 600 icing encounters were logged by three airlines operating in the United States, one operating in Canada, and one operating up the Pacific Coast to Alaska. The data provide relative frequencies of icing cloud variables such as horizontal extent of icing, vertical thickness of icing clouds, air temperature, icing rate, liquid-water content, and total ice accumulation.

Liquid-water contents were higher than those from earlier research flights in layer-type clouds but slightly lower than previous ones from cumulus clouds. Broken-cloud conditions, indicated by intermittent icing, accounted for nearly one-half of all the icing encounters. About 90 percent of the encounters did not exceed a distance of 120 miles, and continuous icing did not exceed 50 miles for 90 percent of the unbroken conditions. Icing-cloud thicknesses measured during climbs and descents were less than 4,500 feet for 90 percent of the vertical cloud traverses.

ICING PROBLEMS

Droplet Impingment

Experimental studies have been made in the NACA icing tunnel to determine the effect of a flapped truncated airfoil on surface velocity distribution and droplet-impingement rates and limits. A 6-foot-chord NACA 65_1–212 airfoil was cut successively at the 50- and 30-percent-chord stations to produce the truncated airfoil sections, which were equipped with trailing-edge flaps to alter the flow field. The results indicated that the correct use of such airfoils may permit impingement and icing studies to be conducted with full-scale leading-edge sections in existing small icing tunnels.

The paths of icing cloud droplets into two engine inlets have been calculated (Technical Note 3593) for 0° angle of attack and for a wide range of meteorological and flight conditions. In both types of inlets, the inlet air velocity of one being 0.7 that of the other, a prolate ellipsoid of revolution (10 percent thick) represents either part or all of the forebody at the center of an annular inlet to an engine. The configurations can also represent the fuselage of an airplane with side ram-scoop inlets. Results indicated that the amount of water ingested is not sensitive to small changes in shape of the outer wall, that impingement on the cowl (i. e., amount and distribution) is quite sensitive to the physical shape and surface condition of the wall, and that the use of screens and boundary-layer-removal scoops at the entrance requires careful design because of the shadow zone (zero water concentration) and regions of high concentration. In addition, a general concept showed that lowering the inlet velocity ratio lowers the ingestion efficiency.

The impingement characteristics of several other bodies have been obtained from droplet-trajectory calculations. For an NACA 65A004 airfoil at 0° angle of attack, the amount of water in droplet from impinging on the airfoil, the area of droplet impingement, and the rate of droplet impingement per unit area of the airfoil surface were calculated as given in Technical Note 3586. The results were compared with those previously reported for the same airfoil at angles of attack of 4° and 8°.

For a sphere in an ideal fluid flow, droplet impingement data and equations for determining the collection efficiency, the area, and the distribution of impingement have been presented in terms of dimensionless parameters (Technical Note 3587). The range of flight and atmospheric conditions covered in the calculations was extended considerably beyond the range covered by previously reported calculations for a sphere.

A study has also been made of water-droplet impingement on a rectangular half body in a two-dimensional incompressible flow field (Technical Note 3658). Data on collection efficiency and distribution of water-droplet impingement were obtained by means of a mechanical differential analyzer.

Icing Protection

A better understanding of the performance and penalties of pneumatic de-icers can aid in selecting ice-protection systems for aircraft. Accordingly, an evaluation in icing conditions was made of two types of pneumatic de-icers, one having spanwise inflatable tubes and the other having chordwise inflatable tubes (Technical Note 3564). Measurements were made to determine lift, drag, and pitching-moment changes caused by inflation of the de-icer boots and by ice formations on the boots. In order to help determine the aerodynamic effects of size and location of ridge-type ice formations on an airfoil, spanwise spoilers mounted on the airfoil at various chordwise locations were also studied.

A preliminary experimental study was conducted to determine the feasibility of preventing rain from impinging on aircraft windshields by use of a high-velocity jet-air blast. By this means, raindrops are broken up into a multitude of small droplets by the jet-air blast and deflected around the windshield. The deflection appears feasible for flight speeds up to 150 miles per hour for low-angle (35° or less) windshields. However, visibility through the mist generated by raindrop breakup is a problem requiring solution.

RESEARCH PUBLICATIONS

REPORTS

1210. Analysis of Turbulent Heat Transfer, Mass Transfer, and Friction in Smooth Tubes at High Prandtl and Schmidt Numbers. By Robert G. Deissler.
1211. Experimental Investigation of Free-Convection Heat Transfer in Vertical Tube at Large Grashof Numbers. By E. R. G. Eckert and A. J. Diaguila.
1212. Analog Study of Interacting and Noninteracting Multiple-Loop Control Systems for Turbojet Engines. By George J. Pack and W. E. Phillips, Jr.
1213. Minimum-Drag Ducted and Pointed Bodies of Revolution Based on Linearized Supersonic Theory. By Hermon M. Parker.
1214. Statistical Measurements of Contact Conditions of 478 Transport-Airplane Landings During Routine Daytime Operations. By Norman S. Silsby.
1215. Impingement of Cloud Droplets on a Cylinder and Procedure for Measuring Liquid-Water Content and Droplet Sizes in Supercooled Clouds by Rotating Multicylinder Method. By R. J. Brun, W. Lewis, P. J. Perkins, and J. S. Serafini.
1216. Charts for Estimating Tail-Rotor Contribution to Helicopter Directional Stability and Control in Low-Speed Flight. By Kenneth B. Amer and Alfred Gessow.
1217. Theoretical Prediction of Pressure Distributions on Nonlifting Airfoils at High Subsonic Speeds. By John R. Spreiter and Alberta Alksne.
1218. Effect of Ground Interference on the Aerodynamic and Flow Characteristics of a 42° Sweptback Wing at Reynolds Numbers up to 6.8×10^6. By G. Chester Furlong and Thomas V. Bollech.
1219. Measurement and Analysis of Wing and Tail Buffeting Loads on a Fighter Airplane. By Wilber B. Huston and T. H. Skopinski.
1220. Calculations of Laminar Heat Transfer Around Cylinders of Arbitrary Cross Section and Transpiration-Cooled Walls With Application to Turbine Blade Cooling. By E. R. G. Eckert and J. N. B. Livingood.
1221. Theoretical Study of the Tunnel-Boundary Lift Interference Due to Slotted Walls in the Presence of the Trailing-Vortex System of a Lifting Model. By Clarence W. Matthews.
1222. A Free-Flight Wind Tunnel for Aerodynamic Testing at Hypersonic Speeds. By Alvin Seiff.
1223. Theoretical and Experimental Investigation of Heat Transfer by Laminar Natural Convection Between Parallel Plates. By A. F. Lietzke.
1224. Effects of Wing Position and Fuselage Size on the Low-Speed Static and Rolling Stability Characteristics of a Delta-Wing Model. By Alex Goodman and David F. Thomas, Jr.
1225. Determination of Lateral-Stability Derivatives and Transfer-Function Coefficients from Frequency-Response Data for Lateral Motions. By James J. Donegan, Samuel W. Robinson, Jr., and Ordway B. Gates, Jr.
1226. A Method for the Design of Sweptback Wings Warped to Produce Specified Flight Characteristics at Supersonic Speeds. By Warren A. Tucker.
1227. An Investigation of the Maximum Lift of Wings at Supersonic Speeds. By James J. Gallagher and James N. Mueller.
1228. Calculated Spanwise Lift Distributions, Influence Functions, and Influence Coefficients for Unswept Wings in Subsonic Flow. By Franklin W. Diederich and Martin Zlotnick.
1229. Exact Solutions of Laminar-Boundary-Layer Equations with Constant Property Values for Porous Wall with Variable Temperature. By Patrick L. Donoughe and John N. B. Livingood.
1230. Generalized Indicial Forces on Deforming Rectangular Wings in Supersonic Flight. By Harvard Lomax, Franklyn B. Fuller, and Loma Sluder.
1231. NACA Transonic Wind-Tunnel Test Sections. By Ray H. Wright and Vernon G. Ward.
1232. A Theoretical and Experimental Investigation of the Lift and Drag Characteristics of Hydrofoils at Subcritical and Supercritical Speeds. By Kenneth L. Wadlin, Charles L. Shuford, Jr., and John R. McGehee.
1233. Shock-Turbulence Interaction and the Generation of Noise. By H. S. Ribner.
1234. On the Kernel Function of the Integral Equation Relating the Lift and Downwash Distributions of Oscillating Finite Wings in Subsonic Flow. By Charles E. Watkins, Harry L. Runyan, and Donald S. Woolston.
1235. Standard Atmosphere—Tables and Data for Altitudes to 65,800 feet. By International Civil Aviation Organization and Langley Aeronautical Laboratory.
1236. Arrangement of Fusiform Bodies to Reduce the Wave Drag at Supersonic Speeds. By Morris D. Friedman and Doris Cohen.
1237. A Flight Evaluation of the Longitudinal Stability Characteristics Associated with the Pitch-Up of a Swept-Wing Airplane in Maneuvering Flight at Transonic Speeds. By Seth B. Anderson and Richard S. Bray.
1238. Investigation at Supersonic Speeds of 22 Triangular Wings Representing Two Airfoil Sections for Each of 11 Apex Angles. By Eugene S. Love.
1239. Error in Airspeed Measurement Due to the Static-Pressure Field Ahead of an Airplane at Transonic Speeds. By Thomas C. O'Bryan, Edward C. B. Danforth, and J. Ford Johnston.
1240. An Investigation of the Effects of Heat Transfer on Boundary-Layer Transition on a Parabolic Body of Revolution (NACA RM-10) at a Mach Number of 1.61. By K. R. Czarnecki and Archibald R. Sinclair.
1241. Theoretical and Analog Studies of the Effects of Nonlinear Stability Derivatives on the Longitudinal Motions of an Aircraft in Response to Step Control Deflections and to the Influence of Proportional Automatic Control. By Howard J. Curfman, Jr.
1242. Transonic Flow Past Cone Cylinders. By George E. Solomon.
1243. High-Resolution Autoradiography. By George C. Towe, Henry J. Gomberg, and J. W. Freeman.
1244. Free-Stream Boundaries of Turbulent Flows. By Stanley Corrsin and Alan L. Kistler.
1245. Analysis and Calculation by Integral Methods of Laminar Compressible Boundary Layer With Heat Transfer and

With and Without Pressure Gradient. By Morris Morduchow.

1246. The Hydrodynamic Characteristics of Modified Rectangular Flat Plates Having Aspect Ratios of 1.00, 0.25, and 0.125 and Operating Near a Free Water Surface. By Kenneth L. Wadlin, John A. Ramsen, and Victor L. Vaughan, Jr.

1247. Characteristics of Turbulence in a Boundary Layer With Zero Pressure Gradient. By P. S. Klebanoff.

1248. An Experimental Study of Applied Ground Loads in Landing. By Benjamin Milwitzky, Dean C. Lindquist, and Dexter M. Potter.

1249. A Unified Two-Dimensional Approach to the Calculation of Three-Dimensional Hypersonic Flows, With Application to Bodies of Revolution. By A. J. Eggers, Jr., and Raymond C. Savin.

1250. The Dynamic-Response Characteristics of a 35° Swept-Wing Airplane as Determined From Flight Measurements. By William C. Triplett, Stuart C. Brown, and G. Allen Smith.

1251. Stress Analysis of Circular Semimonocoque Cylinders With Cutouts. By Harvey G. McComb, Jr.

1252. Quasi-Cylindrical Theory of Wing-Body Interference at Supersonic Speeds and Comparison With Experiment. By Jack N. Nielsen.

1253. A Correlation by Means of Transonic Similarity Rules of Experimentally Determined Characteristics of a Series of Symmetrical and Cambered Wings of Rectangular Plan Form. By John B. McDevitt.

TECHNICAL NOTES [1]

3218. Flight Determination of the Drag and Pressure Recovery of an NACA 1–40–250 Nose Inlet at Mach Numbers From 0.9 to 1.8. By R. I. Sears and C. F. Merlet.

3271. Thermodynamic Properties of Gaseous Nitrogen. By Harold W. Woolley.

3272. Generalized Tables of Corrections to Thermodynamic Properties for Nonpolar Gases. By Harold W. Woolley and William S. Benedict.

3274. Some Linear Dynamics of Two-Spool Turbo Jet Engines. By David Novik.

3275. Investigation of the Effect of Impact Damage on Fatigue Strength of Jet-Engine Compressor Rotor Blades. By Albert Kaufman and André J. Meyer, Jr.

3277. Space Heating Rates for Some Premixed Turbulent Propane-Air Flames. By Burton D. Fine and Paul Wagner.

3293. Cumulative Fatigue Damage of Axially Loaded Alclad 75S–T6 and Alclad 24S–T3 Aluminum-Alloy Sheet. By Ira Smith, Darnley M. Howard, and Frank C. Smith.

3294. Friction Study of Aircraft Tire Material on Concrete. By W. G. Hample.

3298. A Low-Density Wind-Tunnel Study of Shock-Wave Structure and Relaxation Phenomena in Gases. By F. S. Sherman.

3384. Effect of Hydrocarbon Structure on Reaction Processes Leading to Spontaneous Ignition. By Donald E. Swarts and Charles E. Frank.

3413. Investigation of the Use of a Rubber Analog in the Study of Stress Distribution in Riveted and Cemented Joints. By Louis R. Demarkles.

3414. Influence of Temperature on Creep, Stress-Rupture, and Static Properties of Melamine-Resin and Silicone-Resin Glass-Fabric Laminates By William N. Findley, Harlan W. Peithman, and Will J. Worley.

[1] The missing numbers in the series of Technical Notes were released before or after the period covered by this report.

3415. A Universal Column Formula for Load at Which Yielding Starts. By L. H. Donnell and V. C. Tsien.

3419. NACA Model Investigations of Seaplanes in Waves. By John B. Parkinson.

3421. Aerodynamics of a Rectangular Wing of Infinite Aspect Ratio at High Angles of Attack and Supersonic Speeds. By John C. Martin and Frank S. Malvestuto, Jr.

3422. Noise Survey of a 10-Foot Four-Blade Turbine-Driven Propeller Under Static Conditions. By Max C. Kurbjun.

3455. Recovery and Time-Response Characteristics of Six Thermocouple Probes in Subsonic and Supersonic Flow. By Truman M. Stickney.

3456. Propagation of a Free Flame in a Turbulent Gas Stream. By William R. Mickelsen and Norman E. Ernstein.

3458. Unstable Convection in Vertical Channels With Heating From Below, Including Effects of Heat Sources and Frictional Heating. By Simon Ostrach.

3460. Tables of Coefficients for the Analysis of Stresses About Cutouts in Circular Semimonocoque Cylinders With Flexible Rings. By Harvey G. McComb, Jr., and Emmet F. Low, Jr.

3462. Tensile Properties of 7075–T6 and 2024–T3 Aluminum-Alloy Sheet Heated at Uniform Temperature Rates Under Constant Load. By George J. Heimerl and John E. Inge.

3463. Investigation of the Vibrations of a Hollow Thin-Walled Rectangular Beam. By Eldon E. Kordes and Edwin T. Kruszewski.

3464. Influence of Shear Deformation of the Cross Section on Torsional Frequencies of Box Beams. By Edwin T. Kruszewski and William W. Davenport.

3465. Theoretical Investigation of Flutter of Two-Dimensional Flat Panels With One Surface Exposed to Supersonic Potential Flow. By Herbert C. Nelson and Herbert J. Cunningham.

3466. An Investigation of the Discharge and Drag Characteristics of Auxiliary-Air Outlets Discharging Into a Transonic Stream. By Paul E. Dewey and Allen R. Vick.

3467. Effect of Interaction on Landing-Gear Behavior and Dynamic Loads in a Flexible Airplane Structure. By Francis E. Cook and Benjamin Milwitzky.

3468. Effects of Sweep on the Maximum-Lift Characteristics of Four Aspect-Ratio-4 Wings at Transonic Speeds. By Thomas R. Turner.

3469. Summary of Results Obtained by Transonic-Bump Method on Effects of Plan Form and Thickness on Lift and Drag Characteristics of Wings at Transonic Speeds. By Edward C. Polhamus.

3470. Gust-Tunnel Investigation of the Effect of a Sharp-Edge Gust on the Flapwise Blade Bending Moments of a Model Helicopter Rotor. By Domenic J. Maglieri and Thomas D. Reisert.

3471. Theoretical Analyses to Determine Unbalanced Trailing-Edge Controls Having Minimum Hinge Moments Due to Deflection at Supersonic Speeds. By Kennith L. Goin.

3472. Flow Studies on Flat-Plate Delta Wings at Supersonic Speed. By William H. Michael, Jr.

3473. Effects of Sweep and Angle of Attack on Boundary-Layer Transition on Wings at Mach Number 4.04. By Robert W. Dunning and Edward F. Ulmann.

3474. Rapid Radiant-Heating Tests of Multiweb Beams. By Joseph N. Kotanchik, Aldie E. Johnson, Jr., and Robert D. Ross.

3475. An Analysis of Acceleration, Airspeed, and Gust-Velocity Data From One Type of Four-Engine Transport Airplane Operated Over Two Domestic Routes. By Martin R. Copp and Thomas L. Coleman.

3476. Calculated Spanwise Lift Distributions and Aerodynamic Influence Coefficients for Swept Wings in Subsonic Flow. By Franklin W. Diederich and Martin Zlotnick.

3477. Hydrodynamic Pressure Distributions Obtained During a Planing Investigation of Five Related Prismatic Surfaces. By Walter J. Kapryan and George M. Boyd, Jr.

3478. On Boattail Bodies of Revolution Having Minimum Wave Drag. By Keith C. Harder and Conrad Rennemann, Jr.

3479. Analysis of the Horizontal-Tail Loads Measured in Flight on a Multiengine Jet Bomber. By William S. Aiken, Jr. and Bernard Wiener.

3480. Free-Spinning-Tunnel Investigation of Gyroscopic Effects of Jet-Engine Rotating Parts (Or of Rotating Propellers) on Spin and Spin Recovery. By James S. Bowman, Jr.

3481. Wind-Tunnel Investigation at Low Speed of Effect of Size and Position of Closed Air Ducts on Static Longitudinal and Static Lateral Stability Characteristics of Unswept-Midwing Models Having Wings of Aspect Ratio 2, 4, and 6. By Byron M. Jaquet and James L. Williams.

3482. Supplementary Charts for Estimating Performance of High-Performance Helicopters. By Robert J. Tapscott and Alfred Gessow.

3483. An Analysis of Acceleration, Airspeed, and Gust-Velocity Data From a Four-Engine Transport Airplane in Operations on an Eastern United States Route. By Thomas L. Coleman and Mary W. Fetner.

3484. On Spectral Analysis of Runway Roughness and Loads Developed During Taxiing. By John C. Houbolt, James H. Walls and Robert F. Smiley.

3485. An Approximate Solution for Axially Symmetric Flow Over a Cone With an Attached Shock Wave. By Richard A. Hord.

3486. Measurements of Turbulent Skin Friction on a Flat Plate at Transonic Speeds. By Raimo Jaakko Hakkinen.

3487. Acoustic Radiation From Two-Dimensional Rectangular Cutouts in Aerodynamic Surfaces. By K. Krishnamurty.

3488. Some Measurements of Flow in a Rectangular Cutout. By Anatol Roshko.

3489. Contributions on the Mechanics of Boundary-Layer Transition. By G. B. Schubauer and P. S. Klebanoff.

3490. Experimental and Calculated Temperature and Mass Histories of Vaporizing Fuel Drops. By M. M. El Wakil, R. J. Priem, H. J. Brikowski, P. S. Myers, and O. A. Uyehara.

3491. Experimental Investigation of Eccentricity Ratio, Friction, and Oil Flow of Long and Short Journal Bearings With Load-Number Charts. By George B. DuBois, Fred W. Ocvirk, and R. L. Wehe.

3492. Determination of Inflow Distributions From Experimental Aerodynamic Loading and Blade-Motion Data on a Model Helicopter Rotor in Hovering and Forward Flight. By Gaetano Falabella, Jr., and John R. Meyer, Jr.

3493. Development of Equipment and of Experimental Techniques for Column Creep Tests. By Sharad A. Patel, Martin Bloom, Burton Erickson, Alexander Chwick, and Nicholas John Hoff.

3494. Sound Propagation Into the Shadow Zone in a Temperature-Stratified Atmosphere Above a Plane Boundary. By David C. Pridmore-Brown and Uno Ingard.

3495. Failure of Materials Under Combined Repeated Stresses With Superimposed Static Stresses. By George Sines.

3497. Summary of Results of a Wind-Tunnel Investigation of Nine Related Horizontal Tails. By Jules B. Dods, Jr. and Bruce E. Tinling.

3500. Correction of Additional Span Loadings Computed by the Weissinger Seven-Point Method for Moderately Tapered Wings of High Aspect Ratio. By John DeYoung and Walter H. Barling, Jr.

3503. Reduction of Profile Drag at Supersonic Velocities by the Use of Airfoil Sections Having a Blunt Trailing Edge. By Dean R. Chapman.

3505. An Experimental Investigation of Regions of Separated Laminar Flow. By Donald E. Gault.

3506. Criterions for Prediction and Control of Ram-Jet Flow Pulsations. By William H. Sterbentz and John C. Evvard.

3507. Practical Considerations in Specific Applications of Gas-Flow Interferometry. By Walton L. Howes and Donald R. Buchele.

3508. Laminar Free Convection on a Vertical Plate With Prescribed Nonuniform Wall Heat Flux or Prescribed Nonuniform Wall Temperature. By E. M. Sparrow.

3509. A Study of Boundary-Layer Transition and Surface Temperature Distributions at Mach 3.12. By Paul F. Brinich.

3510. An Automatic Viscometer for Non-Newtonian Materials. By Ruth N. Weltmann and Perry W. Kuhns.

3511. Extrapolation Techniques Applied to Matrix Methods in Neutron Diffusion Problems. By Robert R. McCready.

3512. Effect of Some Selected Heat Treatments on the Operating Life of Cast HS–21 Turbine Blades. By Francis J. Clauss, Floyd B. Garrett and John W. Weeton.

3513. Heat Transfer at the Forward Stagnation Point of Blunt Bodies. By Eli Reshotko and Clarence B. Cohen.

3514. Response of Homogeneous and Two-Material Laminated Cylinders to Sinusoidal Environmental Temperature Change, With Applications to Hot-Wire Anemometry and Thermocouple Pyrometry. By Herman H. Lowell and Norman A. Patton.

3515. Analysis of Two-Dimensional Compressible-Flow Loss Characteristics Downstream of Turbomachine Blade Rows in Terms of Basic Boundary-Layer Characteristics. By Warner L. Stewart.

3516. Summary Evaluation of Toothed-Nozzle Attachments as a Jet-Noise-Suppression Device. By Warren J. North.

3517. Approximate Method for Determining Equilibrium Operation of Compressor Component of Turbojet Engine. By Merle C. Huppert.

3518. Rotating-Stall Characteristics of a Rotor With High Hub-Tip Radius Ratio. By Eleanor L. Costilow and Merle C. Huppert.

3519. Visualization Study of Secondary Flows in Turbine Rotor Tip Regions. By Hubert W. Allen and Milton G. Kofskey.

3520. Flame Propagation Limits of Propane and $\underline{n}$-Pentane in Oxides of Nitrogen. By Riley O. Miller.

3521. A Comparison of the Measured and Predicted Lateral Oscillatory Characteristics of a 35° Swept-Wing Fighter Airplane. By Walter E. McNeill and George E. Cooper.

3522. Measurements of the Effects of Finite Span on the Pressure Distribution Over Double-Wedge Wings at Mach Numbers Near Shock Attachment. By Walter G. Vincenti.

3523. The Effectiveness of Wing Vortex Generators in Improving the Maneuvering Characteristics of a Swept-Wing Airplane at Transonic Speeds. By Normam M. McFadden, George A. Rathert, Jr., and Richard S. Bray.

3524. The Effect of Reynolds Number on the Stalling Characteristics and Pressure Distributions of Four Moderately Thin Airfoil Sections. By George B. McCullough.

3525. Vortex Interference on Slender Airplanes. By Alvin H. Sacks.

3526. Flight Calibration of Four Airspeed Systems on a Swept-Wing Airplane at Mach Numbers up to 1.04 by the NACA Radar-Phototheodolite Method. By Jim Rogers Thompson, Richard S. Bray, and George E. Cooper.

3527. A Second-Order Shock-Expansion Method Applicable to Bodies of Revolution Near Zero Lift. By Clarence A. Syvertson and David H. Dennis.

3528. A Theoretical Study of the Aerodynamics of Slender Cruciform-Wing Arrangements and Their Wakes. By John R. Spreiter and Alvin H. Sacks.

3529. The Transonic Characteristics of 36 Symmetrical Wings of Varying Taper, Aspect Ratio, and Thickness as Determined by the Transonic-Bump Technique. By Warren H. Nelson, Edwin C. Allen, and Walter J. Krumm.

3530. Minimum Wave Drag for Arbitrary Arrangements of Wings and Bodies. By Robert T. Jones.

3531. Pilot's Loss of Orientation in Inverted Spins. By Stanley H. Scher.

3532. Low-Speed Static Lateral and Rolling Stability Characteristics of a Series of Configurations Composed of Intersecting Triangular Plan-Form Surfaces. By David F. Thomas, Jr.

3533. The Proper Combination of Lift Loading for Least Drag on a Supersonic Wing. By Frederick C. Grant.

3534. Instrumentation for Measurement of Free-Space Sound Pressure in the Immediate Vicinity of a Propeller in Flight. By William D. Mace, Francis J. Haney, and Edmund A. Brummer.

3535. Flight Investigation of the Surface-Pressure Distribution and the Flow Field Around a Conical and Two Spherical Nonrotating Full-Scale Propeller Spinners. By Jerome B. Hammack, Milton L. Windler, and Elwood F. Scheithauer.

3536. A Limited Flight Investigation of the Effect of Three Vortex-Generator Configurations on the Effectiveness of a Plain Flap on an Unswept Wing. By Garland J. Morris and Lindsay John Lina.

3537. Helicopter Instrument Flight and Precision Maneuvers as Affected by Changes in Damping in Roll, Pitch, and Yaw. By James B. Whitten. John P. Reeder and Almer D. Crim.

3538. Summary of Derived Gust Velocities Obtained From Measurements Within Thunderstorms. By Harold B. Tolefson.

3539. Some Effects of System Nonlinearities in the Problem of Aircraft Flutter. By Donald S. Woolston, Harry L. Runyan, and Thomas A. Byrdsong.

3540. A Reevaluation of Gust-Load Statistics for Applications in Spectral Calculations. By Harry Press and May T. Meadows.

3541. A Method for Obtaining Statistical Data on Airplane Vertical Velocity at Ground Contact From Measurements of Center-of-Gravity Acceleration. By Robert C. Dreher.

3542. Analysis of Stresses in the Plastic Range Around a Circular Hole in a Plate Subjected to Uniaxial Tension. By Bernard Budiansky and Robert J. Vidensek.

3543. Some Effects of Fuselage Flexibility on Longitudinal Stability and Control. By Bernard B. Klawans and Harold I. Johnson.

3544. Comparison Between Theoretical and Experimental Stresses in Circular Semimonocoque Cylinders With Rectangular Cutouts. By Harvey G. McComb, Jr., and Emmet F. Low, Jr.

3545. Investigation of the Effect of Short Fixed Diffusers on Starting Blowdown Jets in the Mach Number Range From 2.7 to 4.5. By John A. Moore.

3546. Exploratory Investigation of Boundary-Layer Transition on a Hollow Cylinder at a Mach Number of 6.9. By Mitchel H. Bertram.

3547. Aerodynamic Characteristics of a Small-Scale Shrouded Propeller at Angles of Attack From 0° to 90°. By Lysle P. Parlett.

3548. Flight Investigation at Mach Numbers From 0.6 to 1.7 to Determine Drag and Base Pressures on a Blunt-Trailing-Edge Airfoil and Drag of Diamond and Circular-Arc Airfoils at Zero Lift. By John D. Morrow and Ellis Katz.

3549. Flight Investigation at Mach Numbers From 0.8 to 1.5 to Determine the Effects of Nose Bluntness on the Total Drag of Two Fin-Stabilized Bodies of Revolution. By Roger G. Hart.

3550. Measurements of the Effect of Trailing-Edge Thickness on the Zero-Lift Drag of Thin Low-Aspect-Ratio Wings. By John D. Morrow.

3551. Experimental Investigation at Low Speed of Effects of Fuselage Cross Section on Static Longitudinal and Lateral Stability Characteristics of Models Having 0° and 45° Sweptback Surfaces. By William Letko and James L. Williams.

3552. Investigation of the Compressive Strength and Creep Lifetime of 2024-T3 Aluminum-Alloy Plates at Elevated Temperatures. By Eldon E. Mathauser and William D. Deveikis.

3553. Compressive Crippling of Structural Sections. By Melvin S. Anderson.

3554. A Preliminary Investigation of the Effects of Frequency and Amplitude on the Rolling Derivatives of an Unswept-Wing Model Oscillating in Roll. By Lewis R. Fisher, Jacob H. Lichtenstein, and Katherine D. Williams.

3555. A Method for Calculating the Contour of Bodies of Revolution With a Prescribed Pressure Gradient at Supersonic Speed With Experimental Verification. By Paige B. Burbank.

3556. Grain-Boundary Behavior in Creep of Aluminum Bicrystals. By F. N. Rhines, W. E. Bond, and M. A. Kissel.

3557. A Theoretical Analysis of the Field of a Random Noise Source Above an Infinite Plane. By Peter A. Franken.

3558. Heat Capacity Lag of Gaseous Mixtures. By Thomas D. Rossing, Robert C. Amme, and Sam Legvold.

3559. Laminar Separation Over a Transpiration-Cooled Surface in Compressible Flow. By Morris Morduchow.

3560. Spontaneous Ignition Studies Relating to Lubricants of Reduced Flammability. By Kenneth T. Mecklenborg.

3561. Intensity, Scale, and Spectra of Turbulence in Mixing Region of Free Subsonic Jet. By James C. Laurence.

3562. Variation of Boundary-Layer Transition With Heat Transfer on Two Bodies of Revolution at a Mach Number of 3.12. By John R. Jack and N. S. Diaconis.

3563. Heat Loss From Yawed Hot Wires at Subsonic Mach Numbers. By Virgil A. Sandborn and James C. Laurence.

3564. Effect of Pneumatic De-Icers and Ice Formations on Aerodynamic Characteristics of an Airfoil. By Dean T. Bowden.

3565. Chemical Action of Halogenated Agents in Fire Extinguishing. By Frank E. Belles.
3566. A Polar-Coordinate Survey Method for Determining Jet-Engine Combustion-Chamber Performance. By Robert Friedman and Edward R. Carlson.
3567. Study of Screeching Combustion in a 6-Inch Simulated Afterburner. By Perry L. Blackshear, Warren D. Rayle, and Leonard K. Tower.
3568. Averaging of Periodic Pressure Pulsations by a Total-Pressure Probe. By R. C. Johnson.
3569. Compressible Laminar Boundary Layer and Heat Transfer for Unsteady Motions of a Flat Plate. By Simon Ostrach.
3570. An Experimental Comparison of the Lagrangian and Eulerian Correlation Coefficients in Homogeneous Isotropic Turbulence. By William R. Mickelsen.
3571. Lift Hysteresis at Stall as an Unsteady Boundary-Layer Phenomenon. By Franklin K. Moore.
3572. Amplitude of Supersonic Diffuser Flow Pulsations. By William H. Sterbentz and Joseph Davids.
3573. Effect of Exhaust-Nozzle Ejectors on Turbojet Noise Generation. By Warren J. North and Willard D. Coles.
3574. Acoustic Analysis of Ram-Jet Buzz. By Harold Mirels.
3575. Burning Velocities of Various Premixed Turbulent Propane Flames on Open Burners. By Paul Wagner.
3577. The Nickel Dip: A Radioisotope Study of Metallic Deposits in Porcelain Enameling. By Joseph C. Richmond, Harry B. Kirkpatrick, and William N. Harrison.
3578. Influence of Large Amplitudes on Flexural Motions of Elastic Plates. By George Herrmann.
3579. Vapor-Phase Oxidation and Spontaneous Ignition-Correlation and Effect of Variables. By Donald E. Swarts and Milton Orchin.
3580. Stall Propagation in Axial-Flow Compressors. By Alan H. Stenning, Anthony R. Kriebel, and Stephen R. Montgomery.
3581. Experimental Investigation of Blade Flutter in an Annular Cascade. By J. R. Rowe and A. Mendelson.
3582. Effect of Climb Technique on Jet-Transport Noise. By Warren J. North.
3583. Charts of Boundary-Layer Mass Flow and Momentum for Inlet Performance Analysis Mach Number Range, 0.2 to 5.0. By Paul C. Simon and Kenneth L. Kowalski.
3584. Free-Convection Effects on Heat Transfer for Turbulent Flow Through a Vertical Tube. By E. R. G. Eckert, Anthony J. Diaguila, and John N. B. Livingood.
3586. Impingement of Water Droplets on NACA 65A004 Airfoil at 0° Angle of Attack. By Rinaldo J. Brun and Dorothea E. Vogt.
3587. Impingement of Water Droplets on a Sphere. By Robert G. Dorsch, Paul G. Saper, and Charles F. Kadow.
3588. Summary of Laminar-Boundary-Layer Solutions for Wedge-Type Flow Over Convection- and Transpiration-Cooled Surfaces. By John N. B. Livingood and Patrick L. Donoughe.
3589. Design Criteria for Axisymmetric and Two-Dimensional Supersonic Inlets and Exits. By James F. Connors and Rudolph C. Meyer.
3590. Investigation of Far Noise Field of Jets. I—Effect of Nozzle Shape. By Edmund E. Callaghan and Willard D. Coles.
3591. Investigation of Far Noise Field of Jets. II—Comparison of Air Jets and Jet Engines. By Willard D. Coles and Edmund E. Callaghan.
3592. An Oil-Stream Photomicrographic Aeroscope for Obtaining Cloud Liquid-Water Content and Droplet Size Distributions in Flight. By Paul T. Hacker.
3593. Cloud-Droplet Ingestion in Engine Inlets With Inlet Velocity Ratios of 1.0 and 0.7. By Rinaldo J. Brun.
3594. Effect of Transvere Body Force on Channel Flow With Small Heat Addition. By Simon Ostrach and Franklin K. Moore.
3595. Wear of Typical Carbon-Base Sliding Seal Materials at Temperatures to 700° F. By Robert L. Johnson, Max A. Swikert, and John M. Bailey.
3596. On the Permeability of Porous Materials. By E. Carson Yates, Jr.
3597. Analysis of a Vane-Controlled Gust-Alleviation System. By Robert W. Boucher and Christopher C. Kraft, Jr.
3598. Method and Tables for Determining the Time Response to a Unit Impulse From Frequency-Response Data and for Determining the Fourier Transform of a Function of Time. By Carl R. Huss and James J. Donegan.
3599. Turbulent Heat-Transfer Measurements at a Mach Number of 0.87. By Maurice J. Brevoort and Bernard Rashis.
3600. Correlation of Crippling Strength of Plate Structures With Material Properties. By Roger A. Anderson and Melvin S. Anderson.
3601. Pressure Rise Associated With Shock-Induced Boundary-Layer Separation. By Eugene S. Love.
3602. Laboratory Investigation of an Autopilot Utilizing a Mechanical Linkage With a Dead Spot to Obtain an Effective Rate Signal. By Ernest C. Seaberg.
3603. Theoretical Study of the Lateral Frequency Response to Gusts of a Fighter Airplane, Both With Controls Fixed and With Several Types of Autopilots. By James J. Adams and Charles W. Mathews.
3604. Low-Speed Yawed-Rolling Characteristics and Other Elastic Properties of a Pair of 26-Inch-Diameter, 12-Ply-Rating, Type VII Aircraft Tires. By Walter B. Horne, Robert F. Smiley, and Bertrand H. Stephenson.
3605. Theoretical Span Load Distributions and Rolling Moments for Sideslipping Wings of Arbitrary Plan Form in Incompressible Flow. By M. J. Queijo.
3606. Tabulation of the $f\lambda$ Functions Which Occur in the Aerodynamic Theory of Oscillating Wings in Supersonic Flow. By Vera Huckel.
3607. Effect of Thickness, Camber, and Thickness Distribution on Airfoil Characteristics at Mach Numbers up to 1.0. By Bernard N. Daley and Richard S. Dick.
3608. Hydrodynamic Impact Loads in Smooth Water for a Prismatic Float Having an Angle of Dead Rise of 10°. By Philip M. Edge, Jr.
3609. Linearized Lifting-Surface and Lifting-Line Evaluations of Sidewash Behind Rolling Triangular Wings at Supersonic Speeds. By Percy J. Bobbitt.
3610. Comparison of Landing-Impact Velocities of First and Second Wheel to Contact From Statistical Measurements of Transport Airplane Landings. By Eziaslav N. Harrin.
3611. Analysis of a Spin and Recovery From Time Histories of Attitudes and Velocities as Determined for a Dynamic Model of a Contemporary Fighter Airplane in the Free-Spinning Tunnel. By Stanley H. Scher.
3612. Initial Results of a Flight Investigation of a Gust-Alleviation System. By Christopher C. Kraft, Jr.
3613. The Problem of Reducing the Speed of a Jet Transport in Flight. By Don. D. Davis, Jr.
3614. Flow Studies on Drooped-Leading-Edge Delta Wings at Supersonic Speed. By William H. Michael, Jr.
3615. An Experimental Investigation of the Scale Relations for the Impinging Water Spray Generated by a Planing Surface. By Ellis E. McBride.

3616. Charts for Estimating Rotor-Blade Flapping Motion of High-Performance Helicopters. By Robert J. Tapscott and Alfred Gessow.
3617. Theoretical Analysis of Linked Leading-Edge and Trailing-Edge Flap-Type Controls at Supersonic Speeds. By E. Carson Yates, Jr.
3618. Experimental Investigation of the Vibrations of a Built-Up Rectangular Box Beam. By Eldon E. Kordes and Edwin T. Kruszewski.
3619. Effect of Carriage Mass Upon the Loads and Motions of a Prismatic Body During Hydrodynamic Impact. By Melvin F. Markey.
3620. The Design of a Miniature Solid-Propellant Rocket. By Robert H. Heitkotter.
3621. Gust-Load and Airspeed Data From One Type of Two-Engine Airplane on Six Civil Airline Routes From 1947 to 1955. By Walter G. Walker.
3622. Preliminary Study of Some Factors Which Affect the Stall-Flutter Characteristics of Thin Wings. By A. Gerald Rainey.
3623. Correlation of Supersonic Convective Heat-Transfer Coefficients From Measurements of the Skin Temperature of a Parabolic Body of Revolution (NACA RM-10). By Leo T. Chauvin and Carlos A. deMoraes.
3624. Investigation of the Use of the Thermal Decomposition of Nitrous Oxide to Produce Hypersonic Flow of a Gas Closely Resembling Air. By Alexander P. Sabol and John S. Evans.
3625. Investigation of the Propulsive Characteristics of a Helicopter-Type Pulse-Jet Engine Over a Range of Mach Numbers and Angle of Yaw. By Paul J. Carpenter, James P. Shivers, and Edwin E. Lee, Jr.
3626. Experimental Investigation of the Flow Around Lifting Symmetrical Double-Wedge Airfoils at Mach Numbers of 1.30 and 1.41. By Paul B. Gooderum and George P. Wood.
3627. Boundary-Layer Growth and Shock Attenuation in a Shock Tube With Roughness. By Paul W. Huber and Donald R. McFarland.
3628. An Analysis of Estimated and Experimental Transonic Downwash Characteristics as Affected by Plan Form and Thickness for Wing and Wing-Fuselage Configurations. By Joseph Weil, George S. Campbell and Margaret S. Diederich.
3629. Investigation of the Effects of Ground Proximity and Propeller Position on the Effectiveness of a Wing With Large-Chord Slotted Flaps in Redirecting Propeller Slipstreams Downward for Vertical Take-Off. By Richard E. Kuhn.
3630. Hovering-Flight Tests of a Model of a Transport Vertical-Take-off Airplane With Tilting Wing and Propellers. By Powell M. Lovell, Jr., and Lysle P. Parlett.
3631. Results of Axial-Load Fatigue Tests on Electrio-Polished 2024-T3 and 7075-T6 Aluminum-Alloy-Sheet Specimens With Central Holes. By Charles B. Landers and Herbert F. Hardrath.
3632. Correlation, Evaluation, and Extension of Linearized Theories for Tire Motion and Wheel Shimmy. By Robert F. Smiley.
3633. Analysis of the Ultimate Strength and Optimum Proportions of Multiweb Wing Structures. By B. Walter Rosen.
3634. Calculations of the Rate of Thermal Dissociation of Air Behind Normal Shock Waves at Mach Numbers of 10, 12, and 14. By George P. Wood.
3635. Analytical Study of Modifications to the Autopilot of a Fighter Airplane in Order to Reduce the Response to Side Gusts. By Charles W. Mathews and James J. Adams.
3636. The Accuracy of the Substitute-Stringer Approach for Determining the Bending Frequencies of Multistringer Box Beams. By William W. Davenport.
3637. Flight Investigation of the Effectiveness of an Automatic Aileron Trim Control Device for Personal Airplanes. By William H. Phillips, Helmut A. Kuehnel and James B. Whitten.
3638. On Panel Flutter and Divergence of Infinitely Long Unstiffened and Ring-Stiffened Thin-Walled Circular Cylinders. By Robert W. Leonard and John M. Hedgepeth.
3639. Approximate Indicial Lift Functions for Several Wings of Finite Span in Incompressible Flow as Obtained From Oscillatory Lift Coefficients. By Joseph A. Drischler.
3640. A Method for Deflection Analysis of Thin Low-Aspect-Ratio Wings. By Manuel Stein and J. Lyell Sanders, Jr.
3641. Wind-Tunnel Investigation of a Number of Total-Pressure Tubes at High Angles of Attack. Subsonic, Transonic, and Supersonic Speeds. By William Gracey.
3642. Effect of Shallow Water on the Hydrodynamic Characteristics of a Flat-Bottom Planing Surface. By Kenneth W. Christopher.
3643. Measurement of Aerodynamic Forces for Various Mean Angles of Attack on an Airfoil Oscillating in Pitch and on Two Finite-Span Wings Oscillating in Bending With Emphasis on Damping in the Stall. By A. Gerald Rainey.
3645. Wind-Tunnel Investigation of Effects of Fuselage Cross-Sectional Shape, Fuselage Bend, and Vertical-Tail Size on Directional Characteristics of Nonoverlap-Type Helicopter Fuselage Models Without Rotors. By James L. Williams.
3646. A Theory for the Elastic Deflections of Plates Integrally Stiffened on One Side. By Robert F. Crawford.
3647. Investigation of the Compressive Strength and Creep Lifetime of 2024-T Aluminum-Alloy Skin-Stringer Panels at Elevated Temperatures. By Eldon E. Mathauser and William D. Deveikis.
3648. Investigation of Boundary-Layer Transition on 10° Cone in Langley 4- by 4-Foot Supersonic Pressure Tunnel at Mach Numbers of 1.41, 1.61, and 2.01. By Archibald R. Sinclair and K. R. Czarnecki.
3649. Static Longitudinal and Lateral Stability Characteristics at Low Speed of Unswept-Midwing Models Having Wings With an Aspect Ratio of 2, 4, or 6. By Walter D. Wolhart and David F. Thomas, Jr.
3650. Results of a Flight Investigation to Determine the Zero-Lift Drag Characteristics of a 60° Delta Wing With NACA 65-006 Airfoil Section and Various Double-Wedge Sections at Mach Numbers From 0.7 to 1.6. By Clement J. Welsh.
3651. Cross Flows in Laminar Incompressible Boundary Layers. By Arthur G. Hansen and Howard Z. Herzig.
3652. Experimental Investigation of Air-Flow Uniformity and Pressure Level on Wire Cloth for Transpiration-Cooling Applications. By Patrick L. Donoughe and Roy A. McKinnon.
3653. Some Effects of Bluntness on Boundary-Layer Transition and Heat Transfer at Supersonic Speeds. By W. E. Moeckel.
3654. Performance Analysis of Fixed- and Free-Turbine Helicopter Engines. By Richard P. Krebs and William S. Miller, Jr.
3655. Method of Calculating Core Dimensions of Crossflow Heat Exchanger With Prescribed Gas Flows and Inlet and

Exit States. By E. R. G. Eckert and Anthony J. Diaguila.

3657. Friction Studies of Graphite and Mixtures of Graphite With Several Metallic Oxides and Salts at Temperatures to 1000° F. By Marshall B. Peterson and Robert L. Johnson.

3658. Impingement of Water Droplets on a Rectangular Half Body in a Two-Dimensional Incompressible Flow Field. By William Lewis and Rinaldo J. Brun.

3659. Effect of Leading-Edge Geometry on Boundary-Layer Transition at Mach 3.1. By Paul F. Brinich.

3660. Investigation of the Ni_3Al Phase of Nickel-Aluminum Alloys. By Edward M. Grala.

3661. Self Shielding in Rectangular and Cylindrical Geometries. By Harold Schneider, Paul G. Saper, and Charles F. Kadow.

3662. Theoretical Loss Relations for Low-Speed Two-Dimensional-Cascade Flow. By Seymour Lieblein and William H. Roudebush.

3663. Discharge Coefficients for Combustor-Liner Air-Entry Holes. I—Circular Holes With Parallel Flow. By Ralph T. Dittrich and Charles C. Graves.

3664. Summary of Scale-Model Thrust-Reverser Investigation. By John H. Povolny, Fred W. Steffen, and Jack G. McArdle.

3665. Performance and Operational Studies of a Full-Scale Jet-Engine Thrust Reverser. By Robert C. Kohl.

3666. Bodies of Revolution Having Minimum Drag at High Supersonic Airspeeds. By A. J. Eggers, Jr., Meyer M. Resnikoff, and David H. Dennis.

3667. Wing-Body Combinations With Certain Geometric Restraints Having Low Zero-Lift Wave Drag at Low Supersonic Mach Numbers. By Harvard Lomax.

3668. Preliminary Investigation of a Family of Diffusers Designed for Near Sonic Inlet Velocities. By Richard Scherrer and Warren E. Anderson.

3669. Perforated Sheets as a Porous Material for Distributed Suction and Injection. By Robert E. Dannenberg, Bruno J. Gambucci, and James A. Weiberg.

3670. Determination of Vortex Paths by Series Expansion Technique With Application to Cruciform Wings. By Alberta Y. Alksne.

3671. Wind-Tunnel Investigation of the Effect of Clipping the Tips of Triangular Wings of Different Thickness, Camber, and Aspect Ratio—Transonic Bump Method. By Horace F. Emerson.

3672. Investigation at High Subsonic Speeds of a Body-Contouring Method for Alleviating the Adverse Interference at the Root of a Sweptback Wing. By John B. McDevitt and William M. Haire.

3673. On the Range of Applicability of the Transonic Area Rule. By John R. Spreiter.

3674. Theoretical Pressure Distributions for Some Slender Wing-Body Combinations at Zero Lift. By Paul F. Byrd.

3676. Investigation of Lateral Control Near the Stall. Flight Tests With High-Wing and Low-Wing Monoplanes of Various Configurations. By Fred E. Weick and H. Norman Abramson.

3677. Investigation of Lateral Control Near the Stall. Analysis for Required Longitudinal Trim Characteristics and Discussion of Design Variables. By Fred E. Weick and H. Norman Abramson.

3678. Influence of Alloying Upon Grain-Boundary Creep. By F. N. Rhines, W. E. Bond, and M. A. Kissel.

3679. Influence of Copper Ions on Adherence of Viterous Coatings to Stainless Steel. By D. G. Moore and A. G. Eubanks.

3681. Investigation of Plastic Behavior of Binary Aluminum Alloys by Internal-Friction Methods. By R. E. Maringer, L. L. Marsh, and G. K. Manning.

3682. Time Correlator for Problems in Aerodynamics. By George Tolmie Skinner.

3685. Fatigue Crack Propagation in Severely Notched Bars. By W. S. Hyler, E. D. Abraham, and H. J. Grover.

3686. Experimental Measurements of Forces and Moments on a Two-Dimensional Oscillating Wing at Subsonic Speeds. By Sherman A. Clevenson and Edward Widmayer, Jr.

3687. Some Wind-Tunnel Experiments on Single-Degree-of-Freedom Flutter of Ailerons in the High Subsonic Speed Range. By Sherman A. Clevenson.

3689. Investigation by the Transonic-Bump Method of a 35° Sweptback Semispan Model Equipped With a Flap Operated by a Series of Servovanes Located Ahead of and Geared to the Flap. By William H. Phillips and Robert F. Thompson.

3690. Normal Component of Induced Velocity in the Vicinity of a Lifting Rotor With a Nonuniform Disk Loading. By Harry H. Heyson and S. Katzoff.

3691. Analysis and Comparison With Theory of Flow-Field Measurements Near a Lifting Rotor in the Langley Full-Scale Tunnel. By Harry H. Heyson.

3692. Investigation at Zero Forward Speed of a Leading-Edge Slat as a Longitudinal Control Device for Vertically Rising Airplanes that Utilize the Redirected-Slipstream Principle. By Richard E. Kuhn.

3693. Preliminary Investigation of the Effectiveness of a Sliding Flap in Deflecting a Propeller Slipstream Downward for Vertical Take-Off. By Richard E. Kuhn and Kenneth P. Spreemann.

3696. A Study of the High-Speed Performance Characteristics of 90° Bends in Circular Ducts. By James T. Higginbotham, Charles C. Wood, and E. Floyd Valentine.

3697. Flight Tests at Supersonic Speeds to Determine the Effect of Taper on the Zero-Lift Drag of Sweptback Low-Aspect-Ratio Wings. By Murray Pittel.

3698. Preliminary Investigation of Self-Excited Vibrations of Single Planing Surfaces. By Elmo J. Mottard.

3699. Some Effects of Joint Conductivity on the Temperatures and Thermal Stresses in Aerodynamically Heated Skin-Stiffener Combinations. By George E. Griffith and Georgene H. Miltonberger.

3702. Measurements of Atmospheric Turbulence Over a Wide Range of Wavelength for One Meteorological Condition By Harold L. Crane and Robert G. Chilton.

3703. The Flow Past and Unswept- and a Swept-Wing-Body Combination and Their Equivalent Bodies of Revolution at Mach Numbers Near 1.0. By Walter F. Lindsey.

3705. An Investigation of Forward-Located Fixed Spoilers and Deflectors as Gust Alleviators on an Unswept-Wing Model. By Delwin R. Croom, C. C. Shufflebarger, and Jarrett K. Huffman.

3708. Investigation at Supersonic Speeds of the Variation With Reynolds Number and Mach Number of the Total, Base, and Skin-Friction Drag of Seven Boattail Bodies of Revolution Designed for Minimum Wave Drag. By August F. Bromm, Jr., and Julia M. Goodwin.

3711. Some Effects of Guide-Vane Turning and Stators on the Rotating Stall Characteristics of a High Hub-Tip Ratio Single-Stage Compressor. By Eleanor L. Costilow and Merle C. Huppert.

3712. Boundary Layer Behind Shock or Thin Expansion Wave Moving Into Stationary Fluid. By Harold Mirels.

3713. Selection of Optimum Configurations for Heat Exchanger With One Dominating Film Resistance. By E. R. G. Eckert and T. F. Irvine, Jr.

3714. A Sonic-Flow Orifice Probe for the Inflight Measurement of Temperature Profiles of a Jet Engine Exhaust With Afterburning. By C. Dewey Havill and L. Stewart Rolls.
3715. Comparison of the Experimental and Theoretical Distributions of Lift on a Slender Inclined Body of Revolution at $M=2$. By Edward W. Perkins and Donald M. Kuehn.
3716. Comparison of Experimental and Theoretical Normal-Force Distributions (Including Reynolds Number Effects) on an Ogive-Cylinder Body at Mach Number 1.98. By Edward W. Perkins and Leland H. Jorgensen.
3718. Theoretical Wave Drag of Shrouded Airfoils and Bodies. By Paul F. Byrd.
3720. Comparison Between Experimental and Predicted Downwash at a Mach Number of 0.25 Behind a Wing-Body Combination Having a Triangular Wing of Aspect Ratio 2.0. By Norman E. Sorensen and Edward J. Hopkins.

TECHNICAL MEMORANDUMS [1]

1330. Theory of Dynamic Creep. By A. A. Predvoditelev and B. A. Smirnov. From Vestnik Moskovskogo Univ., Phys., vol. 8, no. 8, 1953.
1369. Flat Plate Cascades at Supersonic Speed. By Rashad M. El Badrawy. From Mitteilungen aus dem Institut für Aerodynamik an der E. T. H., no. 19, 1952.
1377. The Theories of Turbulence. By L. Agostini and J. Bass. From Publications Scientifiques et Techniques du Ministére de L'Air, No. 237, 1950.
1384. Metallography of Aluminum and Its Alloys Use of Electrolytic Polishing. By P. A. Jacquet. From Office National d'Etudes et de Recherches Aéronautiques, Publication No. 51, 1952.
1385. On the Gas Dynamics of a Rotating Impeller. By A. Busemann. From Zeitschrift für angewandte Mathematik und Mechanik, vol. 18, issue 1, Feb. 1938.
1386. Remark on the Theory of Lifting Surfaces. By Aldo Muggia. From Atti della Accademia delle Scienze di Torino, vol. 87, 1952–1953.
1388. General Solutions of Optimum Problems in Nonstationary Flight. By Angelo Miele. From L'Aerotecnica, n. 3, vol. XXXII, 1952.
1389. Optimum Flight Paths of Turbojet Aircraft. By Angelo Miele. From L'Aerotecnica, n. 4, vol. XXXII, 1952.
1390. On the Mechanism of Buckling of a Circular Cylindrical Shell Under Axial Compression. By Y. Yoshimura.
1391. Reduction of the Shimmy Tendency of Tail and Nose-Wheel Landing Gears by Installation of Specially Designed Tires. By H. Schrode. From Bericht der Deutschen Versuchsanstalt für Luftfahrt E. V., Berlin-Adlershof. Technische Berichte, Bd. 10, 1943.
1392. On the Buckling of Bars and Plates in the Plastic Range. Part. II. By J. P. Benthem. From Nationaal Luchtvaartlaboratorium, Amsterdam, Rapport S. 423, Jan. 1954.
1393. Flow of Gas Through Turbine Lattices. By M. E. Deich. From (Tekhnickeskaia gazodinamika) ch. 7, 1953.
1394. A Flat Wing With Sharp Edges in a Supersonic Stream. By A. E. Donov. From Izvestiia-Akademia, NAUK, USSR, 1939.
1396. From Linear Mechanics to Nonlinear Mechanics. By Julien Loeb. From Annales des Télécommunications, vol. 5, no. 2, Feb. 1950.
1397. Interim Report on Fatigue Characteristics of a Typical Metal Wing. By J. L. Kepert and A. O. Payne. From Aeronautical Research Laboratories Melbourne, Australia.
1398. Formation of a Vortex at the Edge of a Plate. By Leo Anton. From Göttinger Dissertation, Ingenieur-Archiv, vol. X, 1939.
1399. Acoustics of a Nonhomogeneous Moving Medium. By D. I. Blokhintsev. From Ogiz, Gosudarstvennoe Izdatel'stvo, Tekhniko-Teoreticheskoi Literatury, Moskva, 1946, Leningrad.
1400. Boundary Layer. By L. G. Loitsianskii. From Mechanics in the U.S.S.R. over Thirty Years, 1917–1947.
1401. Directional Stability of Towed Airplanes. By W. Söhne. From Deutsches Ingenieur-Archiv, vol. 21, no. 4, 1953.
1403. On the Instability of Methods for the Integration of Ordinary Differential Equations. By Heinz Rutishauser. From ZAMP, Kurze Mitteilungen, vol. III, 1952.
1415. Laminar Flow About a Rotating Body of Revolution in an Axial Airstream. By H. Schlichting. From Ingenieur-Archiv, vol. XXI, no. 4, 1953.

OTHER TECHNICAL PAPERS BY STAFF MEMBERS

Allen, Gabriel, Webeler, Rayjor W., and Barile, Sam: Multiple Scattering of Low-Energy Alpha Particles in Gas. Phys. Rev., vol. 99, no. 2, July 15, 1955, pp. 556–558.

Allen, H. Julian: Development of Two Hypersonic Test Facilities at the National Advisory Committee for Aeronautics Ames Aeronautical Laboratory. Presented at the Sixth Meeting of the Wind Tunnel and Model Testing Panel (Paris, Nov. 2–6, 1954), Advisory Group for Aeronautical Research and Development AG 17/7, pp. 333–372.

Allen, H. Julian: Transonic Wind Tunnel Development at the National Advisory Committee for Aeronautics. Presented at the Sixth Meeting of the Wind Tunnel and Model Testing Panel (Paris, Nov. 2–6, 1954), Advisory Group for Aeronautical Research and Development AG 17/7, pp. 198–217.

Altshuller, Aubrey P.: Lattice Energies and Related Thermodynamic Properties of the Alkali Metal Borohydrides and of the Borohydride Ion. Jour. Am. Chem. Soc., vol. 77, no. 21, Nov. 5, 1955, pp. 5455–5457.

Anderson, Roger A.: Weight Efficiency Analysis of Thin Wing Construction. Paper 56–AV–13, A. S. M. E., 1956.

Aron, Jack, and Groetzinger, Gerhart: Longitudinal Photomagnetoelectric Effect in Germanium. Phys. Rev., vol. 100, no. 4, Nov. 15, 1955, pp. 1128–1129.

Auble, Carmon M., and Heidmann, Marcus F.: The Application of Radiation Measurement Techniques to the Determination of Gas Temperatures in Liquid Propellant Flames. Jet Propulsion, vol. 25, no. 9, pt. 1, Sept. 1955, pp. 449–453, 467.

Benser, William A., and Finger, Harold B.: Compressor-Stall Problems in Gas-Turbine Type Aircraft Engines. Preprint 751, SAE, 1956.

Berlad, Abraham L., and Potter, Andrew E.: Prediction of the Quenching Effect of Various Surface Geometries. Fifth Symposium (International) on Combustion (Combustion in Engines and Combustion Kinetics), University of Pittsburgh, Aug. 30–Sept. 3, 1954. Reinhold Pub. Corp., N. Y., 1955, pp. 728–735.

Brokaw, Richard S.: Estimating Thermal Conductivities for Nonpolar Gas Mixtures. Ind. and Eng. Chem., vol. 47, no. 11, Nov. 1955, pp. 2398–2400.

Brokaw, Richard S.: Thermal Ignition, With Particular Reference to High Temperatures. Selected Combustion Problems II—Combustion Colloquium, Advisory Group for Aeronautical Research and Development (Liege, Belgium, Dec.

[1] The missing numbers in the series of Technical Memorandums were released before or after the period covered by this report.

5–9, 1955), Butterworths Sci. Pubs. (London), 1956, pp. 115–138.

Brooks, George W.: Analytical Determination of the Natural Couple Frequencies of Tandem Helicopters. Preprint 620, Inst. Aero. Sci., 1956.

Buckner, Howard A., Jr., and Rebeske, John J., Jr.: Application of High-Speed Strain-Gage Torquemeter to Turbomachinery Research. Trans. A. S. M. E., vol. 77, no. 5, July 1955, pp. 597–603.

Budiansky, Bernard, and Mayers, Jean: Influence of Aerodynamic Heating on the Effective Torsional Stiffness of Thin Wings. Preprint 579, Inst. Aero. Sci., 1956.

Busemann, Adolf: The Relation Between Minimizing Drag and Noise at Supersonic Speeds. Proceedings of the Conference on High-Speed Aeronautics (Brooklyn, Jan. 20–22, 1955), Polytechnic Inst. of Brooklyn, 1955, pp. 133–144.

Cooper, H., Schwed, Philip, and Webeler, Rayjor W.: Thermoelectric Power of AuCu in Nonequilibrium States. Jour. Appl. Phys., vol. 27, no. 5, May 1956, pp. 516–518.

Cortright, Edgar M., Jr.: Some Aerodynamic Considerations of Nozzle-Afterbody Combinations. Preprint 614, Inst. Aero. Sci., 1956.

Crocco, Luigi, and Cohen, Clarence B.: Compressible Laminar Boundary Layer With Heat Transfer and Pressure Gradient. 50 Jahre Grenzschichtforschung, Eine Festschrift in Originalbeitragen, H. Görtler and W. Tollmien, eds., Friedr. Vieweg & Sohn (Braunschweig, Germany), 1955, pp. 280–293.

Deissler, Robert G., and Loeffler, Albert L., Jr.: Turbulent Flow and Heat Transfer on a Flat Plate at High Mach Number With Variable Fluid Properties. Paper 55–A–133, A. S. M. E., 1955.

Deissler, Robert G.: Turbulent Heat Transfer and Friction in the Entrance Regions of Smooth Passages. Trans. A. S. M. E., vol. 77, no. 8, Nov. 1955, pp. 1221–1233.

Dimeff, John, Carson, James A., and Charters, Alex C., Jr.: Piston-Type Strain Gauge for Measuring Pressures in Interior Ballistics Research. Rev. Sci. Instr., vol. 26, no. 9, Sept. 1955, pp. 879–883.

Dryden, Hugh L., and Duberg, John E.: Aeroelastic Effects of Aerodynamic Heating. Presented at the Fifth General Assembly (Ottawa, June 10–17, 1955), Advisory Group for Aeronautical Research and Development AG20/P10, pp. 102–107.

Dryden, Hugh L.: Ballistics Research—The Scientific Bases of Airplane, Projectile, and Missile Development. Ordnance, vol. 40, no. 215, Mar./Apr. 1956, pp. 893–897.

Dryden, Hugh L.: The International Geophysical Year. Nat. Geographic, vol. 109, no. 2, Feb. 1956, pp. 285–298.

Dryden, Hugh L.: Problems in Ultra-High-Speed Flight. Inst. Radio Engrs.—Trans. on Telemetry and Remote Control, vol. TRU-1, no. 3, Aug. 1955, pp. 2–4.

Dryden, Hugh L.: Recent Investigations on the Problem of Transition. Zeit. für Flugwissenschaften, vol. 4, no. 3/4, Mar./Apr. 1956, pp. 89–95.

Dryden, Hugh L.: Transition From Laminar to Turbulent Flow at Subsonic and Supersonic Speeds. Proceedings of the Conference on High-Speed Aeronautics (Brooklyn, Jan. 20–22, 1955), Polytechnic Inst. of Brooklyn, 1955, pp. 41–74.

Duberg, John E.: High Temperature Structural Research at the National Advisory Committee for Aeronautics. Proceedings of the Conference on High-Speed Aeronautics (Brooklyn, Jan. 20–22, 1955), Polytechnic Inst. of Brooklyn, 1955, pp. 213–232.

Duberg, John E.: Some NACA Research on the Effect of Transient Heating on Aircraft Structures. Paper 56–AV–16, A. S. M. E., 1956.

Fryburg, George C.: The Conductometric Method Applied to the High Temperature Oxidation of Iron. Corrosion, vol. 12, no. 2, Feb. 1956, pp. 40–42.

Fryburg, George C.: Enhanced Oxidation of Platinum in Activated Oxygen. Jour. Chem. Phys., vol. 24, no. 2, Feb. 1956, pp. 175–180.

Gerstein, Melvin, and Coffin, Kenneth P.: Combustion of Solid Fuels. High Speed Aerodynamics and Jet Propulsion, Vol. II—Combustion Processes, Princeton University Press (Princeton), 1956, pp. 444–469.

Gessow, Alfred: The Future Role of the Helicopter (Editorial). Jour. Am. Helicopter Soc., vol. 1, no. 2, April 1956, pp. 1–2.

Godfrey, Douglas: A Study of Fretting Wear in Mineral Oil. Lubrication Eng., vol. 12, no. 1, Jan./Feb. 1956, pp. 37–42.

Golosman, Bernard S.: Analysis of a Regenerative Amplifier With Distributed Amplification (Extract From a Thesis Submitted for M. S. Degree at Cal. U.). Proc. Inst. Radio Engineers, vol. 44, no. 4, April 1956, pp. 533–534.

Gustafson, Frederic B.: A History of NACA Research on Rotating-Wing Aircraft. Jour. Am. Helicopter Soc., vol. 1, no. 1, Jan. 1956, pp. 16–26.

Hamrick, Joseph T.: Some Aerodynamic Investigations in Centrifugal Impellers. Trans. A. S. M. E., vol. 78, no. 3, Apr. 1956, pp. 591–602.

Heaslet, Maxwell A.: Reducing Supersonic Wave Drag. Aviation Age, vol. 25, no. 6, June 1956, pp. A:6–A:9.

Heldenfels, Richard R.: Some Elevated Temperature Structural Problems of High-Speed Aircraft. Preprint 599, SAE, 1956.

Herzig, Howard Z., and Hansen, Arthur G.: Experimental and Analytical Investigation of Secondary Flows in Ducts. Preprint 593, Inst. Aero. Sci., 1956.

Hibbard, Robert R., and Barnett, Henry C.: Fuels for Turbojet Powered Aircraft. Selected Combustion Problems II—Combustion Colloquium, Advisory Group for Aeronautical Research and Development (Liege, Belgium, Dec. 5–9, 1955), Butterworths Sci. Pubs. (London), 1956, pp. 30–53.

Huntsberger, Ralph F., and Parsons, John P.: The Design of Large High-Speed Wind Tunnels. Presented at the Fifth Meeting of the Wind Tunnel and Model Testing Panel (The Hague, Netherlands, May 3–7, 1954). Advisory Group for Aeronautical Research and Development AG15/P6, pp. 127–152.

Jones, Melvin H., and Brown, William F., Jr.: An Axial Loading Creep Machine. A. S. T. M. Bull. no. 211, Jan. 1956, pp. 53–60.

Jones, Melvin H., Brown, William F., Jr., and Newman, David P.: Creep Damage in a Cr-Mo-V Steel as Measured by Retained Stress Rupture Properties. Paper 55–A–175, A. S. M. E., 1955.

Jones, Robert T.: Possibilities of Efficient High-Speed Transport Airplanes. Proceedings of the Conference on High-Speed Aeronautics (Brooklyn, Jan. 20–22, 1955), Polytechnic Inst. of Brooklyn, 1955, pp. 145–156.

Kauffman, William M.: Flight Application of Target-Simulator Principles. Preprint 649, Inst. Aero. Sci., 1956.

Kauffman, William M., and Drinkwater, Fred J., III: Variable-Stability Airplanes in Lateral-Stability Research. Aero. Eng. Rev., vol. 14, no. 8, Aug. 1955, pp. 29–35.

Kuhn, Paul: Effect of Geometric Size on Notch Fatigue. International Union of Theoretical and Applied Mechanics (IUTAM) Colloquium on Fatigue (Stockholm, Sweden, May 25–27, 1955), Proc., Springer (Berlin-Göttingen-Heidelberg, Germany), 1956, pp. 131–140.

Kuhn, Paul: Stresses in Aircraft Structures. McGraw-Hill Publications in Aeronautical Science, McGraw-Hill Book Co., Inc., (N. Y.), 1956.

Lad, Robert A., and Metz, Florence I.: An Experimental Investigation of the Effect of Vacancy and F-Centre Concentrations on the Transient Creep of Sodium Chloride Single Crystals. Jour. Mech. of Phys. of Solids, vol. 4, no. 1, Oct. 1955, pp. 28–37.

Ladanyi, Dezso J., and Miller, Riley O.: Two Methods for Measuring Ignition Delays of Self-Igniting Rocket Propellant Combinations. Jet Propulsion, vol. 26, no. 3, Mar. 1956, pp. 157–163.

Lassiter, Leslie W., Hess, Robert W., and Hubbard, Harvey H.: An Experimental Study of the Response of Simple Panels to Intense Acoustic Loading. Preprint 632, Inst. Aero. Sci., 1956.

Leider, R. Herman: Effect of X-Irradiation on Surface Structure of Sodium Chloride Crystals. Phys. Rev., vol. 101, no. 1, Jan. 1, 1956, pp. 56–58.

Lomax, Harvard, and Heaslet, Max A.: Recent Developments in the Theory of Wing-Body Wave Drag. Preprint 617, Inst. Aero. Sci., 1956.

McKeown, Anderson B., and Belles, Frank E.: Nitric Acid-Nitrogen Dioxide-Water System. Vapor Pressures and Related Properties. Ind. and Eng. Chem., vol. 47, no. 12, Dec. 1955, pp. 2540–2543.

McKinney, Marion O., Kuhn, Richard E., and Hammack, Jerome B.: Problems in the Design of Propeller-Driven Vertical Take-Off Transport Airplanes. Aero. Eng. Rev., vol. 15, no. 4, Apr. 1956, pp. 68–75, 84.

McLellan, Charles H.: An Investigation of the Melting of Bodies Due to Aerodynamic Heating. Trans. A. S. M. E., vol. 77, no. 5, July 1955, pp. 727–733.

McNulty, James F.: Thrust Loading on Piles. Am. Soc. Civil Engineers Proc., vol. 82 (SM 2, no. 940), Apr. 1956, pp. 1–25.

Manson, Samuel S., and Smith, Robert W.: Quantitative Evaluation of Thermal-Shock Resistance. Trans. A. S. M. E., vol. 78, no. 3, Apr. 1956, pp. 533–544.

Martin, Frank E., and Raring, Richard H.: High Speed Quenching Dilatometer. Jour. Metals, vol. 8, no. 2, Sec. 2, Feb. 1956, pp. 191–195.

Maslen, Stephen H., and Moore, Franklin K.: On Strong Transverse Waves Without Shocks in a Circular Cylinder. Jour. Aero. Sci., vol. 23, no. 6, June 1956, pp. 583–593.

Mendelson, Alexander, and Manson, Samuel S.: Approximate Solution to Thermal-Shock Problems in Plates, Hollow Spheres, and Cylinders With Heat Transfer at Two Surfaces. Trans. A. S. M. E., vol. 78, no. 3, Apr. 1956, pp. 545–553.

Metz, Florence I., and Lad, Robert A.: The Effect of Substrate on the Crystallization of Metallic Films. Jour. Phys. Chem., vol. 60, no. 3, Mar. 1956, pp. 277–280.

Miller, William S., Jr., Krebs, Richard P., and Blaschke, T. C.: Shaft Gas Turbines for Helicopters. Preprint 515, SAE, 1955.

Moore, Franklin K.: Three-Dimensional Boundary Layer Theory. Advances in Applied Mechanics, vol. IV, H. L. Dryden and Th. von Karman, eds., Acad. Press, Inc., (N. Y.), 1955, pp. 160–228.

Moshos, George J.: Analog Interpolator for Automatic Control. Jour. Assoc. Computing Machinery, vol. 2, no. 2, Apr. 1955, pp. 83–91.

Murray, Sylvester F., Johnson, Robert L., and Swikert, Max A.: Difluorodichloromethane as Boundary Lubricant for Steel and Other Metals. Mech. Eng., vol. 78, no. 3, Mar. 1956, pp. 233–236.

Neihouse, Anshal I.: Design and Operating Techniques of Vertical Spin Tunnels. Presented at the Sixth Meeting of the Wind Tunnel and Model Testing Panel (Paris, Nov. 2–6, 1954), Advisory Group for Aeronautical Research and Development AG 17/7, pp. 399–420.

Nemeth, Zolton N., and Anderson, William J.: Effect of Air and Nitrogen Atmospheres on the Temperature Limitations of Liquid and Solid Lubricants in Ball Bearings. Lubrication Eng., vol. 11, no. 4, July/Aug. 1955, pp. 267–273.

Nemeth, Zolton N., and Anderson, William J.: Effect of Atmospheric Moisture and Oxygen Content on High-Temperature Lubrication of Ball Bearings With Graphite. Lubrication Eng., vol. 12, no. 3, May/June 1956, p. 169.

Nemeth, Zolton N., and Anderson, William J.: Effect of Oxygen Concentration in Atmosphere on Oil Lubrication of High-Temperature Ball Bearings. Paper 55–Lub–8, A. S. M. E., 1955.

Nemeth, Zolton N., and Anderson, William J.: Temperature Limitations of Petroleum, Synthetic, and Other Lubricants in Rolling-Contact Bearings. Trans. SAE, vol. 63, 1955, pp. 556–566.

Olson, Walter T., Childs, J. Howard, and Jonash, Edmund R.: The Combustion-Efficiency Problem of the Turbojet at High Altitude. Trans. A. S. M. E., vol. 77, no. 5, July 1955, pp. 605–615.

Ostrach, Simon: Convection Phenomena in Fluids Heated From Below. Paper 55–A–88, A. S. M. E., 1955.

Ostrach, Simon: On the Flow, Heat Transfer, and Stability of Viscous Fluids Subject to Body Forces and Heated From Below in Vertical Channels. 50 Jahre Grenzschichtforschung, Eine Festschrift in Originalbeitragen, H. Görtler and W. Tollmien, eds., Friedr. Vieweg & Sohn (Braunschweig, Germany), 1955, pp. 226–235.

O'Sullivan, William J., Jr.: Some Thermal and Mechanical Properties of Inconel at High Temperatures for Use in Aerodynamic Heating Research. Proc. A. S. T. M., vol. 55, 1955, pp. 757–764.

Peters, Roger W.: The NACA Combined Load Testing Machine. Proc. Soc. Exp. Stress Analysis, vol. 13, no. 1, 1955, pp. 181–198.

Peterson, Marshall B., and Johnson, Robert L.: Factors Influencing Friction and Wear With Solid Lubricants. Lubrication Eng., vol. 11, no. 5, Sept./Oct., 1955, pp. 325–331.

Peterson, Marshall B., and Johnson, Robert L.: Solid Lubricants for Titanium. Lubrication Eng., vol. 11, no. 5, Sept./Oct., 1955, pp. 297, 299.

Pinkel, I. Irving: Crash-Fire Research With Jet Aircraft. Aero. Eng. Rev., vol. 15, no. 1, Jan. 1956, pp. 53–57.

Potter, Andrew E., and Berlad, Abraham L.: The Quenching of Flames of Propane-Oxygen-Argon and Propane-Oxygen-Helium Mixtures. Jour. Phys. Chem., vol. 60, no. 1, Jan. 1956, pp. 97–101.

Povolny, John H., and McArdle, Jack G.: NACA Investigation of Thrust Reversal Techniques. Preprint 591, SAE, 1955.

Press, Harry: Time Series Problems in Aeronautics. Jour. Am. Statistical Assoc., vol. 50, no. 272, Dec. 1955, pp. 1022–1039.

Regier, Arthur A.: Noise, Vibration, and Aircraft Structures. Preprint 631, Inst. Aero. Sci., 1956.

Regier, Arthur A.: Why Do Airplanes Make Noise? Trans. SAE, vol. 63, 1955, pp. 275–283.

Reshotko, Eli: Heat Transfer to a Yawed Infinite Cylinder in Compressible Flow. 1956 Heat Transfer and Fluid Mechanics Institute (Stanford Univ., June 21–23, 1956), Stanford Univ. Press (Stanford, Cal.), 1956, pp. 275–220.

Rosenblum, Louis: The Thermal Decomposition of Tri-n-Butylborane. Jour. Am. Chem. Soc., vol. 77, no. 19, Oct. 5, 1955, pp. 5016–5017.

Sanders, Newell D., and Laurence, James C.: Fundamental Investigation of Noise Generation by Turbulent Jets. Preprint 744, SAE, 1956.

Schmidt, W. C., and Anderson, William J.: Detecting Bearing Failures by Measuring Temperature Acceleration. Lubrication Eng., vol. 11, no. 4, July/Aug. 1955, pp. 274–276.

Sharp, Elmer M.: Experiences With Automatic Digital Data Processing. Am. Documentation, vol. 7, no. 1, Jan. 1956, pp. 22–28.

Shortal, Joseph A.: Techniques of Model Testing in Free Flight. Presented at Fifth Meeting of the Wind Tunnel and Model Testing Panel (The Hague, Netherlands, May 3–7, 1954), Advisory Group for Aeronautical Research and Development AG15/P6, pp. 56–68.

Silverstein, Abe: Concepts on Turbojet Engines for Transport Application. Preprint 721, SAE, 1956.

Silverstein, Abe: The Future in Ramjets. Aviation Age, vol. 25, no. 6, June 1956, pp. B:6–B:9.

Simon, Dorothy M., and Wagner, Paul: Characterization of Turbulent Combustion by Flame Space and Space Heating Rates. Propane-Oxygen-Nitrogen Flames. Ind. and Eng. Chem., vol. 48, no. 1, Jan. 1956, pp. 129–133.

Sommer, Simon C., and Short, Barbara J.: Free-Flight Measurements of Skin Friction of Turbulent Boundary Layers With High Rates of Heat Transfer at High Supersonic Speeds. Jour. Aero. Sci., vol. 23, no. 6, June 1956, pp. 536–542.

Sparrow, Ephriam M., and Gregg, John L.: Laminar Free Convection From a Vertical Plate With Uniform Surface Heat Flux. Trans. A. S. M. E., vol. 78, no. 2, Feb. 1956, pp. 435–440.

Tapscott, Robert J., and Gustafson, Frederic B.: Helicopter Blade Flapping. Aero. Eng. Rev., vol. 14, no. 9, Sept. 1955, pp. 46–51.

Van Dyke, Milton D.: The Slender Elliptic Cone as a Model for Non-Linear Supersonic Flow Theory. Jour. Fluid Mechanics, vol. 1, no. 1, May 1956, pp. 1–15.

Warshawsky, Isidore: Multiple-Bridge Circuits for Measurement of Small Changes in Resistance. Rev. Sci. Instr., vol. 26, no. 7, July 1955, pp. 711–715.

Weltmann, Ruth N.: Friction Factors for Flow of Non-Newtonian Materials in Pipelines. Ind. and Eng. Chem., vol. 48, no. 3, pt. 1, Mar. 1956, pp. 386–387.

Whitcomb, Richard T.: NACA Details Area Rule Breakthrough. Aviation Week, vol. 63, no. 12, Sept. 19, 1955, pp. 28–31, 33, 35–36, 38, 41–42, 44, 46–47.

Whitcomb, Richard T.: Zero-Lift-Drag Characteristics of Wing-Body Combinations at Transonic Speeds. Aero. Eng. Rev., vol. 15, no. 6, June 1956, pp. 42–45.

Wiener, Bernard, Groetzinger, Gerhart, and McCollum, Rathuel: Specification of Thermally and Mechanically Induced Nonequilibrium States in AuCu by Resistivity and Magnetoresistivity. Jour. Appl. Phys., vol. 26, no. 7, July 1955, pp. 857–862.

Williams, Walter C.: Flight Research at High Altitudes and High Speeds With Rocket-Propelled Research Airplanes. Preprint 601, SAE, 1955.

Woolston, Donald S., Runyan, Harry L., and Andrews, Robert E.: An Investigation of Effects of Certain Types of Structural Nonlinearities on Wing and Control Surface Flutter. Preprint 633, Inst. Aero. Sci., 1956.

Yeates, John E., Jr.: A Discussion of Helicopter Vibration Studies Including Flight Test and Analysis Methods Used to Determine the Coupled Response of a Tandem Type. Preprint 625, Inst. Aero. Sci., 1956.

Zimmerman, Charles H.: Some General Considerations Concerning VTOL Aircraft. Preprint 737, SAE, 1956.

Zimmerman, Charles H.: Some Stability Problems of Vertically Rising Aircraft. Proc. of Second Annual Western Forum of American Helicopter Society (Los Angeles, Sept. 21–22, 1955), Am. Helicopter Soc., Inc. (N. Y.), 1955, pp. 6–32.

Part II—COMMITTEE ORGANIZATION AND MEMBERSHIP

The National Advisory Committee for Aeronautics was established by Act of Congress approved March 3, 1915 (U. S. Code, title 50, sec. 151). The Committee consists of seventeen members appointed by the President, and includes two representatives each of the Department of the Air Force, the Department of the Navy, and the Civil Aeronautics Authority; one representative each of the Smithsonian Institution, the United States Weather Bureau, and the National Bureau of Standards; and "one Department of Defense representative who is acquainted with the needs of aeronautical research and development." In addition seven members are appointed for five-year terms from persons "acquainted with the needs of aeronautical science, either civil or military, or skilled in aeronautical engineering or its allied sciences." The representatives of the Government organizations serve for indefinite periods, and all members serve as such without compensation.

The following changes in membership have taken place during the past year:

The Committee lost a valuable member by the death on January 4, 1956, of Mr. Ralph S. Damon, President of Trans World Air Lines, Inc., who had been serving as Chairman of the important NACA Committee on Operating Problems. In its tribute to Mr. Damon's memory, the NACA at its meeting on January 19, 1956, said: "His intelligence, enthusiasm, sound judgment, and high qualities of integrity and sincerity, together with his wealth of experience, enabled him to support most effectively the responsibilities of the Committee and to provide highly competent leadership."

To succeed Mr. Damon, President Eisenhower on April 14, 1956, appointed the well-known World War I ace and aviation executive, Captain Edward V. Rickenbacker, Chairman of the Board of Eastern Air Lines, Inc., to membership on the NACA.

On January 6, 1956, the President appointed Hon. Clifford C. Furnas, Assistant Secretary of Defense (Research and Development), a member of NACA. Dr. Furnas succeeded Hon. Donald A. Quarles, Secretary of the Air Force, who had previously served in Dr. Furnas' present post in the Department of Defense.

Vice Admiral William V. Davis, USN, Deputy Chief of Naval Operations (Air), was appointed a member of the NACA on August 2, 1956, succeeding Vice Admiral Thomas S. Combs, who had just been detached from the same Navy post and assigned to other duty.

In accordance with the regulations of the Committee as approved by the President, the chairman and vice chairman and the chairman and vice chairman of the Executive Committee are elected annually.

Prior to the annual meeting of the NACA on October 17, 1956, Dr. Jerome C. Hunsaker, who had been chairman since August 1941, indicated his desire to retire from the chairmanship of the NACA and of the Executive Committee. At the meeting the NACA elected Dr. James H. Doolittle chairman of the NACA and of the Executive Committee. Dr. Leonard Carmichael was re-elected vice chairman of the NACA and Dr. Detlev W. Bronk vice chairman of the Executive Committee.

The Committee membership is as follows:

James H. Doolittle, Sc. D., Shell Oil Company, Chairman.
Leonard Carmichael, Ph. D., Secretary, Smithsonian Institution, Vice Chairman.
Joseph P. Adams, LL. B., Vice Chairman, Civil Aeronautics Board.
Allen V. Astin, Ph. D., Director, National Bureau of Standards.
Preston R. Bassett, M. A., Vice President, Sperry Rand Corporation.
Detlev W. Bronk, Ph. D., President, Rockefeller Institute for Medical Research.
Frederick C. Crawford, Sc. D., Chairman of the Board, Thompson Products, Inc.
William V. Davis, Jr., Vice Admiral, United States Navy, Deputy Chief of Naval Operations (Air).
Clifford C. Furnas, Ph. D., Assistant Secretary of Defense (Research and Development).
Jerome C. Hunsaker, Sc. D., Massachusetts Institute of Technology.
Carl J. Pfingstag, Rear Admiral, United States Navy, Assistant Chief for Field Activities, Bureau of Aeronautics.
Donald L. Putt, Lieutenant General, United States Air Force, Deputy Chief of Staff, Development.
Arthur E. Raymond, Sc. D., Vice President—Engineering, Douglas Aircraft Company, Inc.
Francis W. Reichelderfer, Sc. D., Chief, United States Weather Bureau.
Edward V. Rickenbacker, Sc. D., Chairman of the Board, Eastern Air Lines, Inc.
Louis S. Rothschild, Under Secretary of Commerce for Transportation.
Nathan F. Twining, General, United States Air Force, Chief of Staff.

Assisting the Committee in its coordination of aeronautical research and the formulation of its research programs are four main technical committees: Aerodynamics, Power Plants for Aircraft, Aircraft Construction, and Operating Problems. Each of these committees is assisted by four or more subcommittees. Effective January 1, 1956, two new subcommittees were established under the Committee on Aerodynamics in place of the Subcommittee on Stability and Control, namely: Aerodynamic Stability and Control, and Automatic Stabilization and Control. This action was taken because of the increase in the importance of the problems of automatic stabilization and control in connection with both piloted aircraft and missiles.

The Committee is advised on matters of policy affecting the aircraft industry by an Industry Consulting Committee.

The membership of the committees and their subcommittees is as follows:

COMMITTEE ON AERODYNAMICS

Mr. Preston R. Bassett, Vice President, The Sperry Rand Corp., Chairman.
Dr. Theodore P. Wright, Vice President for Research, Cornell University, Vice Chairman.
Col. Daniel D. McKee, USAF, Wright Air Development Center.
Rear Adm. W. A. Schoech, USN, Assistant Chief of the Bureau of Aeronautics for Research and Development, Department of the Navy.
Mr. F. A. Louden, Bureau of Aeronautics, Department of the Navy.
Dr. H. H. Kurzweg, Associate Technical Director for Aeroballistic Research, Naval Ordnance Laboratory.
Maj. Gen August Schomburg, USA, Assistant Chief of Ordnance for Research and Development, Department of the Army.
Mr. D. M. Thompson, Office of the Chief of Transportation, Department of the Army.
Mr. Harold D. Hoekstra, Civil Aeronautics Administration.
Dr. Hugh L. Dryden (ex officio).
Mr. Floyd L. Thompson, NACA Langley Aeronautical Laboratory.
Mr. Russell G. Robinson, NACA Ames Aeronautical Laboratory.
Capt. W. S. Diehl, USN (Ret.).
Mr. L. L. Douglas, Vice President—Engineering, VERTOL Aircraft Corp.
Rear Adm. R. S. Hatcher, USN (Ret.), Professor and Chairman, Department of Aeronautical Engineering, New York University.
Mr. Clarence L. Johnson, Chief Engineer, Lockheed Aircraft Corp.
Dr. A. Kartveli, Vice President—Engineering, Republic Aviation Corp.
Mr. Schuyler Kleinhans, Assistant Chief Engineer, Santa Monica Division, Douglas Aircraft Co.
Dr. Albert E. Lombard, Jr., Director of Research, McDonnell Aircraft Corp.
Dr. Clark B. Millikan, Director, Daniel Guggenheim Aeronautical Laboratory, California Institute of Technology.
Dr. William J. O'Donnell, Assistant Chief Engineer—Development and Experimental, Republic Aviation Corp.
Mr. Kendall Perkins, Vice President—Engineering, McDonnell Aircraft Corp.
Mr. H. A. Storms, Jr., Chief, Technical Engineering, North American Aviation, Inc.
Mr. Charles Tilgner, Jr., Chief Aeronautical Engineer (Staff), Grumman Aircraft Engineering Corp.
Mr. George S. Trimble, Jr., Vice President—Chief Engineer, The Martin Co.
Mr. Robert J. Woods, Chief Design Engineer, Bell Aircraft Corp.

Mr. Milton B. Ames, Jr., Secretary

Subcommittee on Fluid Mechanics

Dr. William R. Sears, Cornell University, Chairman.
Maj. Eugene W. Geniesse, USAF, Air Research and Development Command.
Mr. E. Haynes, Air Research and Development Command.
Mr. Phillip Eisenberg, Office of Naval Research, Department of the Navy.
Mr. John D. Nicolaides, Bureau of Ordnance, Department of the Navy.
Dr. Joseph Sternberg, Ballistic Research Laboratories, Aberdeen Proving Ground.
Dr. G. B. Schubauer, Chief, Fluid Mechanics Section, National Bureau of Standards.
Dr. Adolf Busemann, NACA Langley Aeronautical Laboratory.
Mr. John Stack, NACA Langley Aeronautical Laboratory.
Dr. D. R. Chapman, NACA Ames Aeronautical Laboratory.
Mr. Robert T. Jones, NACA Ames Aeronautical Laboratory.
Dr. John C. Evvard, NACA Lewis Flight Propulsion Laboratory.
Prof. Walker Bleakney, Princeton University.
Dr. J. V. Charyk, Aeronutronics Systems, Inc.
Dr. Francis H. Clauser, The Johns Hopkins University.
Dr. Wallace D. Hayes, Princeton University.
Dr. Hans W. Liepmann, California Institute of Technology.
Prof. C. C. Lin, Massachusetts Institute of Technology.
Prof. Wilbur C. Nelson, Chairman, Aeronautical Engineering Department, University of Michigan.
Prof. E. L. Resler, Jr., Cornell University.

Mr. Ernest O. Pearson, Jr., Secretary.

Subcommittee on High-Speed Aerodynamics

Dr. Clark B. Millikan, Director, Daniel Guggenheim Aeronautical Laboratory, California Institute of Technology, Chairman.
Maj. Eugene W. Geniesse, Jr., USAF, Air Research and Development Command.
Mr. Joseph Flatt, Wright Air Development Center.
Mr. Oscar Seidman, Bureau of Aeronautics, Department of the Navy.
Dr. H. H. Kurzweg, Associate Technical Director for Aeroballistic Research, Naval Ordnance Laboratory.
Mr. C. L. Poor, 3d, Chief, Exterior Ballistics Laboratory, Ballistic Research Laboratories, Aberdeen Proving Ground.
Mr. John Beebe, Office of the Chief of Transportation, Department of the Army.
Mr. John Stack, NACA Langley Aeronautical Laboratory.
Mr. H. Julian Allen, NACA Ames Aeronautical Laboratory.
Mr. Abe Silverstein, NACA Lewis Flight Propulsion Laboratory.
Mr. Walter C. Williams, NACA High-Speed Flight Station.
Mr. John R. Clark, Assistant Chief Engineer, Chance Vought Aircraft, Inc.
Mr. Philip A. Colman, Chief Preliminary Design Engineer, Lockheed Aircraft Corp.
Mr. Alexander H. Flax, Vice President—Technical Operations, Cornell Aeronautical Laboratory, Inc.
Mr. L. P. Greene, Chief Aerodynamicist, North American Aviation, Inc.
Mr. Robert L. Gustafson, Chief of Aerodynamics, Grumman Aircraft Engineering Corp.
Mr. C. J. Koch, The Martin Co.
Mr. John G. Lee, Director of Research, United Aircraft Corp.
Mr. David S. Lewis, Jr., McDonnell Aircraft Corp.
Mr. Harlowe J. Longfelder, Chief—Preliminary Design, Seattle Division, Boeing Airplane Co.

Prof. John R. Markham, Professor of Aeronautical Engineering, Massachusetts Institute of Technology.
Mr. K. E. Van Every, Chief, Aerodynamics Section, El Segundo Division, Douglas Aircraft Co., Inc.

Mr. Albert J. Evans, Secretary

Subcommittee on Aerodynamic Stability and Control

Capt. W. S. Diehl, USN (Ret.), Chairman.
Mr. Melvin Shorr, Wright Air Development Center.
Mr. Jerome Teplitz, Bureau of Aeronautics, Department of the Navy.
Mr. L. L. Liccini, Bureau of Ordnance, Department of the Navy.
Maj. William H. Brabson, Jr., USA, Office of the Chief of Research and Development, Department of the Army.
Mr. John A. Carran, Civil Aeronautics Administration.
Mr. Thomas A. Harris, NACA Langley Aeronautical Laboratory.
Dr. J. N. Nielsen, NACA Ames Aeronautical Laboratory.
Mr. Hubert M. Drake, NACA High-Speed Flight Station.
Mr. M. J. Abzug, Douglas Aircraft Co., Inc.
Prof. Joseph Bicknell, Massachusetts Institute of Technology.
Mr. E. A. Bonney, Applied Physics Laboratory, The Johns Hopkins University.
Mr. J. E. Goode, Jr., Convair, Division of General Dynamics Corp.
Mr. George S. Graff, Chief of Aerodynamics, McDonnell Aircraft Corp.
Mr. William T. Hamilton, Chief Aerodynamics Engineer, Boeing Airplane Co.
Mr. Maxwell W. Hunter, Assistant Chief Project Engineer—Missiles, Douglas Aircraft Co., Inc.
Mr. R. B. Katkov, Northrop Aircraft, Inc.
Mr. Conrad A. Lau, Chance Vought Aircraft, Inc.
Mr. W. F. Milliken, Jr., Manager, Flight Research, Cornell Aeronautical Laboratory, Inc.
Mr. Frank J. Mulholland, Assistant Chief Development Engineer, Republic Aviation Corp.

Mr. Jack D. Brewer, Secretary

Subcommittee on Automatic Stabilization and Control

Mr. Warren E. Swanson, North American Aviation, Inc. Chairman.
Mr. George L. Yingling, Wright Air Development Center.
Mr. William Koven, Bureau of Aeronautics, Department of the Navy.
Mr. Marvin Schuldenfrei, Bureau of Aeronautics, Department of the Navy.
Mr. J. M. Lee, Bureau of Ordnance, Department of the Navy.
Mr. Paul R. Miles, Signal Corps Engineering Laboratories.
Mr. Charles W. Mathews, NACA Langley Aeronautical Laboratory.
Mr. Harry J. Goett, NACA Ames Aeronautical Laboratory.
Mr. M. J. Abzug, Douglas Aircraft Co., Inc.
Mr. Frank A. Gaynor, General Electric Co.
Dr. William J. Jacobi, The Ramo-Wooldridge Corp.
Mr. W. F. Milliken, Jr., Manager, Flight Research, Cornell Aeronautical Laboratory, Inc.
Mr. Louis A. Payne, Convair, Division of General Dynamics Corp.
Mr. Thomas L. Phillips, Raytheon Manufacturing Co.
Mr. Donald J. Povejsil, Westinghouse Electric Corp.
Dr. Allen E. Puckett, Head, Missile Aerodynamics Department, Hughes Aircraft Co.
Mr. O. H. Schuck, Minneapolis-Honeywell Regulator Co.
Dr. Robert C. Seamans, Jr., RCA Aviation Systems Laboratory.

Mr. Bernard Maggin, Secretary

Subcommittee on Internal Flow

Dr. William J. O'Donnell, Assistant Chief Engineer—Development and Experimental, Republic Aviation Corp., Chairman.
Mr. Frederick T. Rall, Jr., Wright Air Development Center.
Mr. Robert E. Roy, Wright Air Development Center.
Mr. R. T. Miller, Bureau of Aeronautics, Department of the Navy.
Dr. Thomas W. Williams, Office of Naval Research, Department of the Navy.
Mr. V. S. Kupelian, U. S. Naval Ordnance Experimental Unit at National Bureau of Standards.
Mr. John V. Becker, NACA Langley Aeronautical Laboratory.
Mr. Wallace F. Davis, NACA Ames Aeronautical Laboratory.
Mr. DeMarquis D. Wyatt, NACA Lewis Flight Propulsion Laboratory.
Mr. J. S. Alford, General Electric Co.
Mr. Bernard F. Beckelman, Boeing Airplane Co.
Mr. William J. Blatz, McDonnell Aircraft Corp.
Mr. John A. Drake, Director of Long-Range Planning and Research Programs, Marquardt Aircraft Co.
Mr. Harry Drell, Group Engineer—Power Plant Analysis, Lockheed Aircraft Corp.
Dr. Antonio Ferri, Polytechnic Institute of Brooklyn.
Mr. Donald J. Jordan, Pratt & Whitney Aircraft, United Aircraft Corp.
Mr. M. A. Sulkin, Chief Thermodynamicist, North American Aviation, Inc.
Mr. William M. Zarkowsky, Chief of Propulsion, Grumman Aircraft Engineering Corp.

Mr. Albert J. Evans, Secretary

Subcommittee on Propellers for Aircraft

Mr. D. H. Jacobson, Aeroproducts Operations, Allison Division, General Motors Corp., Chairman.
Capt. William G. Alexander, USAF, Air Research and Development Command.
Mr. Daniel A. Dickey, Wright Air Development Center.
Lt. Commander Hugh L. H. Collins, USN, Bureau of Aeronautics, Department of the Navy.
Mr. John Beebe, Office of the Chief of Transportation, Department of the Army.
Mr. John C. Morse, Civil Aeronautics Administration.
Mr. Eugene C. Draley, NACA Langley Aeronautical Laboratory.
Mr. Donald H. Wood, NACA Ames Aeronautical Laboratory.
Mr. George W. Brady, Director of Engineering, Propeller Division, Curtiss-Wright Corp.
Mr. Frank W. Caldwell.
Mr. R. Richard Heppe, Department Head, Aerodynamics, Lockheed Aircraft Corp.
Mr. R. S. Kelso, Cornell Aeronautical Laboratory, Inc.
Mr. Frank W. Kolk, American Airlines, Inc.
Mr. Thomas B. Rhines, Assistant Chief Engineer, Hamilton Standard Division, United Aircraft Corp.
Mr. Kenneth E. Ward, Convair, Division of General Dynamics Corp.

Mr. Ralph W. May, Secretary

Subcommittee on Seaplanes

Rear Adm. R. S. Hatcher, USN (Ret.), Professor and Chairman, Department of Aeronautical Engineering, New York University, Chairman.
Mr. Robert F. Robinson, Air Research and Development Command.
Mr. Eugene H. Handler, Bureau of Aeronautics, Department of the Navy.

Mr. F. W. S. Locke, Jr., Bureau of Aeronautics, Department of the Navy.
Mr. Marshall P. Tulin, Office of Naval Research, Department of the Navy.
Mr. M. St. Denis, David W. Taylor Model Basin.
Comdr. H. C. Weart, USN, Naval Air Test Center, Patuxent.
Mr. Joseph Matulaitis, Office of the Chief of Transportation, Department of the Army.
Capt. Reinhold R. Johnson, USCG, Coast Guard Station, Brooklyn.
Mr. Robert Rosenbaum, Civil Aeronautics Administration.
Mr. John B. Parkinson, NACA Langley Aeronautical Laboratory.
Mr. H. E. Brooke, Chief of Hydrodynamics, Convair, Division of General Dynamics Corp.
Mr. Robert B. Cotton, Vice President, All American Engineering Co.
Mr. C. L. Fenn, Chief Engineer, Edo Corp.
Mr. Wilfred C. Hugli, Jr., Stevens Institute of Technology.
Mr. Grover Loening.
Mr. J. D. Pierson, The Martin Co.

Mr. Ralph W. May, Secretary

Subcommittee on Helicopters

Mr. L. L. Douglas, Vice President—Engineering, VERTOL Aircraft Corp., Chairman.
Mr. Bernard Lindenbaum, Wright Air Development Center.
Mr. Paul A. Simmons, Jr., Wright Air Development Center.
Capt. James W. Klopp, USN, Bureau of Aeronautics, Department of the Navy.
Mr. T. L. Wilson, Office of Naval Research, Department of the Navy.
Lt. Col. M. J. Strok, USA, Office of the Chief of Research and Development, Department of the Army.
Mr. J. Wallace McDonald, Office of the Chief of Transportation, Department of the Army.
Comdr. James W. Williams, USCG, Headquarters, U. S. Coast Guard.
Mr. Herbert H. Slaughter, Jr., Civil Aeronautics Administration.
Honorable Joseph P. Adams (ex officio), Vice Chairman, Civil Aeronautics Board.
Mr. Richard C. Dingeldein, NACA Langley Aeronautical Laboratory.
Mr. F. B. Gustafson, NACA Langley Aeronautical Laboratory.
Mr. Charles W. Harper, NACA Ames Aeronautical Laboratory.
Mr. Friedrich L. V. Doblhoff, Chief Engineer, Helicopter Engineering Division, McDonnell Aircraft Corp.
Mr. Jack E. Gallagher, Chief Engineer and Operations Manager, New York Airways, Inc.
Mr. Bartram Kelley, Chief Helicopter Engineer, Bell Aircraft Corp.
Mr. Ralph B. Lightfoot, Sikorsky Aircraft, United Aircraft Corp.
Prof. R. H. Miller, Associate Professor of Aeronautical Engineering, Massachusetts Institute of Technology.
Mr. Charles M. Seibel, Chief Engineer, Helicopter Division, Cessna Aircraft Co.
Mr. N. M. Stefano, Chief—Rotary Wing, Fairchild Aircraft Division, Fairchild Engine and Airplane Corp.
Mr. Robert Wagner, Chief Engineer, Hiller Helicopters

Mr. P. M. Lovell, Jr., Secretary

COMMITTEE ON POWER PLANTS FOR AIRCRAFT

Dr. Frederick C. Crawford, Chairman of the Board, Thompson Products, Inc., Chairman.
Dean C. R. Soderburg, Dean of Engineering, Massachusetts Institute of Technology, Vice Chairman.
Col. Donald Heaton, USAF, Directorate of Research and Development.
Col. John J. B. Calderbank, USAF, Wright Air Development Center.
Capt. Thomas B. Haley, USN, Bureau of Aeronautics, Department of the Navy.
Col. C. L. Register, USA, Ballistic Research Laboratories, Aberdeen Proving Ground.
Lt. Col. Michael J. Strok, USA, Office of Chief of Research and Development, Department of the Army.
Mr. Stephen H. Rolle, Chief, Power Plant Branch, Aircraft Engineering Division, Civil Aeronautics Administration.
Dr. Hugh L. Dryden (ex officio).
Mr. Abe Silverstein, NACA Lewis Flight Propulsion Laboratory.
Mr. John G. Borger, Pan American Airways System.
Mr. Allan Chilton, Chief Engineer, Aircraft Gas Turbine Division, Westinghouse Electric Corp.
Mr. D. Cochran, General Manager, AGT Development Department, General Electric Co.
Mr. J. T. Cooley, Vice President, California Research Corp.
Mr. Dimitrius Gerdan, Director of Engineering, Allison Division, General Motors Corp.
Mr. Wilton G. Lundquist, Vice President, Curtiss-Wright Corp.
Mr. Thomas E. Myers, North American Aviation, Inc.
Mr. Wright A. Parkins, General Manager, Pratt & Whitney Aircraft, United Aircraft Corp.
Mr. Ivar L. Shogran, Douglas Aircraft Co., Inc.
Mr. Rudolf H. Thielemann, Senior Metallurgist, Stanford Research Institute.

Mr. William H. Woodward, Secretary

Subcommittee on Aircraft Fuels

Mr. J. L. Cooley, Vice President, California Research Corp., Chairman.
Maj. Eugene Finke, USAF, Directorate of Research and Development, U. S. Air Force.
Mr. Marc P. Dunnam, Wright Air Development Center.
Comdr. B. L. Towle, USN, Bureau of Aeronautics, Department of the Navy.
Mr. Donald D. Weidhuner, Office of Chief of Transportation, Department of the Army.
Mr. N. L. Klein, Office of the Chief of Ordnance, Department of the Army.
Mr. Ralph S. White, Civil Aeronautics Administration.
Mr. Henry C. Barnett, NACA Lewis Flight Propulsion Laboratory.
Dr. D. P. Barnard, Standard Oil Co. of Indiana.
Mr. A. J. Blackwood, Esso Research and Engineering Co.
Mr. C. S. Brandt, Convair, Division of General Dynamics Corp.
Mr. F. G. Dougherty, Allison Division, General Motors Corp.
Mr. E. A. Droegemueller, Pratt & Whitney Aircraft, United Aircraft Corp.
Mr. D. N. Harris, Shell Oil Co.
Dr. J. Bennett Hill, Director, Research and Development Department, Sun Oil Co.
Mr. W. M. Holaday, Deputy Assistant Secretary of Defense (Research and Development).
Mr. J. N. Krebs, General Electric Co.
Prof. Carl C. Monrad, Head, Department of Chemical Engineering, Carnegie Institute of Technology.
Mr. James S. Reid, Phillips Petroleum Co.

Mr. Harold F Hipsher, Secretary

Subcommittee on Combustion

Dr. Alfred G. Cattaneo, Shell Development Co., Chairman.
Mr. Howard P. Barfield, Wright Air Development Center.
Dr. Lloyd A. Wood, Wright Air Development Center.
Mr. Nelson F. Rekos, Bureau of Aeronautics, Department of the Navy.
Mr. Alfred G. Lundquist, Office of Naval Research, Department of the Navy.
Dr. Frank E. Marble, Jet Propulsion Laboratory, California Institute of Technology (representing Department of the Army).
Mr. F. R. Caldwell, National Bureau of Standards.
Dr. Walter T. Olson, NACA Lewis Flight Propulsion Laboratory.
Dr. W. H. Avery, Applied Physics Laboratory, The Johns Hopkins University.
Mr. William J. Bennet, Marquardt Aircraft Co.
Mr. William V. Hanzalek, Assistant to General Manager, Research Division, Curtiss-Wright Corp.
Dr. Bernard Lewis, Combustion and Explosives Research, Inc.
Dr. John P. Longwell, Esso Research and Engineering Co.
Dr. S. S. Penner, California Institute of Technology.
Mr. Paul A. Pitt, Chief Development Engineer, Solar Aircraft Co.
Mr. W. D. Pouchot, Supervising Engineer, Combustion Section, Aviation Gas Turbine Division, Westinghouse Eelectric Corp.
Prof. Glenn C. Williams, Massachusetts Institute of Technology.
Dr. Kurt Wohl, Professor of Chemical Engineering, University of Delaware.

Mr. Benson E. Gammon, Secretary.

Subcommittee on Lubrication and Wear

Dr. Robert G. Larsen, Research Director, Martinez Refinery, Shell Oil Co., Chairman.
Mr. C. M. Michaels, Wright Air Development Center.
Mr. Bernard Rubin, Wright Air Development Center.
Mr. Charles C. Singleterry, Bureau of Aeronautics, Department of the Navy.
Mr. R. E. Streets, Office of the Chief of Ordnance, Department of the Army.
Mr. Joseph Matulaitis, Office of the Chief of Transportation, Department of the Army.
Mr. Edmond E. Bisson, NACA Lewis Flight Propulsion Laboratory.
Dr. W. E. Campbell.
Mr. A. B. Crampton, Standard Oil Company of New Jersey.
Dr. Merrell R. Fenske, Director, Petroleum Refining Laboratory, School of Chemistry and Physics, The Pennsylvania State University.
Mr. A. S. Irwin, Assistant Chief Engineer—Aircraft, Marlin-Rockwell Corp.
Dr. E. G. Jackson, General Electric Co.
Dr. M. Eugene Merchant, Cincinnati Milling Machine Co.
Mr. V. W. Peterson, Allison Division, General Motors Corp.
Mr. Earle A. Ryder.
Prof. L. M. Tichvinsky, Professor of Mechanical Engineering, University of California.
Mr. George P. Townsend, Jr., Chief Engineer, Sundstrand Aviation—Denver.
Mr. Frank W. Wellons, Assistant Chief Engineer, SKF Industries, Inc.

Mr. Harold F. Hipsher, Secretary.

Subcommittee on Compressors and Turbines

Mr. John M. Wetzler, Allison Division, General Motors Corp., Chairman.
Mr. Ernest C. Simpson, Wright Air Development Center.
Mr. John C. Schettino, Bureau of Aeronautics, Department of the Navy.
Comdr. L. K. Bliss, USN, Office of Naval Research, Department of the Navy.
Mr. Edward F. Blackburne, Detroit Arsenal.
Mr. Donald D. Weidhuner, Office of the Chief of Transportation, Department of the Army.
Mr. John R. Erwin, NACA Langley Aeronautical Laboratory.
Mr. William A. Benser, NACA Lewis Flight Propulsion Laboratory.
Mr. William G. Cornell, General Electric Co.
Dr. Robert C. Dean, Jr., Assistant Professor of Mechanical Engineering, Massahcusetts Institute of Technology.
Mr. Walter Doll, Pratt & Whitney Aircraft, United Aircraft Corp.
Prof. Howard W. Emmons, Harvard University.
Mr. John E. Sanders, Curtiss-Wright Corp.
Mr. V. V. Schloesser, Director—Development, Aviation Gas Turbine Division, Westinghouse Electric Corp.
Mr. M. A. Sulkin, Chief Thermodynamicist, North American Aviation, Inc.
Dr. George F. Wislicenus, Director, Garfield Thomas Water Tunnel, Ordnance Research Laboratory, The Pennsylvania State University.

Mr. Curtis L. Walker, Secretary.

Subcommittee on Engine Performance and Operation

Mr. Perry W. Pratt, Chief Engineer, Pratt & Whitney Aircraft, United Aircraft Corp., Chairman.
Col. Paul F. Nay, USAF, Air Research and Development Command.
Mr. Ewell C. Phillips, Wright Air Development Center.
Mr. Richard J. Maurer, Bureau of Aeronautics, Department of the Navy.
Mr. Edward F. Blackburne, Detroit Arsenal.
Mr. Donald D. Weidhuner, Office of the Chief of Transportation, Department of the Army.
Col. E. O. Meals, Deputy Director, Aircraft Reactor Branch, Division of Reactor Development, Atomic Energy Commission.
Mr. Bruce T. Lundin, NACA Lewis Flight Propulsion Laboratory.
Mr. Rudolph Bodemuller, Bendix Products Division, Bendix Aviation Corp.
Mr. C. J. McDowall, Chief Engineer—Advanced Design and Development, Allison Division, General Motors Corp.
Mr. Maynard L. Pennell, Chief Engineer, Transport Division, Boeing Airplane Co.
Mr. Erold F. Pierce, Assistant Chief Engineer, Technical Services, Wright Aeronautical Division, Curtiss-Wright Corp.
Mr. Arnold H. Redding, Section Manager, Preliminary Design Division, Aviation Gas Turbine Division, Westinghouse Electric Corp.
Mr. Thomas B. Rhines, Assistant Chief Engineer, Hamilton Standard Division, United Aircraft Corp.
Mr. Dale D. Streid, Aircraft Gas Turbine Division, General Electric Co.
Mr. Elwood B. Taylor, Chief Power Plant Engineer, El Segundo Division, Douglas Aircraft Co., Inc.
Mr. Goerge S. Trimble, Jr., Vice President—Chief Engineer, The Martin Co.
Mr. Don L. Walter, Vice President—Engineering, Marquardt Aircraft Co.
Mr. R. H. Widmer, Assistant Chief Engineer, Convair, Division of General Dynamics Corp.
Mr. Lee R. Woodworth, Propulsion Research Corp.

Mr. Richard S. Cesaro, Secretary.

Subcommittee on Power Plant Controls

Mr. Rudolph Bodemuller, Bendix Aviation Corp., Chairman.
Mr. J. G. Barrett, Wright Air Development Center.
Mr. A. S. Atkinson, Bureau of Aeronautics, Department of the Navy.
Maj. William H. Brabson, Jr., USA, Office of Chief of Research and Development, Department of the Army.
Mr. John C. Sanders, NACA Lewis Flight Propulsion Laboratory.
Dr. John L. Barnes, University of California.
Mr. A. B. Chudyk, Assistant Chief Engineer, Design and Development Department, Minneapolis-Honeywell Regulator Co.
Dr. C. Stark Draper, Head, Department of Aeronautical Engineering, Massachusetts Institute of Technology.
Mr. R. T. Dungan, Marquardt Aircraft Co.
Mr. Harold E. Francis, Wright Aeronautical Division, Curtiss-Wright Corp.
Dr. E. H. Gamble, General Electric Co.
Mr. William H. Hand, North American Aviation, Inc.
Mr. James R. Kessler, Supervisor of Aircraft Accessory Design, Aeroproducts Operations, Allison Division, General Motors Corp.
Mr. Bruce N. Torell, Pratt & Whitney Aircraft, United Aircraft Corp.
Mr. James W. Wheeler, Department Head for Engine Instruments, Sperry Gyroscope Co., Division of Sperry Rand Corp.

Mr. Curtis L. Walker, Secretary.

Subcommittee on Power Plant Materials

Mr. Rudolf H. Thielemann, Senior Metallurgist, Stanford Research Institute, Chairman.
Mr. J. B. Johnson, Wright Air Development Center.
Mr. Nathan E. Promisel, Bureau of Aeronautics, Department of the Navy.
Mr. J. J. Harwood, Office of Naval Research, Department of the Navy.
Mr. Normal L. Reed, Watertown Arsenal.
Mr. S. S. Manson, NACA Lewis Flight Propulsion Laboratory.
Mr. W. L. Badger, General Electric Co.
Mr. Lee S. Busch, Mallory-Sharon Titanium Corp.
Dr. F. N. Darmara, Vice President, Utica Drop Forge & Tool Corp.
Mr. Charles T. Evans, Jr., Vice President—Technology and Development, Universal-Cyclops Steel Corp.
Mr. Glenn A. Fritzlen, Technical Director, Development and Technical Services, Haynes Stellite Co.
Prof. Nicholas J. Grant, Massachusetts Institute of Technology.
Mr. Arthur W. F. Green, Technical Assistant to Executive Engineer, Allison Division, General Motors Corp.
Mr. J. J. Heger, United States Steel Corp.
Mr. William D. Manly, Associate Director, Metallurgy Division, Oak Ridge National Laboratory, Union Carbide & Carbon Corp.
Mr. Andrew G. Slachta, Wright Aeronautical Division, Curtiss-Wright Corp.
Dr. L. F. Yntema, Director of Research, Fansteel Metallurgical Corp.

Mr. William H. Woodward, Secretary.

Subcommittee on Rocket Engines

Mr. Thomas E. Myers, North American Aviation, Inc., Chairman.
Lt. Col. Richard T. Hemsley, USAF, Air Research and Development Command.
Lt. Col. L. F. Ayres, USAF, Western Development Division, Air Research and Development Command.
Lt. Comdr. R. J. Kauffman, USN, Bureau of Aeronautics, Department of the Navy.
Mr. Frank I. Tanczos, Bureau of Ordnance, Department of the Navy.
Mr. James R. Patton, Office of Naval Research, Department of the Navy.
Dr. Eugene Miller, Redstone Arsenal.
Mr. John L. Sloop, NACA Lewis Flight Propulsion Laboratory
Mr. Richard B. Canright, Douglas Aircraft Co., Inc.
Dr. H. F. Dunholter, Chief of Thermodynamics, Convair, Division of General Dynamics Corp.
Mr. R. Bruce Foster, Group Leader, Preliminary Design, Rocket Engine Department, Bell Aircraft Corp.
Mr. William P. Munger, Engineering and Research Manager, Reaction Motors, Inc.
Mr. C. C. Ross, Manager, Liquid Engine Division, Aerojet-General Corp.
Dr. C. N. Satterfield, Professor of Chemical Engineering, Massachusetts Institute of Technology.
Mr. Frederick E. Schultz, General Electric Co.
Dr. H. S. Seifert, The Ramo-Wooldridge Corp.
Dr. A. J. Stosick, Union Carbide & Carbon Corp.
Dr. Maurice J. Zucrow, Professor of Jet Propulsion, School of Mechanical Engineering, Purdue University.

Mr. Benson E. Gammon, Secretary.

COMMITTEE ON AIRCRAFT CONSTRUCTION

Dr. Arthur E. Raymond, Vice President—Engineering, Douglas Aircraft Co., Inc., Chairman.
Mr. George Snyder, Chief Project Engineer, Pilotless Aircraft Division, Boeing Airplane Co., Vice Chariman.
Mr. E. H. Schwartz, Wright Air Development Center.
Capt. James W. Klopp, USN, Bureau of Aeronautics, Department of the Navy.
Dr. Wernher von Braun, Army Ballistic Missile Agency.
Mr. D. M. Thompson, Office of the Chief of Transporation, Department of the Army.
Mr. Albert A. Vollmecke, Civil Aeronautics Administration.
Dr. Hugh L. Dryden (ex officio).
Mr. Robert R. Gilruth, NACA Langley Aeronautical Laboratory.
Mr. John F. Parsons, NACA Ames Aeronautical Laboratory.
Dr. William F. Ballhaus, Chief Engineer, Northrop Aircraft, Inc.
Prof. Raymond L. Bisplinghoff, Professor of Aeronautical Engineering, Massachusetts Institute of Technology.
Mr. G. C. Covington, Vice President—Airplane Engineering, McDonnell Aircraft Corp.
Mr. Martin Goland, Vice President, Southwest Research Institute.
Mr. D. R. Kirk, Convair, Division of General Dynamics Corp.
Mr. Jerome F. McBrearty, Chief Structures Engineer, Lockheed Aircraft Corp.
Mr. George D. Ray, Chief Preliminary Design Engineer, Bell Aircraft Corp.
Dr. Leo Schapiro, Head, Metallurgical and Physical Testing Laboratory, Douglas Aircraft Co., Inc.
Mr. Richard L. Schleicher, Chief Structures Engineer, North American Aviation, Inc.
Prof. F. R. Shanley, University of California.
Mr. Robert J. Woods, Chief Design Engineer, Bell Aircraft Corp.

Mr. Franklyn W. Phillips, Secretary.

Subcommittee on Aircraft Structures

Mr. George D. Ray, Chief Preliminary Design Engineer, Bell Aircraft Corp., Chairman.

Capt. W. T. McGinness, USAF, Air Research and Development Command.
Mr. William B. Miller, Wright Air Development Center.
Mr. Ralph L. Creel, Bureau of Aeronautics, Department of the Navy.
Mr. Emil A. H. Hellebrand, Army Ballistic Missile Agency.
Capt. Earl P. Ford, USA, Office of the Chief of Transportation, Department of the Army.
Mr. Milton Jakosky, Civil Aeronautics Administration.
Mr. Richard R. Heldenfels, NACA Langley Aeronautical Laboratory.
Mr. O. W. Boden, Chief of Missile Design Section, North American Aviation, Inc.
Mr. L. M. Hitchcock, Chief—Technical Staff, Seattle Division Boeing Airplane Co.
Dr. Nicholas J. Hoff, Head, Department of Aeronautical Engineering and Applied Mechanics, Polytechnic Institute of Brooklyn.
Mr. Antonio L. LoPresti, North American Aviation, Inc.
Mr. George N. Mangurian, Chief Analytical Engineer, Northrop Aircraft, Inc.
Mr. William R. Micks, The RAND Corp.
Mr. Herman Pusin, Chief Engineer, Engineering Division, The Marin Co.
Prof. Paul E. Sandorff, Massachusetts Institute of Technology.
Prof. E. E. Sechler, Professor of Aeronautics, California Institute of Technology.
Mr. E. H. Spaulding, Division Engineer, Structural Engineering, Lockheed Aircraft Corp.
Mr. C. H. Stevenson, Douglas Aircraft Co., Inc.

Mr. Melvin G. Rosché, Secretary.

Subcommittee on Aircraft Loads

Mr. Jerome F. McBrearty, Chief Structures Engineer, Lockheed Aircraft Corp., Chairman.
Lt. Col. L. S. Jablecki, USAF, Air Research and Development Command.
Mr. Joseph H. Harrington, Wright Air Development Center.
Mr. Clinton T. Newby, Bureau of Aeronautics, Department of the Navy.
Mr. John Carlson, Office of the Chief of Transportation, Department of the Army.
Mr. Burdell L. Springer, Civil Aeronautics Administration.
Mr. Philip Donely, NACA Langley Aeronautical Laboratory.
Mr. Manley J. Hood, NACA Ames Aeronautical Laboratory.
Mr. D. E. Beeler, NACA High-Speed Flight Station.
Mr. Ralph B. Davidson, Director of Engineering Services, Radioplane Co.
Mr. J. A. Dillworth, III, Structural Requirements Division Engineer, Georgia Division, Lockheed Aircraft Corp.
Mr. E. Z. Gray, Boeing Airplane Co.
Mr. H. J. Hoge, North American Aviation, Inc.
Mr. H. W. Huntley, North American Aviation, Inc.
Mr. William W. Jenney, Douglas Aircraft Co., Inc.
Mr. J. A. Johnson, Lockheed Aircraft Corp.
Mr. Alfred I. Sibila, Chief of Engineering Personnel and Planning, Chance Vought Aircraft, Inc.
Mr. Harry Tobey, Chief of Structures, Vertol Aircraft Corp.

Mr. R. Fabian Goranson, Secretary.

Subcommittee on Vibration and Flutter

Mr. Martin Goland, Vice President, Southwest Research Institute, Chairman.
Mr. Fred L. Daum, Wright Air Development Center.
Mr. W. J. Mykytow, Wright Air Development Center.
Mr. Douglas Michel, Bureau of Aeronautics, Department of the Navy.
Mr. Philipp W. Zettler-Seidel, Army Ballistic Missile Agency.
Mr. J. Wallace McDonald, Office of the Chief of Transportation, Department of the Army.
Mr. Robert Rosenbaum, Civil Aeronautics Administration.
Mr. I. E. Garrick, NACA Langley Aeronautical Laboratory.
Mr. Albert Erickson, NACA Ames Aeronautical Laboratory.
Mr. André J. Meyer, Jr., NACA Lewis Flight Propulsion Laboratory.
Prof. Lee Arnold, Columbia University.
Prof. Holt Ashley, Massachusetts Institute of Technology.
Mr. Eugene F. Baird, Chief Flutter and Vibration Engineer, Grumman Aircraft Engineering Corp.
Mr. Douglas G. Dill, Douglas Aircraft Co., Inc.
Mr. Michael Dublin, Chief of Dynamics, Convair, Division of General Dynamics Corp.
Mr. H. Clay Johnson, Jr., Supervisor, Structural Dynamics, The Martin Co.
Mr. William R. Laidlaw, North American Aviation, Inc.
Mr. E. L. Leppert, Jr., Research Specialist, Flutter and Vibration, Lockheed Aircraft Corp.
Mr. M. J. Turner, Unit Chief—Structural Dynamics, Seattle Division, Boeing Airplane Co.

Mr. Harvey H. Brown, Secretary.

Subcommittee on Aircraft Structural Materials

Dr. Leo Schapiro, Head, Metallurgical and Physical Testing Laboratory, Douglas Aircraft Co., Inc., Chairman.
Mr. J. B. Johnson, Wright Air Development Center.
Mr. Nathan E. Promisel, Bureau of Aeronautics, Department of the Navy.
Dr. W. H. Steurer, Redstone Arsenal.
Mr. L. J. Borges, Office of the Chief of Transportation, Department of the Army.
Dr. Gordon M. Kline, Chief, Organic and Fibrous Materials Division, National Bureau of Standards
Mr. James E. Dougherty, Jr., Chief, Materials and Processes Section, Civil Aeronautics Administration.
Mr. Paul Kuhn, NACA Langley Aeronautical Laboratory.
Mr. G. Mervin Ault, NACA Lewis Flight Propulsion Laboratory
Mr. Robert S. Ames, Goodyear Aircraft Corp.
Mr. Harry A. Campbell, Bell Aircraft Corp.
Mr. Edgar H. Dix, Jr., Assistant Director of Research, Aluminum Company of America.
Prof. Pol Duwez, California Institute of Technology.
Dr. Walter L. Finlay, Vice President and Manager of Research, Rem-Cru Titanium, Inc.
Mr. L. R. Jackson, Assistant Director, Battelle Memorial Institute.
Dr. J. C. McDonald, Assistant Technical Director, Magnesium Department, The Dow Chemical Co.
Mr. Peter Payson, Assistant Director of Research, Crucible Steel Company of America.
Dr. Dana W. Smith, Associate Director, Division of Metallurgical Research, Kaiser Aluminum and Chemical Corp.
Dr. George V. Smith, Professor of Metallurgical Engineering, Cornell University.

Mr. R. H. Raring, Secretary.

COMMITTEE ON OPERATING PROBLEMS

Capt. Edward V. Rickenbacker, Chairman of the Board, Eastern Air Lines, Inc., Chairman.
Mr. William Littlewood, Vice President—Equipment Research, American Airlines, Inc., Vice Chairman.

Col. Joseph Davis, Jr., USAF, Wright Air Development Center.
Brig. Gen. Albert T. Wilson, Jr., USAF, Deputy Chief of Staff, Operations, Military Air Transport Service.
Capt. S. R. Ours, USN, Bureau of Aeronautics, Department of the Navy.
Lt. Col. John L. Rowan, USA, Office of the Deputy Chief of Staff for Military Operations, Department of the Army.
Col. George P. Seneff, Jr., USA, Office of the Chief of Research and Development, Department of the Army.
Mr. William B. Davis, Director, Office of Aviation Safety, Civil Aeronautics Administration.
Mr. Donald M. Stuart, Director, Technical Development and Evaluation Center, Civil Aeronautics Administration.
Dr. F. W. Reichelderfer (ex officio), Chief, U. S. Weather Bureau.
Dr. Hugh L. Dryden (ex officio).
Mr. Melvin N. Gough, NACA Langley Aeronautical Laboratory.
Mr. Lawrence A. Clousing, NACA Ames Aeronautical Laboratory.
Mr. Eugene J. Manganiello, NACA Lewis Flight Propulsion Laboratory.
Mr. M. G. Beard, Assistant Vice President—Equipment Research, American Airlines, Inc.
Mr. John G. Borger, Pan American World Airways System.
Mr. Warren T. Dickinson, Assistant to Chief Engineer, Douglas Aircraft Co., Inc.
Mr. Charles Froesch, Vice President—Engineering, Eastern Airlines, Inc.
Mr. Raymond D. Kelly, Superintendent of Technical Development, United Air Lines, Inc.
Mr. Jerome Lederer, Director, Flight Safety Foundation.
Mr. W. C. Mentzer, General Manager—Engineering, United Air Lines, Inc.
Mr. Robert W. Rummel, Vice President—Engineering, Trans World Airlines, Inc.
Mr. Clarence N. Sayen, President, Air Line Pilots Association.
Mr. Arthur E. Smith, Engineering Manager, Pratt & Whitney Aircraft, United Aircraft Corp.
Mr. R. L. Thoren, Chief Flight Test Engineer, Lockheed Aircraft Corp.
Mr. H. W. Withington, Staff Engineer—Systems, Boeing Airplane Co.

Dr. T. L. K. Smull, Secretary.

Subcommittee on Meteorological Problems

Dr. F. W. Reichelderfer, Chief, U. S. Weather Bureau, Chairman.
Brig. Gen. Thomas S. Moorman, Jr., USAF, Commander, Air Weather Service.
Mr. C. N. Touart, Chief, Atmospheric Analysis Laboratory, Geophysics Research Directorate, Air Force Cambridge Research Center.
Capt. Paul R. Drouilhet, USN, Head, Naval Aerology Branch, Office of Chief of Naval Operations.
Mrs. Frances L. Whedon, Office of the Chief Signal Officer, Department of the Army.
Dr. Ross Gunn, Director, Physical Research Division, U. S. Weather Bureau.
Dr. Harry Wexler, Chief, Scientific Services Division, U. S. Weather Bureau.
Mr. Robert W. Craig, Civil Aeronautics Administration.
Mr. George M. French, Civil Aeronautics Board.
Mr. Harry Press, NACA Langley Aeronautical Laboratory.
Mr. William Lewis, NACA Lewis Flight Propulsion Laboratory.
Mr. Robert N. Buck, Trans World Airlines, Inc.
Dr. Horace R. Byers, Professor of Meteorology, The University of Chicago.
Mr. Martin B. Cahill, Engineering Pilot, Northwest Airlines, Inc.
Mr. Joseph J. George, Eastern Air Lines, Inc.

Mr. Henry T. Harrison, Jr., Director—Meteorology, United Air Lines, Inc.
Prof. H. G. Houghton, Massachusetts Institute of Technology.
Mr. H. J. Reid, Manager, Flight Operations, Capital Airlines, Inc.
Dean Athelstan F. Spilhaus, University of Minnesota.
Dr. George F. Taylor, Chief, Upper Atmosphere Department, Missile Systems Division, Lockheed Aircraft Corp.
Mr. Frank C. White, Air Transport Association of America.

Mr. Mason T. Charak, Secretary.

Subcommittee on Icing Problems

Mr. W. W. Reaser, Douglas Aircraft Co., Inc., Chairman.
Lt. Col. George B. Eldridge, USAF, Air Research and Development Command.
Mr. Carl L. Oakes, Jr., Wright Air Development Center.
Dr. Robert M. Cunningham, Air Force Cambridge Research Center.
Mr. R. T. Miller, Bureau of Aeronautics, Department of the Navy.
Mr. Harcourt C. Sontag, Bureau of Aeronautics, Department of the Navy.
Dr. Henri Bader, Chief Scientist, Snow, Ice, Permafrost Research Establishment.
Maj. John W. Elliott, USA, Office of the Chief of Transportation, Department of the Army.
Mr. Dwight B. Kline, U. S. Weather Bureau.
Mr. Robert J. Auburn, Civil Aeronautics Administration.
Mr. Uwe H. von Glahn, NACA Lewis Flight Propulsion Laboratory.
Mr. J. S. Alford, Aircraft Gas Turbine Department, General Electric Co.
Mr. Victor Hudson, Senior Thermodynamics Engineer, Convair, Division of General Dynamics Corp.
Mr. G. Donald Linklater, Senior Meteorologist, Northwest Airlines, Inc.
Mr. Bernard L. Messinger, Department Manager, Thermodynamics, Lockheed Aircraft Corp.
Mr. Robert A. Paselk, North American Aviation, Inc.
Mr. Duane M. Patterson, Director, Aeronautical Icing Research Laboratories, Smith, Hinchman & Grylls, Inc.
Mr. D. A. Richardson, Assistant to Chief Design Engineer, Vertol Aircraft Corp.

Mr. Mason T. Charak, Secretary.

Subcommittee on Flight Safety

Mr. Charles Froesch, Vice President—Engineering, Eastern Air Lines, Inc., Chairman.
Dr. Albert A. Hetherington, Jr., Air Research and Development Command.
Lt. Col. John P. Stapp, USAF, Chief, Aeromedical Field Laboratory, Holloman Air Development Center.
Mr. Sydney D. Berman, Office of the Inspector General, U. S. Air Force.
Comdr. Forrester C. Auman, USN, Office of Deputy Chief of Naval Operations (Air).
Col. James F. Wells, USA, Office of the Deputy Chief of Staff for Military Operations, Department of the Army.
Mr. L. J. Borges, Office of the Chief of Transportation, Department of the Army.
Mr. W. A. Klikoff, Deputy Chief, Aircraft Engineering Division, Civil Aeronautics Administration.
Mr. John M. Chamberlain, Director, Bureau of Safety Regulation, Civil Aeronautics Board.
Honorable Joseph P. Adams (ex officio), Vice Chairman, Civil Aeronautics Board.

Mr. Melvin N. Gough, NACA Langley Aeronautical Laboratory.
Mr. I. Irving Pinkel, NACA Lewis Flight Propulsion Laboratory.
Mr. Carl M. Christenson, United Air Lines, Inc.
Mr. Allen W. Dallas, Director, Engineering Division, Air Transport Association of America.
Dr. Paul M. Fitts, Jr., Ohio State University.
Mr. Scott Flower, Pan American World Airways, Inc.
Mr. A. Howard Hasbrook, Director, Aviation Crash Injury Research of Cornell University.
Mr. Otto E. Kirchner, Sr., Senior Group Engineer, Preliminary Design Unit, Boeing Airplane Co.
Mr. Jerome Lederer, Director, Flight Safety Foundation.
Dr. Ross A. McFarland, Harvard School of Public Health.
Mr. William I. Stieglitz, Design Safety Engineer, Republic Aviation Corp.
Mr. H. H. Young, Flight Safety Engineer, Douglas Aircraft Co., Inc.

Mr. Boyd C. Myers, II, Secretary.

Subcommittee on Aircraft Noise

Mr. William Littlewood, Vice President—Equipment Research, American Airlines, Inc., Chairman.
Dr. H. O. Parrack, Wright Air Development Center.
Capt. R. L. Christy, (MC) USN, Bureau of Aeronautics, Department of the Navy.
Capt. C. P. Phoebus, (MC) USN, Office of Naval Research, Department of the Navy.
Mr. Joseph Matulaitis, Office of the Chief of Transportation, Department of the Army.
Mr. Stephen H. Rolle, Chief, Power Plant Branch, Civil Aeronautics Administration.
Dr. Richard K. Cook, Chief, Sound Section, National Bureau of Standards.
Mr. Macon C. Ellis, Jr., NACA Langley Aeronautical Laboratory.
Mr. Arthur A. Regier, NACA Langley Aeronautical Laboratory.
Mr. Newell D. Sanders, NACA Lewis Flight Propulsion Laboratory.
Dr. Richard H. Bolt, Massachusetts Institute of Technology.
Mr. Allen W. Dallas, Director, Engineering Division, Air Transport Association of America.
Dr. Robert O. Fehr, Manager, Mechanical Engineering Laboratory, General Electric Co.
Dr. Stacy R. Guild, Johns Hopkins Hospital.
Dr. Cyril M. Harris, Director, Acoustics Laboratory, Columbia University.
Dr. Hans W. Liepmann, California Institute of Technology.
Mr. Karl Martinez, Boeing Airplane Co.
Mr. M. M. Miller, Chief, Acoustics Section, Douglas Aircraft Co., Inc.
Dr. Charles T. Molloy, Lockheed Aircraft Corp.
Mr. John M. Tyler, Pratt & Whitney Aircraft, United Aircraft Corp.
Dr. P. J. Westervelt, Assistant Professor, Department of Physics, Brown University.
Mr. John M. Whitmore, Allison Division, General Motors Corp.

Mr. George P. Bates, Jr., Secretary

INDUSTRY CONSULTING COMMITTEE

Mr. William Littlewood, Vice President—Equipment Research, American Airlines, Inc., Chairman.
Mr. L. R. Grumman, Chairman of the Board, Grumman Aircraft Engineering Corp., Vice Chairman.
Mr. J. L. Atwood, President, North American Aviation, Inc.
Mr. J. H. Carmichael, President, Capital Airlines, Inc.
Dr. M. P. Ferguson, President, Bendix Aviation Corp.
Mr. Harvey Gaylord, Vice President—Helicopters, Bell Aircraft Corp.
Mr. L. S. Hobbs, Vice Chairman, United Aircraft Corp.
Mr. C. W. LaPierre, Executive Vice President, General Electric Co.
Mr. Mundy I. Peale, President, Republic Aviation Corp.
Mr. Dwane L. Wallace, President and General Manager, Cessna Aircraft Co.

Dr. T. L. K. Smull, Secretary

Part III—FINANCIAL REPORT

Funds appropriated for the Committee for the fiscal years 1956 and 1957 and obligations against the fiscal year 1956 appropriations are as follows:

	Fiscal year 1956		Fiscal year 1957
	Allotments	Obligations	Allotments
SALARIES AND EXPENSES APPROPRIATION			
NACA Headquarters	$1, 557, 745	$1, 541, 237	$1, 624, 050
Langley Aeronautical Laboratory	22, 141, 400	22, 051, 384	23, 778, 100
Ames Aeronautical Laboratory	10, 929, 250	10, 850, 663	12, 978, 600
Lewis Flight Propulsion Laboratory	20, 237, 805	20, 200, 066	21, 591, 244
High-Speed Flight Station	1, 929, 695	1, 913, 134	2, 090, 950
Pilotless Aircraft Station	928, 500	908, 622	1, 095, 335
Western Coordination Office	23, 935	19, 979	32, 105
Wright-Patterson Liaison Office	15, 604	15, 439	16, 116
Research contracts with educational institutions	750, 300	750, 291	770, 000
Research contracts with Government agencies	198, 000	198, 000	200, 000
Savings reserved for reappropriation	1, 422, 766	1, 500, 000	
Unobligated balance		186, 185	
Total	[1] 60, 135, 000	60, 135, 000	[2] 64, 176, 500
CONSTRUCTION AND EQUIPMENT APPROPRIATION			
Langley Aeronautical Laboratory	3, 325, 000	31, 741	7, 826, 000
Ames Aeronautical Laboratory	1, 055, 000	418, 898	906, 000
Lewis Flight Propulsion Laboratory	8, 395, 000	1, 796, 349	5, 712, 000
Pilotless Aircraft Station	90, 000	1, 595	
Reserve transferred from prior years	−300, 000	−32, 013	−444, 000
Unobligated balance		[3] 10, 348, 430	
Total	[1] 12, 565, 000	12, 565, 000	[2] 14, 000, 000

[1] Appropriated in the Independent Offices Appropriation Act, 1956, approved June 30, 1955.

[2] Appropriated in the Independent Offices Appropriation Act, 1957, approved June 27, 1956, and the First Supplemental Appropriation Act, 1957, approved July 27, 1956. Includes $1,500,000 reappropriation of fiscal year 1956 funds.

[3] This balance remains available until expended.